

2

AFWAL-TR-81-3170



AD A118720

CHARACTERISTICS OF HIGH PERFORMANCE EJECTORS

J. E. Minardi

UNIVERSITY OF DAYTON RESEARCH INSTITUTE
300 COLLEGE PARK AVENUE
DAYTON, OHIO 45469

January 1982

Final Report for Period 30 January through 30 November 1981

Approved for Public Release; Distribution Unlimited.

DTIC FILE COPY

FLIGHT DYNAMICS LABORATORY
AIR FORCE WRIGHT AERONAUTICAL LABORATORIES
AIR FORCE SYSTEMS COMMAND
WRIGHT-PATTERSON AIR FORCE BASE, OHIO 45433

1982

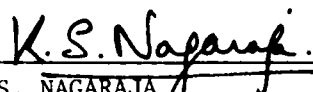
82 08 20 101


NOTICE

When Government drawings, specifications, or other data are used for any purpose other than in connection with a definitely related Government procurement operation, the United States Government thereby incurs no responsibility nor any obligation whatsoever; and the fact that the Government may have formulated, furnished, or in any way supplied the said drawings, specifications, or other data, is not to be regarded by implication or otherwise as in any manner licensing the holder or any other person or corporation, or conveying any rights or permission to manufacture use, or sell any patented invention that may in any way be related thereto.


This report has been reviewed by the Office of Public Affairs (ASD/PA) and is releasable to the National Technical Information Service (NTIS). At NTIS, it will be available to the general public, including foreign nations.

This technical report has been reviewed and is approved for publication.


K. S. NAGARAJA
Air Force Project Engineer


LOWELL C. KEEL
Lt Col, USAF
Chief, Aerodynamics and
Airframe Branch

FOR THE COMMANDER


JOHN R. CHEVALIER
Colonel, USAF
Chief, Aeromechanics Division

"If your address has changed, if you wish to be removed from our mailing list, or if the addressee is no longer employed by your organization please notify FIMM, W-PAFB, OH 45433 to help us maintain a current mailing list".

Copies of this report should not be returned unless return is required by security considerations, contractual obligations, or notice on a specific document.

SECURITY CLASSIFICATION OF THIS PAGE (When Data Entered)

DD FORM 1473 EDITION OF 1 NOV 65 IS OBSOLETE

SECURITY CLASSIFICATION OF THIS PAGE (When Data Entered)

UNCLASSIFIED

SECURITY CLASSIFICATION OF THIS PAGE(When Data Entered)

20.

control-volume approach to analyzing a constant area ejector yields two solutions: one with a subsonic mixed flow and one with a supersonic mixed flow. The supersonic mixed flow produces the best efficiencies and highest total pressures. The properties of the supersonic mixed flow are of necessity related to the properties of the subsonic mixed flow by the normal shock relations. Nonetheless, in practice, the subsonic mixed flow is, in general, not achieved through a normal shock (or pseudo-normal shock) from the supersonic mixed flow solution.

If the ejector has a supersonic primary flow at the inlet and if the resulting mixed flow is supersonic, then the highest efficiencies are achieved with a subsonic secondary flow at the inlet. Thus, this is the most favorable condition to operate an ejector. However, some of the solutions which are consistent with the mathematics of the analyses clearly violate the second law of thermodynamics and would not be possible in an ejector. Other regions of the solution with supersonic mixed flow do not violate the second law but produce mixed flows that have higher kinetic energies when expanded to ambient pressure than the kinematic energy in the primary flow when expanded to the same pressure.

In this paper, these conditions are investigated and thermodynamic processes and associated devices are identified which would be able to achieve this performance, consistent with the control volume requirements upon which the ejector analysis is based. It is important to determine the conditions and range of operation that can actually be achieved in an ejector. This is accomplished in this paper.

If the exit flow from the ejector is subsonic, the back pressure (or the effective back pressure, if there is a diffuser) determines where the ejector will operate; that is, the inlet secondary flow Mach number is determined by the pressure boundary condition at the exit for a given geometry and given stagnation conditions of the primary and secondary fluids. However, if the back pressure is low enough, then the mixed flow at the exit is supersonic and the operating condition is independent of the back pressure at lower values. Thus, for a supersonic mixed flow at the exit, some other condition is required to determine the operating point. This condition is given in the paper and incorporated in the analysis.

> A model is presented that gives a physical interpretation to the various solutions obtained from the mathematics, and more importantly, some fundamental limits are presented and a procedure is developed for determining the efficiency that can be achieved in a constant area ejector when the mixed flow is supersonic.

UNCLASSIFIED

SECURITY CLASSIFICATION OF THIS PAGE(When Data Entered)

TABLE OF CONTENTS

SECTION	PAGE
1 INTRODUCTION	1
2 CONTROL VOLUME ANALYSIS	3
3 ON THE EXISTENCE OF THE SECOND SOLUTION	13
4 CONSIDERATIONS OF THE CONTROL VOLUME ANALYSIS	21
5 FUNDAMENTAL LIMITS OF MIXERS	23
5.1 Reversible Mixing	23
5.2 Constant Kinetic Energy Mixing	29
5.3 Simple Mixing or Straight Mixing	31
5.4 Total Pressure Needed for Thrust Augmentation	33
5.5 Thrust Augmentation as a Function of Mixer Efficiency	39
5.6 Minimum Total Pressure for a Given Bypass Ratio	41
6 DETERMINATION OF THE SUPERSONIC OPERATING POINT	51
7 SUMMARY AND RECOMMENDATION	59
REFERENCES	61
APPENDIX A - Compressible Flow Ejector Analyses from Reference 7	63
APPENDIX B - Detailed Description of Machinery Required to Achieve Any Desired Total Pressure for Constant Energy Steady Flows	85



Accession No.	
	X
A	

LIST OF ILLUSTRATIONS

FIGURE		PAGE
1	Constant Area Ejector	4
2	Efficiency Based on Availability Versus Secondary Inlet Mach Number for a Bypass Ratio of 10	7
3	Efficiency Based on Availability Versus Secondary Inlet Mach Number for a Bypass Ratio of 2	9
4	Subsonic Branch Efficiency Map	10
5	Supersonic Branch Efficiency Map	11
6	Efficiency Based on Availability for a Constant Geometry Solution for the Indicated Conditions	14
7	Total Pressure of the Mixed Flow for the Constant Geometry Solution for the Indicated Conditions	15
8	Mixed Flow Mach Number M_m , for the Constant Geometry Solution for the Indicated Conditions	16
9	Exit Values of Static Pressure of the Mixed Flow for the Constant Geometry Solution for the Indicated Conditions	17
10	A Geometry Which May Give the Same Set of Equations as a Constant Area Geometry. The Exit Area Equals the Sum of the Inlet Areas: $A_m = A_s + A_p$	22
11	Machinery for Producing Any Desired Total Pressure for Constant Enthalpy Steady Flows	24
12	Reversible Mixing of the Primary and Secondary Streams	25
13	Constant Kinetic Energy Mixing	25
14	Total Pressure that Gives a Thrust Augmentation of 1	37
15	T-s Diagram for $P_{op}/P_{os} = 6$ and $T_{op}/T_{os} = 3.7$, Showing States for Reversible Mixing, Constant Kinetic Energy, Simple Mixing, and Thrust Augmentation of 1	38
16	Thrust Augmentation as a Function of Flight Mach Number for a Bypass Ratio of 14.9	42

LIST OF ILLUSTRATIONS (Concluded)

FIGURE		PAGE
17	Thrust Augmentation as a Function of Flight Mach Number for a Bypass Ratio of 5.0	43
18	Thrust Augmentation as a Function of Flight Mach Number for a Bypass Ratio of 2.0	44
19	Fanno Lines for the Mixed Flow on a T-s Diagram	46
20	Composite Curve Showing Various Limit Lines and Ejector Curves for Various Values of Friction	49
21	Inlet Flow Pattern for an Ejector Operating with a Supersonic Mixed Flow and Having a Supersonic Primary Flow and a Subsonic Secondary Flow	52
22	Pressure Ratio Required to Achieve a Given Value of M_g^* Along with Limit Lines and the Supersonic Branch Solution	56
23	Efficiency Versus Mass Flow Ratio for Different Geometry Mixing Tubes	58
A-1	Constant Area Ejector	66
B-1	Machinery for Producing Any Desired Total Pressure for Constant Enthalpy Steady Flows	87

FOREWORD

This report was prepared by the Energy Conversion/Aerodynamics Group, Aerospace Mechanics Division, University of Dayton Research Institute, Dayton, Ohio. The work was funded by the Air Force Wright Aeronautical Laboratories/Flight Dynamics Laboratory, through Project No. 2404, Task No. 10, Work Unit 56, Contract No. F33615-81-K-3017. The Principal Investigator for this research activity was Dr. John E. Minardi, Senior Research Engineer, and the Technical Monitor was Dr. K. S. Nagaraja, Flight Dynamics Laboratory.

The author wishes to express his appreciation to Dr. Nagaraja for his technical assistance and comments during this work. This report covers the total contract period, 30 January to 30 November 1981.

The author wishes to acknowledge the special assistance of Dr. Hans J. P. von Ohain and Mr. Maurice Lawson for many stimulating discussions concerning ejectors. Much of this work is based on their suggestions. Appreciation is also acknowledged to personnel of the University of Dayton Research Institute who assisted in this program: Dr. R. P. Braden, Mr. R. K. Newman, Dr. J. N. Scott, Mr. E. T. Elias, and Mr. G. Kepes. The author would especially like to acknowledge Ms. Ruth Fannin for her assistance in preparation of this report.

SECTION 1

INTRODUCTION

For many years, ejectors have found wide applications in jet pumps, steam-jet refrigeration, mercury diffusion pumps, etc. More recently, ejectors have been investigated for flight applications, especially as a method of thrust augmentation, and their potential usefulness has been demonstrated in experimental aircraft.

The topic of ejectors has been extensively studied over the years -- a recent publication by Porter and Squyers¹ lists over 1,600 references concerning ejector systems and related topics. Analyses of the mixing problem can be divided into two general types: detailed mixing models using the Navier-Stokes equations; or, the control volume approaches which use integrated forms of the conservation equations of mass, momentum, and energy. The one-dimensional control-volume approach, using a compressible fluid, was chosen for this study since it affords the best vehicle for the parametric studies required to understand the potential of ejectors for a given application.

It has been known for some time (see, for example, references 2 through 5) that the analyses of a constant area ejector lead to a double valued solution: one where the mixed flow is subsonic; and the other where the mixed flow is supersonic. Further, it is well known that these two solutions are related by the normal shock relations.

Recently, Alperin and Wu⁶ have pointed out the potential advantages of the supersonic branch for applications to thrust augmentation. Minardi, et al.⁷, who were recently studying two fluid ejectors for applications in turbines at the University of Dayton Research Institute (UDRI), found results for their applications that were consistent with those of Alperin and Wu. Both studies indicated that extremely high efficiencies could be

obtained on the supersonic branch. It was the purpose of this study to determine fundamental performance characteristics and limitations of these high performance ejectors to establish a basis for their application to thrust augmentation.

SECTION 2

CONTROL VOLUME ANALYSIS

Two types of ejectors are widely considered: the constant area ejector and the constant pressure ejector. We will concern ourselves mainly with the constant area ejector, a schematic of which is shown in Figure 1. Of course, a flightworthy ejector used for thrust augmentation would have many essential elements that must be properly integrated. A good discussion of such an integration is given by Alperin and Wu⁶. The major elements are the flight inlet diffusers for the engine and bypass air, the jet engine itself, the inlet nozzle geometry for the secondary air (bypass air) to the ejector, the inlet geometry for the primary gas (engine gas leaving the turbine), the ejector mixing tube and finally, the diffuser (or nozzle) where the mixed flow exits to the atmosphere. We are going to concentrate only on the ejector since the other elements, although not simple, are well understood and have found wide application in flight vehicles.

For example, a better bypass air inlet would simply produce a higher value of secondary inlet air total pressure P_{os} (see Figure 1). The ideal inlet would produce a value of P_{os} equal to the isentropic stagnation pressure determined by the flight Mach number. A better exit diffuser would allow the ejector to exhaust to a higher back pressure, P_{back} (see Figure 1). An ideal isentropic diffuser would allow the ejector to exhaust the flow into a back pressure equal to the total pressure of the mixed flow at the exit, P_{om} (the mixed flow at station m of Figure 1).

However, to understand the essential features of an ejector it is best to first consider only the simple schematic of Figure 1 where the stagnation conditions of the primary and secondary gases are considered given and the back pressure P_{back} can be adjusted to any designed value. In this way, the essential features of the ejector will not be masked by the

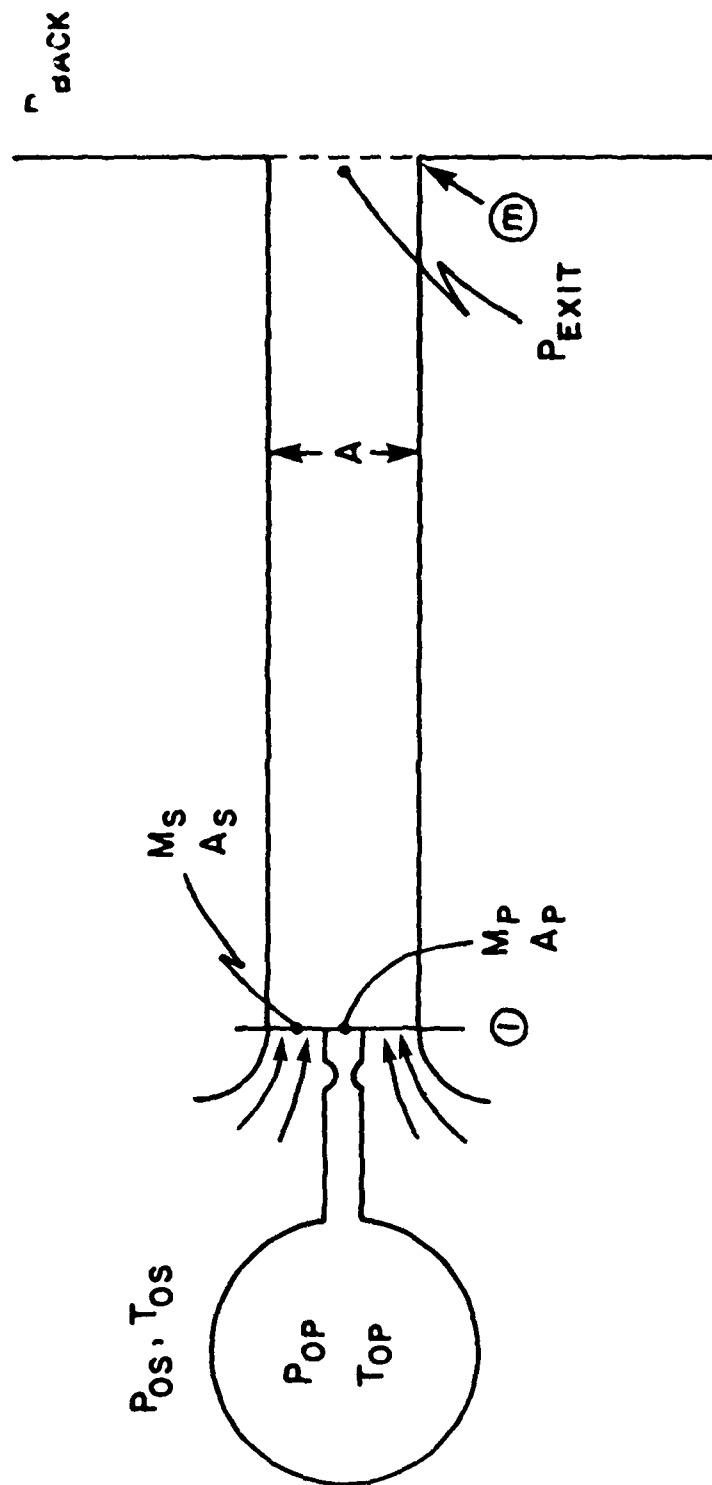


Figure 1. Constant Area Ejector.

features of the other elements, especially the exit diffuser. However, a word of warning may be in order -- a poor diffuser can completely obviate the value of a good ejector.

The usual conditions that are applied to constant area mixing are as follows:

- (1) The flow is steady and the enthalpy is constant;
- (2) The exit area (A in Figure 1) is equal to the sum of the inlet areas of the primary flow A_p and the secondary flow A_s ; and,
- (3) No net pressure forces are acting on the ejector walls (friction forces are frequently accounted for).

Condition 1 is an obvious, reasonable assumption. Conditions 2 and 3 follow directly from the constant area geometry. However, condition 2 could also be valid for a nonconstant area geometry and it is conceivable that condition 3 might also hold for some nonconstant area geometry where the exit area equals the inlet areas. Thus, the constant area geometry is a sufficient condition to yield the three conditions stated above, but not a necessary condition. This will be discussed in greater detail later in this report.

In view of Figure 1 and the conditions stated above, we can write the following equations for one-dimensional flow that is completely mixed at station m.

Continuity:

$$\rho_{1s} A_s V_s + \rho_{1p} A_p V_p = \rho_m A V_m \quad (1)$$

or

$$\dot{m}_s + \dot{m}_p = \dot{m}_m \quad (1')$$

Energy:

$$\dot{m}_s h_{os} + \dot{m}_p h_{op} = \dot{m}_m h_{om} \quad (2)$$

Momentum:

$$P_{1p}A_p + \dot{m}_p V_p + P_{1s}A_s + \dot{m}_s V_s = P_m A + \dot{m}_m V_m \quad (3)$$

also from condition 2

$$A = A_s + A_p \quad (4)$$

If we assume that we have ideal gases then we can solve the above system of equations in a straightforward, though somewhat tedious manner. Our approach to this is given in Reference 7 and in Appendix I. Other equally valid approaches are given in References 2 through 6 and in many of the 1,600 references of Reference 1. It is not our purpose here to review the details of these solutions but rather to discuss some of the results obtained from computer programs based on these solutions.

Figure 2 presents the results for both branches for the solution of the equations for a constant-area ejector with a constant mass flow ratio. The two solution branches are marked subsonic and supersonic on Figure 2. The branch with supersonic mixed flow is referred to by Alperin and Wu⁶ as the "second solution." We have also shown the results for a constant pressure solution on Figure 2. The solutions presented are for air driving air with a pressure ratio, P_r , of 6 ($P_r \equiv P_{op}/P_{os}$) and a temperature ratio, T_r , of 3.7 ($T_r \equiv T_{op}/T_{os}$). These ratios are representative of what might be possible with a modern jet engine. The mass flow ratio ($MR = \dot{m}_p/\dot{m}_s$) was taken as 0.1 (or a bypass ratio of 10). The efficiency based on availability is plotted as a function of the secondary inlet Mach number M_s . The primary inlet Mach number, M_p is adjusted to match the pressure at the inlet (i.e., $P_{1p} = P_{1s}$).

The efficiency based on availability is the ratio of the thermodynamic availability in the mixed flow divided by the availability in the incoming primary flow. The availability for both flows is referenced to the stagnation conditions of the secondary flow. The second law requires that the efficiency

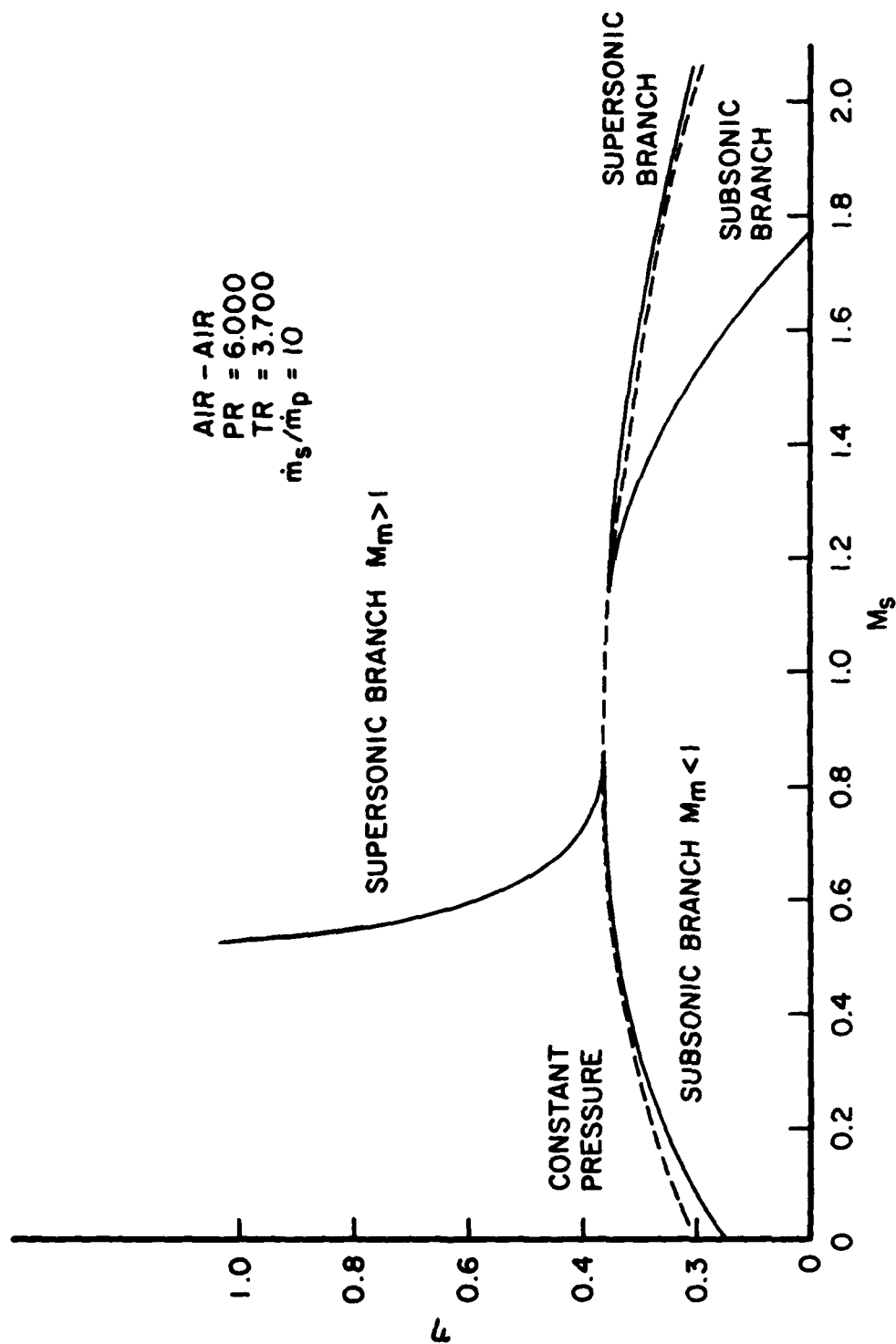


Figure 2. Efficiency Based on Availability Versus Secondary Inlet Mach Number for a Bypass Ratio of 10.

based on this concept be less than or equal to one for an adiabatic system.

As seen in Figure 2, the value of the efficiency, η , exceeds one on the supersonic branch at subsonic inlet Mach numbers, M_s , less than 1. Also note that a choking of the flow takes place in the constant area case and no real solution exists for a range of secondary inlet Mach numbers, M_s . This condition disappears at lower bypass ratios as seen in Figure 3, where all the conditions are the same except that the bypass ratio is 2 instead of 10. Complete tables of data for Figures 2 and 3 are given in Appendix A.

In calculating the data for Figures 2 and 3, we assumed that the inlet pressures of the primary and secondary flows were the same. However, if one of the inlet flows is supersonic, then this condition need not be true. In fact, a map of the performance for all combinations of inlet Mach numbers can be developed for both branches of the solution. We developed a computer program based on the work of Hoge⁴ to construct such maps. Results of these calculations are shown in Figures 4 and 5 where lines of constant efficiency, based on availability, are drawn in the $M_p^*-M_s^*$ plane. (M^* , the ratio of velocity to the speed of sound at Mach one, was used since it has a finite maximum value). For Figures 4 and 5, the pressure ratio and temperature ratio are the same as used for Figures 2 and 3. The mass flow ratio MR is 0.1 (bypass ratio of 10) which is the same as for Figure 2. The region of imaginary solutions, called the forbidden region, is a large, egg-shaped region which is cross-hatched on Figures 4 and 5. The value of the mixed Mach number on the boundary of this region is one.

The locus of points in the plane where the inlet pressures are equal is the solid line labeled $P_{1p} = P_{1s}$ on Figures 4 and 5. If we took a cut through the two surfaces along this line and plotted the efficiencies versus M_s (instead of M_s^*) we would obtain the same results as plotted on Figure 2 for the constant area solutions. The part within the forbidden region, of course,

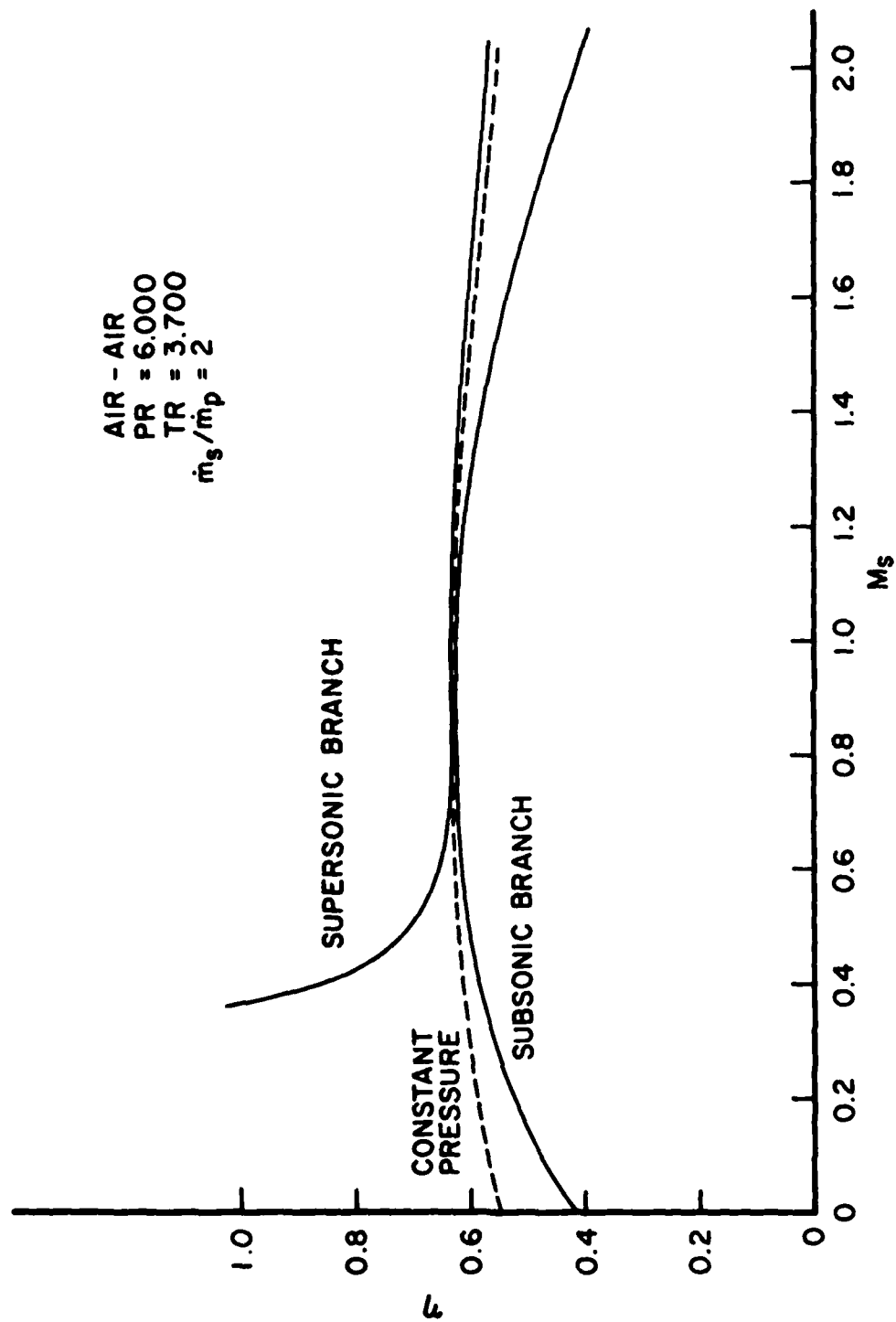


Figure 3. Efficiency Based on Availability Versus Secondary Inlet Mach Number for a Bypass Ratio of 2.

SUBSONIC BRANCH EFFICIENCY
 $MR = 0.10$ $PR = 6.0$ $TR = 3.7$

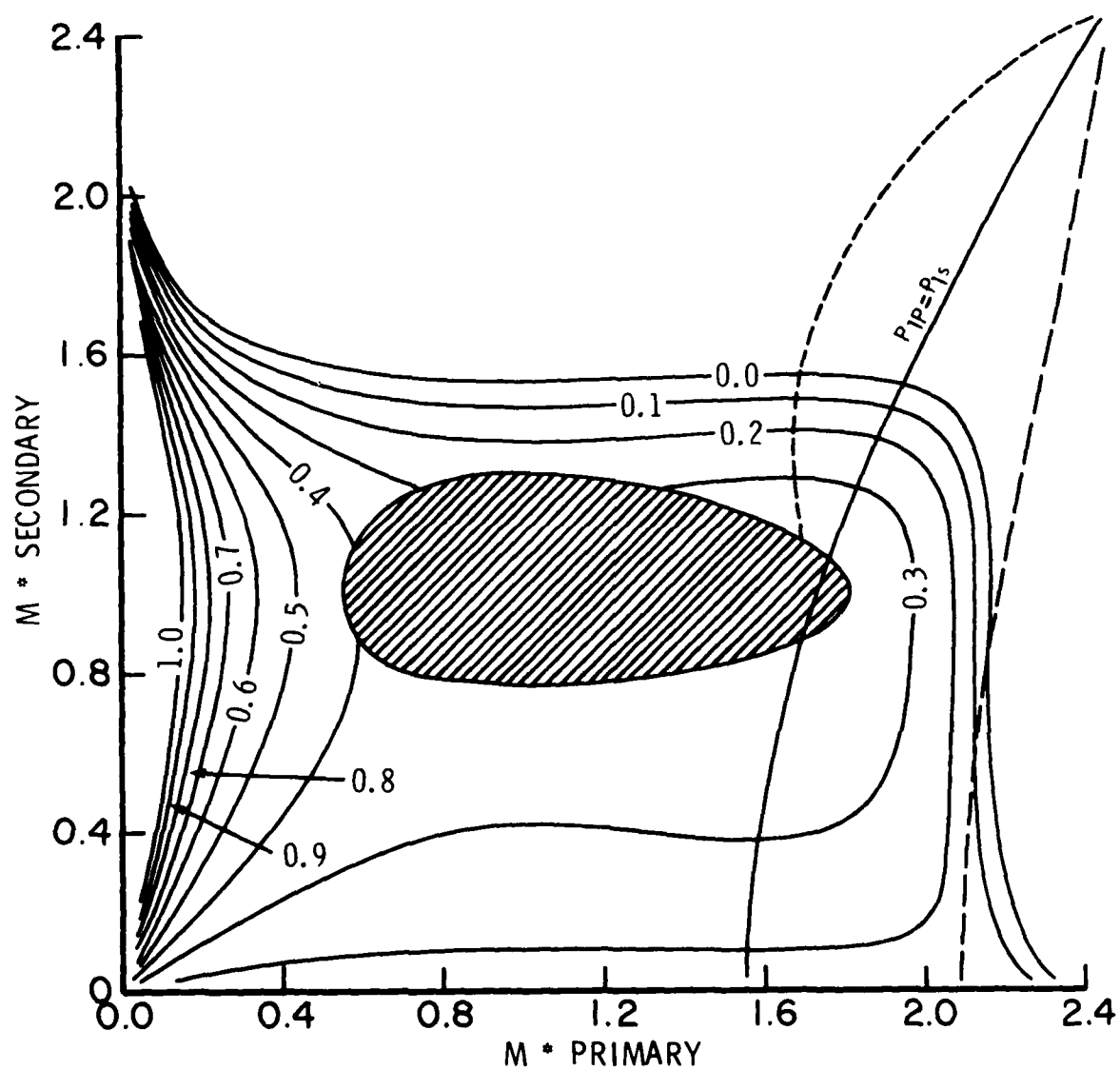


Figure 4. Subsonic Branch Efficiency Map.

SUPERSONIC BRANCH EFFICIENCY
 $MR = 0.10$ $PR = 6.0$ $TR = 3.7$

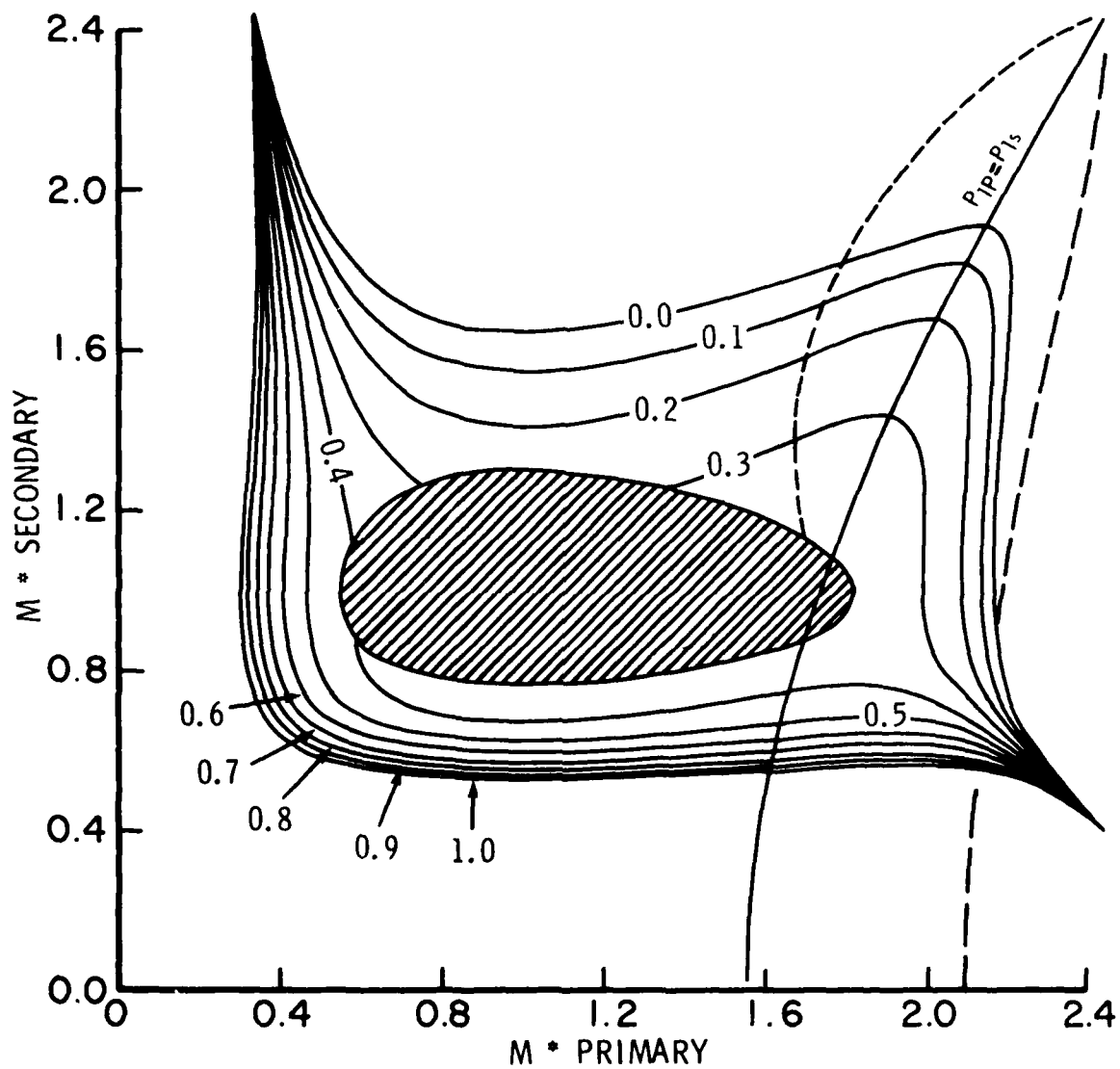


Figure 5. Supersonic Branch Efficiency Map.

has only imaginary solutions and neither branch is shown on Figure 2 for that range of Mach numbers, M_s , that lie within the forbidden region.

It is of interest to note that extremely high efficiencies, equal to or greater than one, are achieved on the subsonic branch (at low M_p^* values of Figure 4) as well as the supersonic branch (see Figure 5). Thus, the high efficiencies are not just a property of the second solution, but can occur on either branch. However, if the condition of equal pressure at the inlet is used, then only the supersonic branch exhibits the extremely high efficiencies.

Figures 4 and 5 illustrate all of the possible solutions that satisfy the equations listed earlier for the given set of conditions. It is quite clear, however, that many of them could not possibly be achieved in an ejector. For example, if both M_s^* and M_p^* are subsonic, then P_{1p} must be equal to P_{1s} if the flows were to enter an ejector. But the locus of points along which this pressure condition holds does not enter the part of the plane where both M_s^* and M_p^* are subsonic. Thus, none of these solutions could occur in an ordinary ejector.

It was considerations such as these that lead to the following set of questions:

1. Can the supersonic solution be achieved at a subsonic value of secondary inlet Mach number M_s ?
2. How does one understand the exceptional solutions exemplified by the values at subsonic inlet Mach numbers of the second solution?
3. What are some fundamental limits of performance of mixers?
4. What are the limits of performance that can actually be achieved on the second solution branch?

In the remainder of the report, we will attempt to answer these questions.

SECTION 3

ON THE EXISTENCE OF THE SECOND SOLUTION

From the theoretical perspective given below, it will become obvious that the second solution can be achieved in the region where the inlet secondary Mach number is one or less. This is most easily seen if we consider the results for the solution of a constant geometry case in response to operation with different back pressures, P_b , of Figure 1. Figures 6 through 9 were obtained for constant geometry. The curves shown on Figure 6 are fundamentally different from those of Figures 2 and 3. All three figures are drawn for constant area ejectors, but the geometry of the ejector is different at each value of M_s in either Figure 2 or Figure 3, while the geometry within the control volume is constant for all values of M_s in Figures 6 through 9. In calculating the data for Figures 2 and 3, the mass flow ratio was held constant and a side condition was set: the inlet pressures of the primary and secondary stream were made equal. Thus, the geometry required to produce the same pressure at the inlet and the constant mass flow ratio changes at each value of M_s in either Figures 2 or 3.

Nonetheless, we see that Figure 6 still exhibits the extremely high values of efficiency at the subsonic inlet Mach numbers of the secondary flow on the supersonic branch of the solution (i.e., second solution). The conditions used for calculating the data for Figures 6 through 9 are given on the figures. Figure 7 presents the total pressure of the mixed flow at the exit divided by the total pressure of the secondary gas. Since the total temperature is fixed by the ratio of the mass flow rates, only one other thermodynamic property from the stagnation state is required to fix the stagnation state of the mixed flow. Therefore, knowledge of either the total pressure (from Figure 7), or the availability (from Figure 6) is adequate to fix the stagnation state of the mixed flow. Thus, either Figure 6 or 7 could be obtained from information on the other.

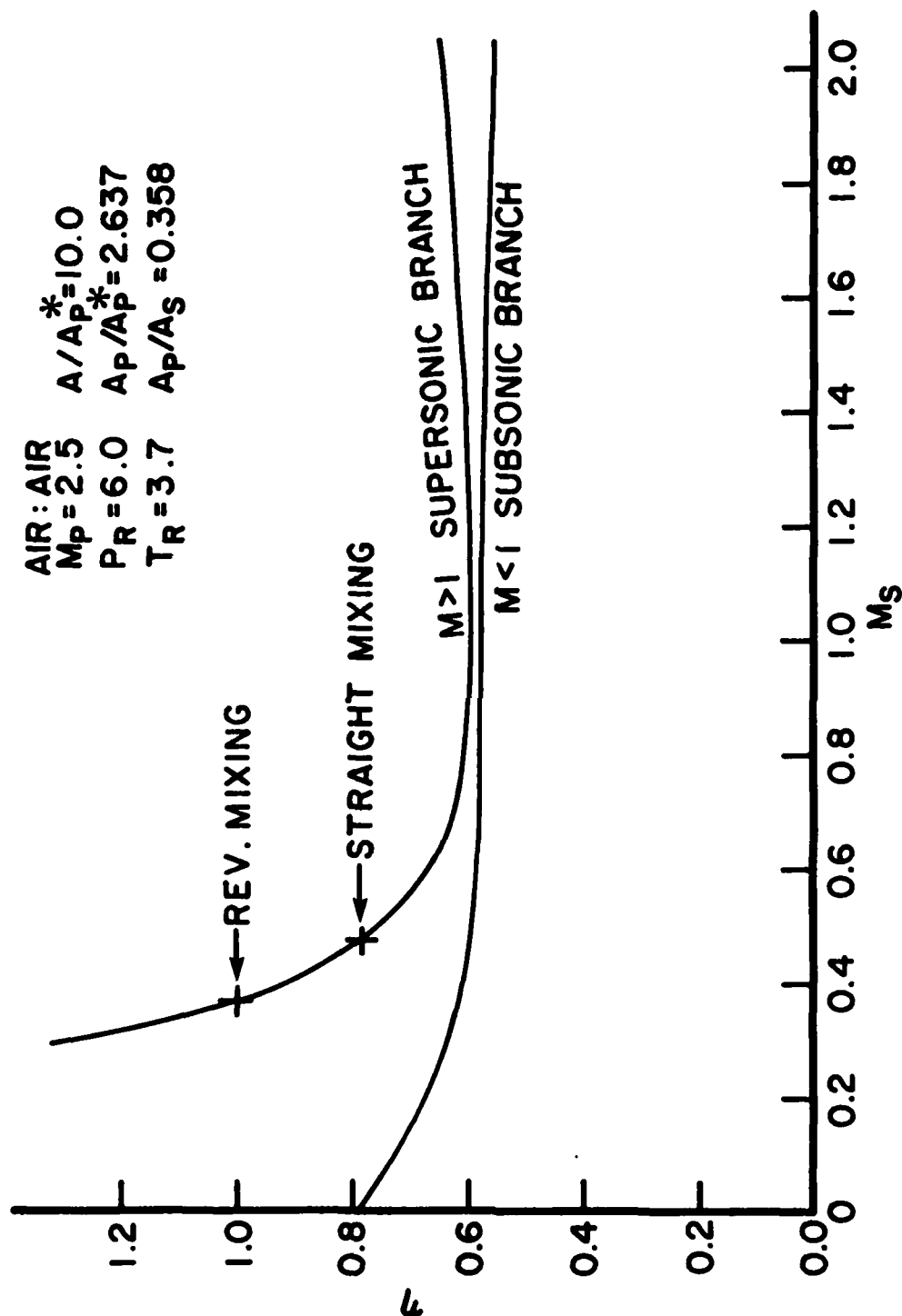


Figure 6. Efficiency Based on Availability for a Constant Geometry Solution for the Indicated Conditions.

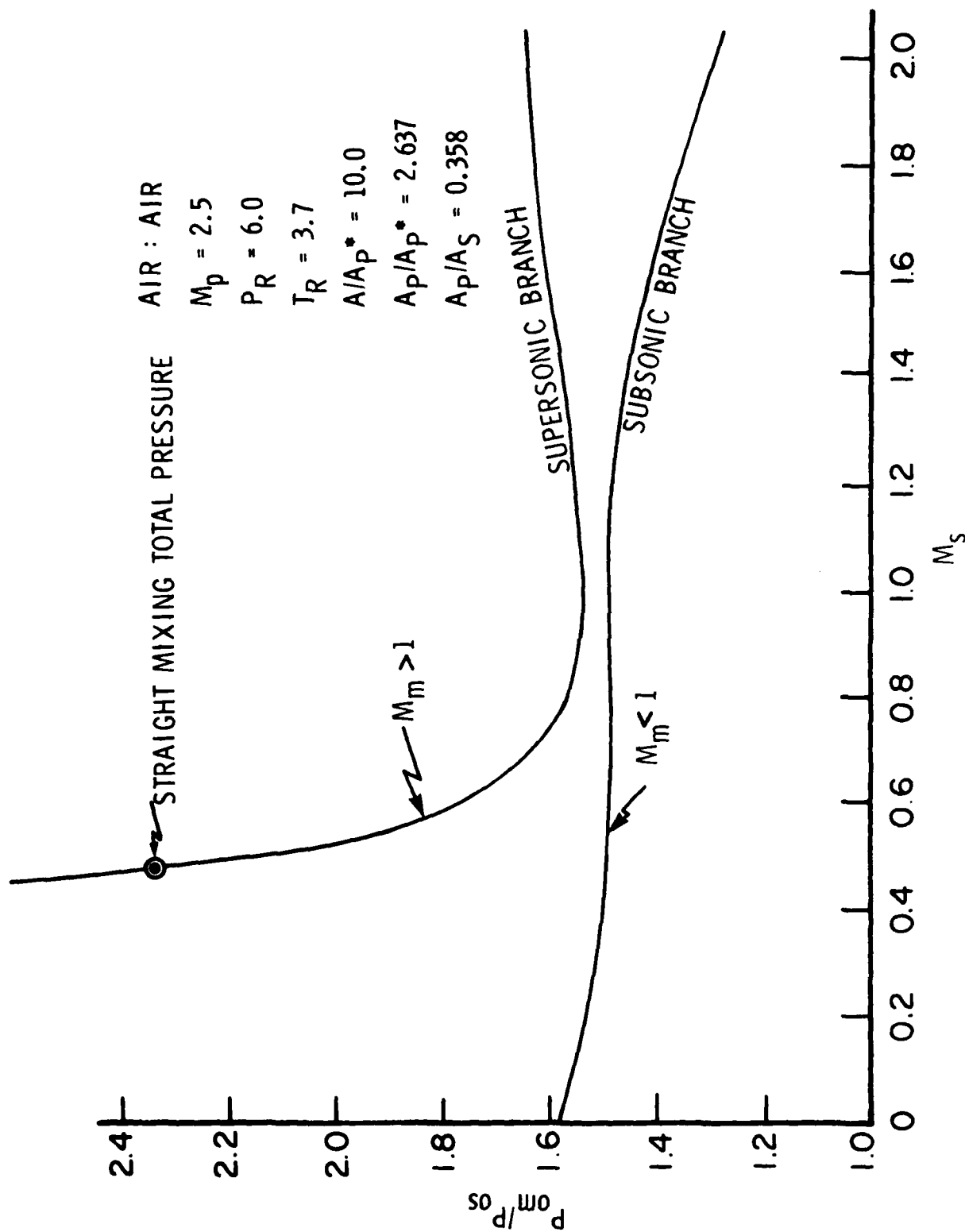


Figure 7. Total Pressure of the Mixed Flow for the Constant Geometry Solution for the Indicated Conditions.

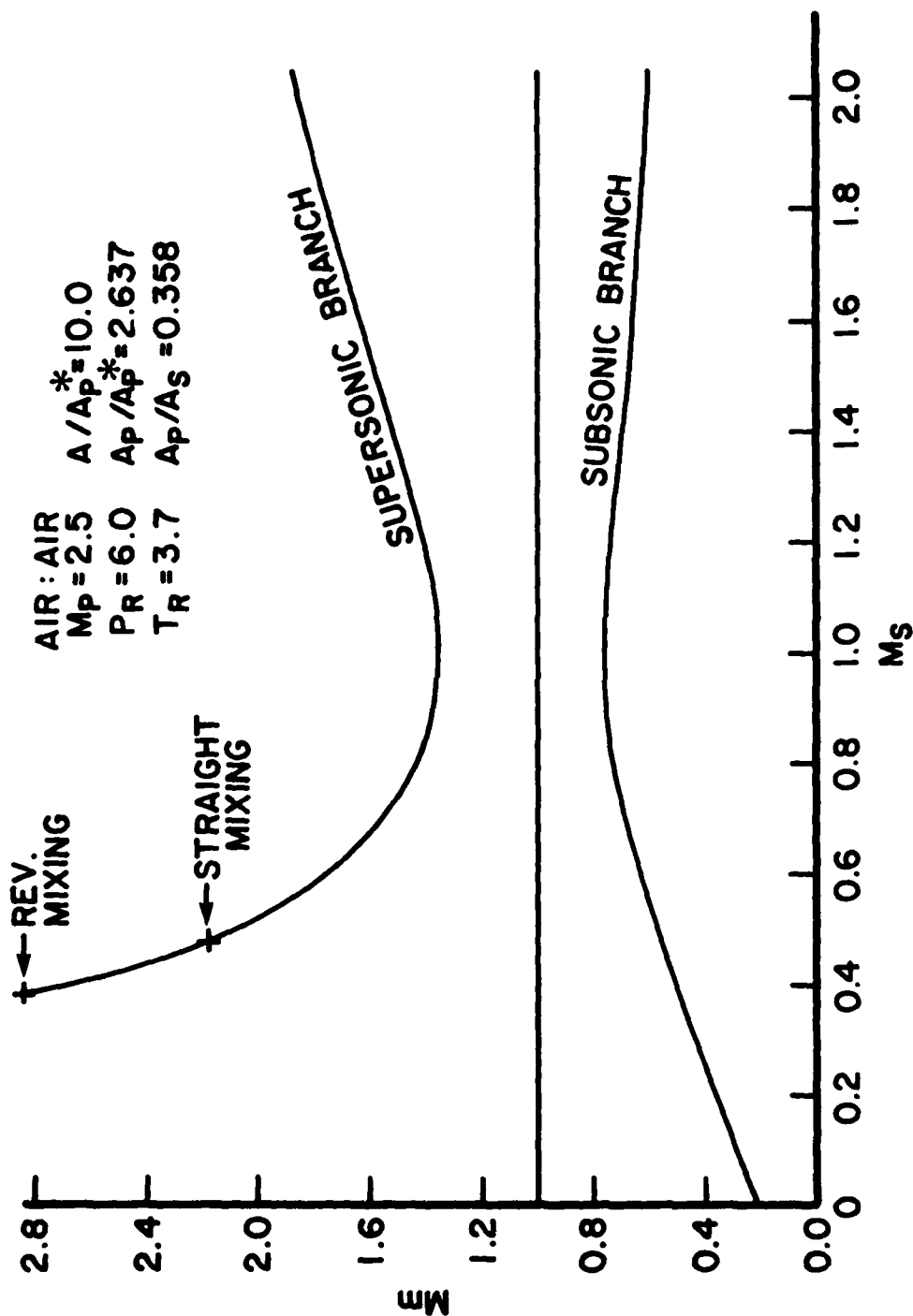


Figure 8. Mixed Flow Mach Number, M_m , for the Constant Geometry Solution for the Indicated Conditions.

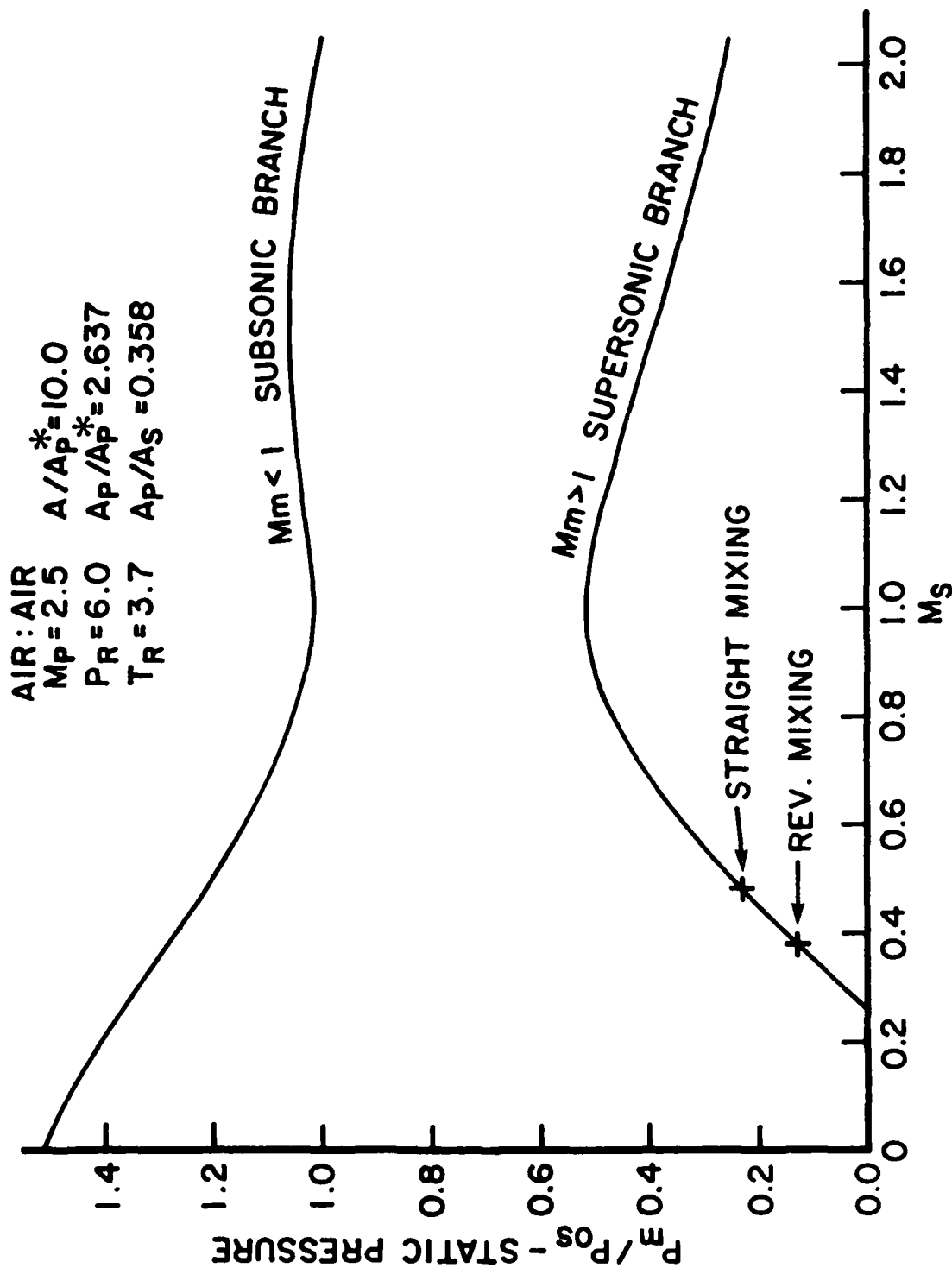


Figure 9. Exit Values of Static Pressure of the Mixed Flow for the Constant Geometry Solution for the Indicated Conditions.

Figure 8 presents the mixed flow Mach number for both solution branches. From Figure 8 it is clear that the mixed flow Mach number on the subsonic branch is well subsonic--less than 0.8, while the supersonic mixed flow Mach number is greater than 1.3.

Figure 9 presents the static pressure in the mixed flow for both branches. Note that the static pressure on the subsonic branch is higher than on the supersonic branch. It is instructive to do a thought experiment with Figure 9 and Figure 1 in view. A particular solution from those presented on Figures 6 through 9 results by setting the back pressure, P_{back} of Figure 1. The setting of this boundary condition actually determines where the ejector will operate. From the geometry of Figure 1 it is clear that M_s must be 1 or less since there is no throat in the secondary flow ahead of the inlet. Therefore, we are only concerned with the solutions where M_s is one or less on Figures 6 through 9.

If the mixed flow Mach number, M_m , is subsonic, then the exit static pressure must be equal to the back pressure. Consequently, in view of Figure 9, the subsonic solution is possible only if the back pressure is in the range of 1.01 to 1.51. If the back pressure is set below 1.01, say 0.8, then the supersonic solution must be achieved at some secondary inlet Mach number of one or less. Of course once the back pressure is low enough so that the supersonic branch is achieved, the operation of the ejector is independent of the back pressure since signals cannot be transmitted upstream. Thus, the ejector will operate at only one point on the supersonic branch, irrespective of the value of the back pressure. Since the ejector operation is independent of the back pressure on the supersonic branch, another condition is required to determine the operating point. This condition will be discussed in detail later in the report. In any event, from our theoretical arguments, it is clear at this time that the

supersonic branch can be achieved. Furthermore, there is substantial data in the literature to support this conclusion (e.g., see Reference 3).

It is still important to understand the physical significance of the extremely high efficiencies that we have seen on both the subsonic and supersonic branches as indicated on Figures 2 through 6. We will consider this in the next section.

SECTION 4

CONSIDERATIONS OF THE CONTROL VOLUME ANALYSIS

As discussed previously, the constant area geometry is a sufficient condition to derive the control volume equations used to obtain the solutions we have discussed. The geometry shown in Figure 10 might also give the same set of equations.

In the geometry of Figure 10 the exit area, A_m , equals the sum of the inlet areas; therefore, the continuity and energy equations are the same as for the constant area geometry. If a turbine-fan combination was included in the control volume, it would exchange energy between the primary and secondary flows, but no heat or work would cross the control volume boundaries. Consequently, the energy equation would not change.

Finally, if the wall shapes were properly chosen, the momentum equation could also be the same. Clearly we could get some results with this device that we could not obtain with the ejector and vice-versa.

Considerations such as these lead to the conclusion that the constant area geometry is a sufficient condition to derive the set of equations used for its analysis but it is not a necessary condition. Since it is not a necessary condition, some of the solutions to the equations may not be possible with an ejector. On the other hand, since it is a sufficient condition, all of the solutions possible with an ejector will be found using the equations.

In order to understand how all of the solutions could be achieved and determine fundamental limits of mixers we have developed, for thought experiments, a set of machinery within our control volume for which the equations are still valid. We will look at some of the fundamental limits in the next section.

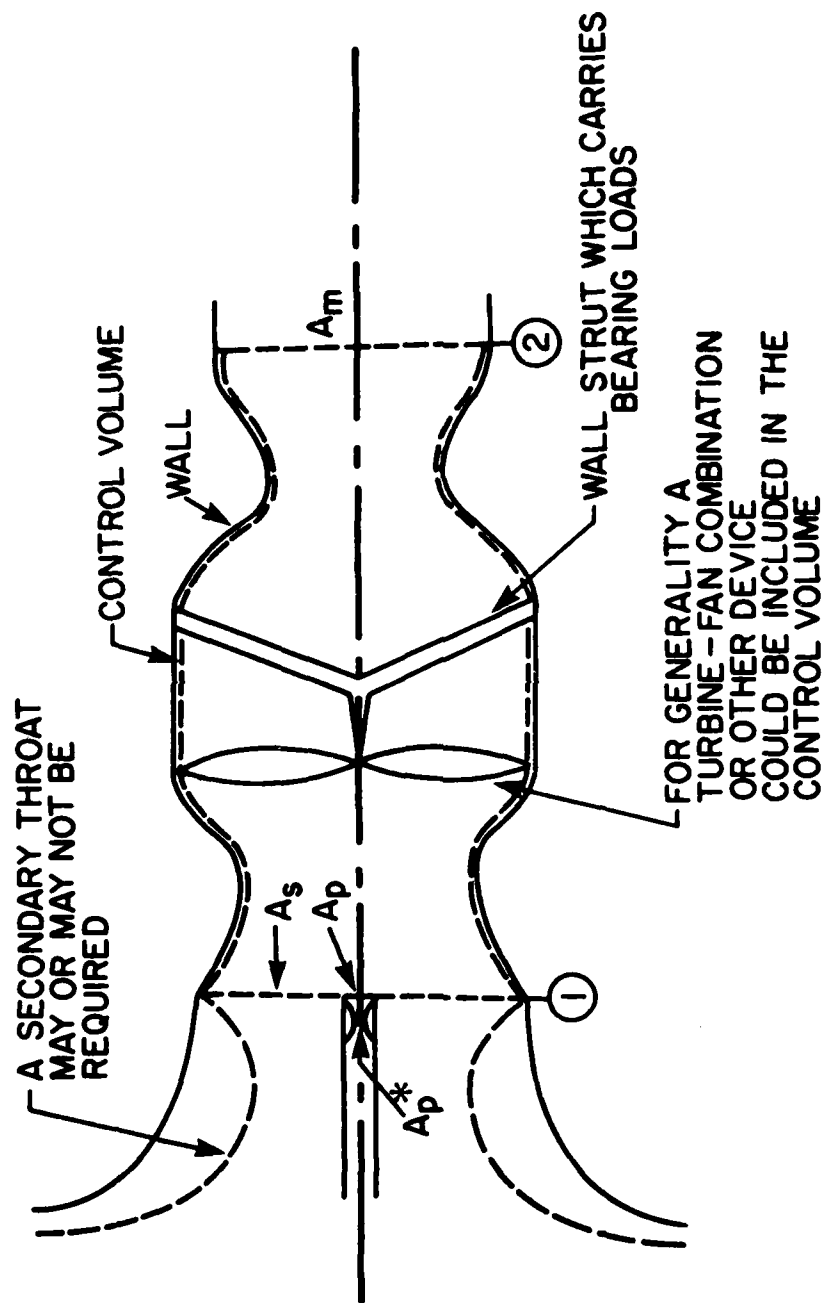


Figure 10. A Geometry Which May Give the Same Set of Equations as a Constant Area Geometry. The Exit Area Equals the Sum of the Inlet Areas: $A_m = A_s + A_p$.

SECTION 5

FUNDAMENTAL LIMITS OF MIXERS

For the purpose of a thought experiment, consider Figure 11 which contains a set of machinery within a control volume. The machinery of Figure 11 is described in detail in Appendix B. We show a jet engine as the source of the primary fluid while the secondary fluid is supplied by the atmosphere.

The first thing we wish to consider is reversible mixing of the two streams.

5.1 REVERSIBLE MIXING

As an aid in understanding reversible mixing and other concepts discussed later, we want to consider the processes shown on the T-s diagrams of Figures 12 and 13. The T-s diagram being used was normalized with the properties of the secondary flow: T_{os} and P_{os} . Further, the entropy is referenced to the secondary flow and then normalized with the gas constant, R. The $\Delta s/R$ on the T-s diagram is $(s-s_{os})/R$.

In the case of reversible mixing, the primary fluid expands in the reversible isentropic turbine to state 2P (see Figures 11 and 12). The work from the turbine is used to compress the secondary gas in the reversible isentropic compressor C4 to the state 2s. The stagnation temperature of the two fluid streams are the same in states 2P and 2s, and we will call this temperature T_{om} .

Equating the work of the turbine to the work of a compressor for arbitrary flow rates yields:

$$\dot{m}_p c_p (T_{op} - T_{om}) = \dot{m}_s c_p (T_{om} - T_{os}) \quad (5)$$

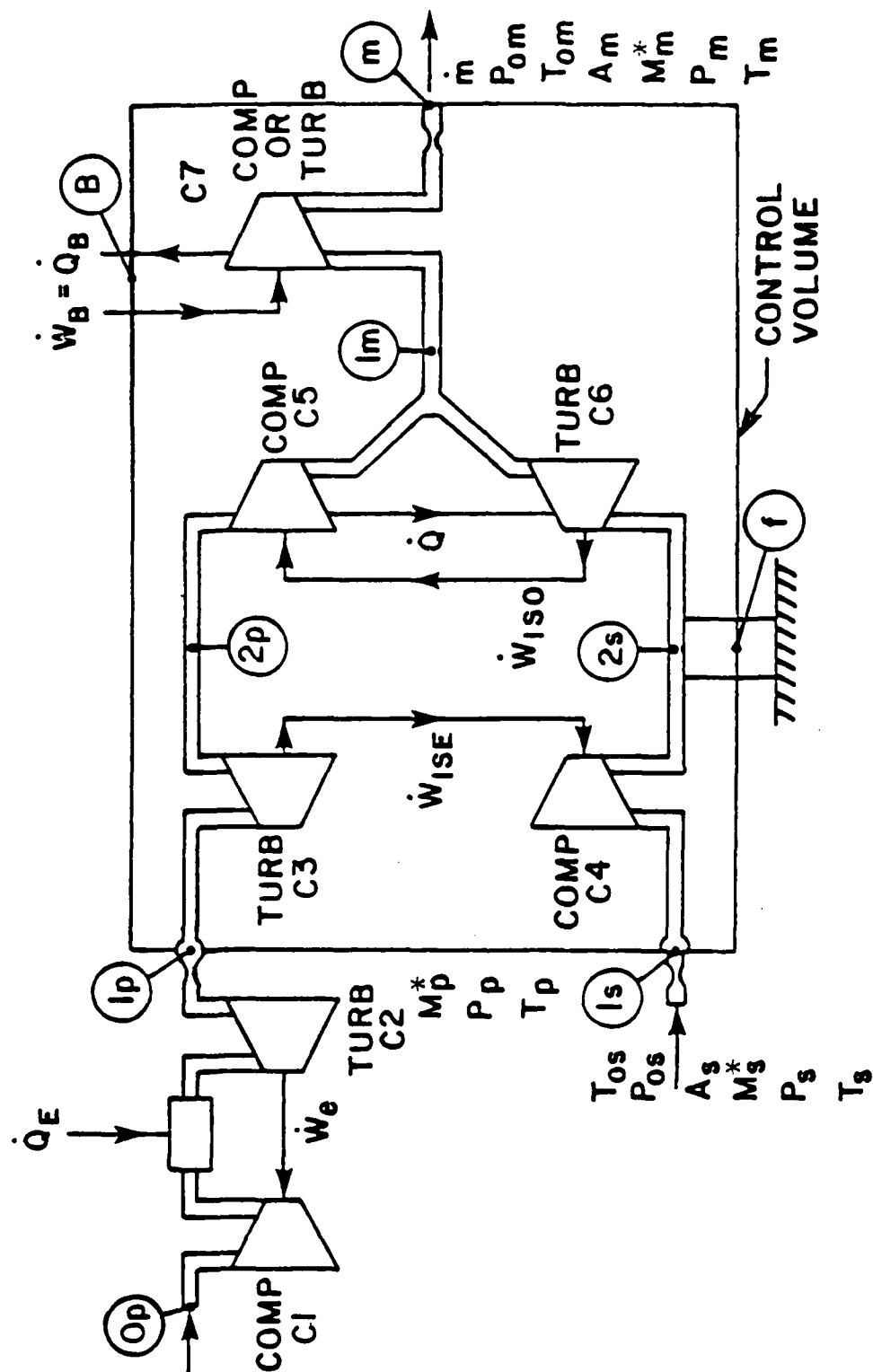


Figure 11. Machinery for Producing Any Desired Total Pressure for Constant Enthalpy Steady Flows.

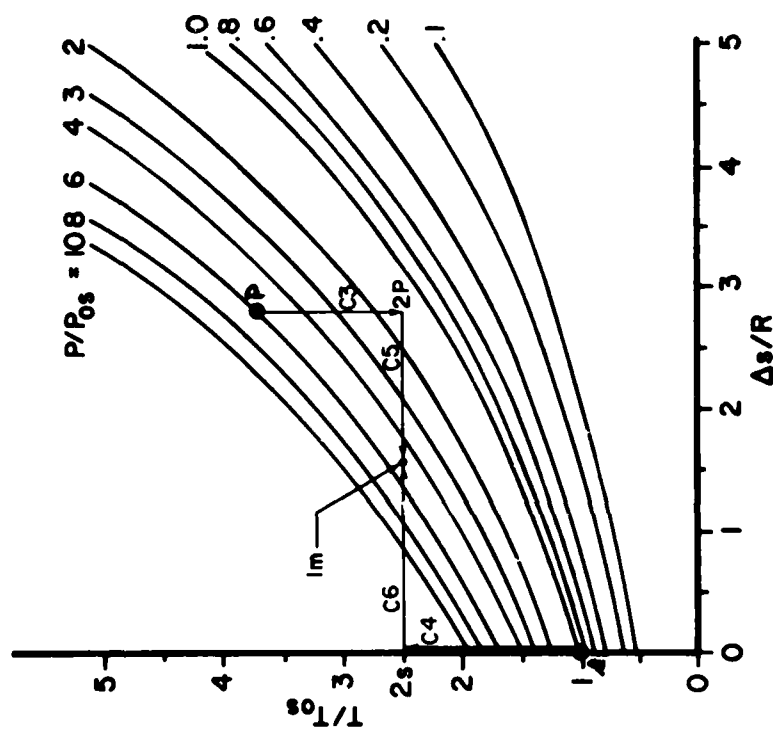


Figure 12. Reversible Mixing of the Primary and Secondary Streams.

Since the work from process C3 drives process C4, the length of C3 is to the length of C4 as m_s is to m_p . A single relation holds p for the lengths of C5 and C6 since the heat transferred from C5 goes to C6. Thus, IM lies on the straight line joining p to s .

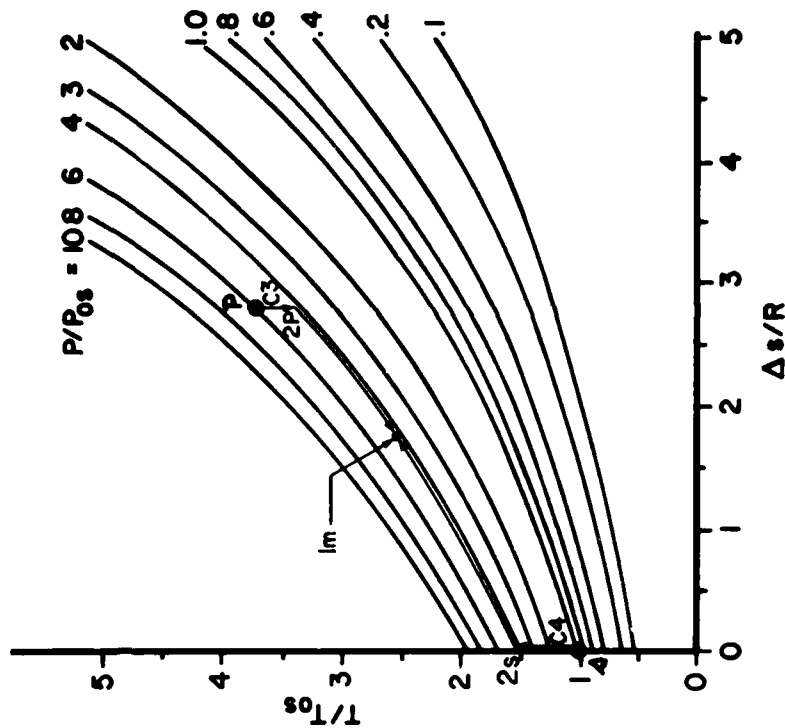


Figure 13. Constant Kinetic Energy Mixing.

Processes C3 and C4 equalize the pressure and then the streams are mixed at constant pressure.

or,

$$\dot{m}_p h_{op} + \dot{m}_s h_{os} = (\dot{m}_p + \dot{m}_s) h_{om}. \quad (5')$$

In view of Equations 1 and 2 we see that the temperature T_{om} is the mixed flow stagnation temperature which depends only on the mass flow ratio or by-pass ratio and the total temperature of the two streams.

The secondary flow then enters the isothermal turbine C6 (see Figures 11 and 12) and the work from the turbine drives the isothermal compressor C5 which compresses the primary gas. The heat transfer from the primary gas required for the isothermal processes is transferred to the turbine C6 to maintain the temperature of the secondary gas. Since we are assuming that the processes are reversible we have for the heat transfers:

$$\dot{m}_p T_{om} (s_{op} - s_{om}) = \dot{m}_s T_{om} (s_{om} - s_{os}) \quad (6)$$

In view of Equations 5 and 6 we have

$$\frac{T_{op} - T_{om}}{T_{om} - T_{os}} = \frac{s_{op} - s_{om}}{s_{om} - s_{os}} \quad (7)$$

From Equation (7) we see that the mixed state in reversible mixing lies on the straight line joining the point s to the point p. Equation (7) can be rearranged to show this more clearly:

$$\frac{T_{om}}{T_{os}} = 1 + \left(\frac{T_{op}}{T_{os}} - 1 \right) \frac{\Delta s_{om}/R}{\Delta s_{op}/R} \quad (8)$$

where $\Delta s = s - s_{os}$.

In order to determine the value of the total pressure, P_{om} for the reversible mixing, we need to use Equation (6) and the equation for the entropy change for an ideal gas:

$$\frac{\Delta s}{R} = \frac{\gamma}{\gamma-1} \ln \frac{T}{T_{os}} - \ln \frac{P}{P_{os}} \quad (9)$$

In view of (6) we can obtain

$$\dot{m}_p \Delta s_{op} = \dot{m}_m \Delta s_{om} \quad (10)$$

Therefore:

$$\frac{\dot{m}_p}{\dot{m}_m} \frac{\gamma}{\gamma-1} \ln \left(\frac{T_{op}}{T_{os}} \right) - \frac{\dot{m}_p}{\dot{m}_m} \ln \left(\frac{P_{op}}{P_{os}} \right) = \frac{\gamma}{\gamma-1} \ln \left(\frac{T_{om}}{T_{os}} \right) - \ln \left(\frac{P_{om}}{P_{os}} \right) \quad (11)$$

From Equation (11) and the energy equation we can show:

$$\frac{P_{om}}{P_{os}} = \left(\frac{P_{op}}{P_{os}} \right)^{\frac{\dot{m}_p}{\dot{m}_m}} \left[\frac{\frac{\dot{m}_p}{\dot{m}_m} \frac{T_{op}}{T_{os}} + \frac{\dot{m}_s}{\dot{m}_m}}{\left(\frac{T_{op}}{T_{os}} \right)^{\frac{\dot{m}_p}{\dot{m}_m}}} \right]^{\frac{\gamma}{\gamma-1}} \quad (12)$$

Equation (12) gives the total pressure of the mixed flow

that can be achieved in reversible mixing at the station 1m and agrees with a similar result obtained by Kennedy². This is the highest value of total pressure that can be obtained without the aid of heat transfer out of the control volume. With the use of the isothermal machine, C7 (see Figure 11), still higher total pressures would be possible. It is very important to realize that the presence of C7 is consistent with the energy equation, Equation (2).

Of course, if the final total pressure exceeds that given by Equation (12), one can say that the second law is violated for an adiabatic control volume (or, we need C7). However, in the cases when the machines C3 through C6 (see Figure 11) are real, the situation is different: the total pressure at 1m would be less than that given by Equation (12). But, the isothermal machine, C7, could bring it closer to the value for reversible mixing without it being an obvious violation of the second law. For this reason, we have called the machine, C7, the "ghost machine" since its effect may be totally masked.

For the thought experiments for the machinery of Figure 11 this ghost machine is not too important, but, for an ejector there must be intrinsic loss mechanisms because we have, in general, differences in velocity, temperature, pressure, and sometimes, species at the entrance to the ejector.

However, the ghost machine, which is consistent with our equations, can completely mask these intrinsic losses without an apparent violation of the second law. The second law, therefore, may not give us a realistic estimate of the maximum performance of an ejector. Some other condition is needed to more realistically estimate the maximum performance; such a condition is available and will be discussed in detail later.

Another interesting point about Equation (12) is the fact that, in general, more kinetic energy can be obtained from an expansion of the mixed flow to any pressure than could be obtained from separate expansion of primary and secondary flows to the same

pressure. The total pressure that yields the same kinetic energy is derived in the next section.

5.2 CONSTANT KINETIC ENERGY MIXING

If the flow mixes such that the gross exit kinetic energy is constant, we can write the following equation:

$$\dot{m}_s T_{os} \left[1 - \left(\frac{P_f}{P_{os}} \right)^{\frac{\gamma-1}{\gamma}} \right] + \dot{m}_p T_{op} \left[1 - \left(\frac{P_f}{P_{op}} \right)^{\frac{\gamma-1}{\gamma}} \right] = \dot{m}_m T_{om} \left[1 - \left(\frac{P_f}{P_{om}} \right)^{\frac{\gamma-1}{\gamma}} \right] \quad (13)$$

In Equation (13), P_f is an arbitrary final pressure to which the flows expand. In view of the energy equation for an ideal gas, Equation (13) becomes

$$- \dot{m}_s T_{os} \left(\frac{P_f}{P_{os}} \right)^{\frac{\gamma-1}{\gamma}} - \dot{m}_p T_{op} \left(\frac{P_f}{P_{op}} \right)^{\frac{\gamma-1}{\gamma}} = - \dot{m}_m T_{om} \left(\frac{P_f}{P_{om}} \right)^{\frac{\gamma-1}{\gamma}} \quad (14)$$

Clearly, since P_f cancels out of Equation (14), the result is independent of the final pressure to which we can expand the flows. In particular, this means the result is independent of the ambient pressure except for its influence on P_{os} . In that case, P_{os} would be the stagnation pressure due to the flight Mach number and P_f would be the ambient pressure. In view of the energy equation, we can solve Equation (14) and obtain:

$$\frac{P_{om}}{P_{os}} = \frac{P_{op}}{P_{os}} \left[\frac{\frac{\dot{m}_p}{\dot{m}_s} \frac{T_{op}}{T_{os}} + 1}{\left(\frac{P_{op}}{P_{os}}\right)^{\frac{\gamma-1}{\gamma}} + \frac{\dot{m}_p}{\dot{m}_s} \frac{T_{op}}{T_{os}}} \right]^{\frac{\gamma}{\gamma-1}} \quad (15)$$

Equation (15) determines the total pressure of the mixed flow that will yield the same kinetic energy as was available in the primary and secondary flows before mixing.

This pressure can be obtained by the machinery of Figure 11 in the following way. The primary flow expands through the reversible adiabatic turbine C3 and compresses the secondary flow to the same value of pressure in the reversible adiabatic compressor C4. The processes are shown on the T-s diagram of Figure 13. The two flows are then mixed and come to the final temperature T_{om} . The processes just described also represent the ideal mixing turbofan.

Since the work of the turbine equals the work of the compressor we have in view of the T-s diagram of Figure 13

$$\dot{m}_s (T_{2s} - T_{os}) = \dot{m}_p (T_{op} - T_{2p}) \quad (16)$$

or

$$\dot{m}_s T_{os} \left(\frac{T_{2s}}{T_{os}} - 1 \right) = \dot{m}_p T_{op} \left(1 - \frac{T_{2p}}{T_{op}} \right) \quad (17)$$

Because of the isentropic processes we have:

$$\dot{m}_s T_{os} \left[\left(\frac{P_{om}}{P_{os}} \right)^{\frac{\gamma-1}{\gamma}} \right] - 1 = \dot{m}_p T_{op} \left[1 - \left(\frac{P_{om}}{P_{op}} \right)^{\frac{\gamma-1}{\gamma}} \right] \quad (18)$$

Equation (18) can easily be rearranged to obtain Equation (15). Hence, the total pressure given by Equation (15), which conserves kinetic energy, can also be considered as the total pressure which is obtained from an ideal mixing turbofan.

In deriving Equation (15) we assumed that the gross exit kinetic energy in the mixed flow was equal to that of the two separated flows before mixing. It can be shown, however, that exactly the same result is obtained if we equate the increase in kinetic energy across the core engine by itself to that of the engine-mixer combination, (i.e., $\dot{m}_p(v_{jp}^2 - v_f^2) = \dot{m}_m(v_{jm}^2 - v_f^2)$), from which we can show that $\dot{m}_p v_{jp}^2 + \dot{m}_s v_f^2 = \dot{m}_m v_{jm}^2$. In these equations we have assumed expansion to atmospheric pressure. The exit-jet, primary velocity is V_{jp} and mixed-flow, exit-jet velocity is V_{jm} . The loss-free, exit-jet velocity of the secondary flow is equal to the flight speed, V_f . Thus, the thermodynamic efficiency of the engine with mixer is the same as that of the core engine. Again this represents an ideal turbofan.

5.3 SIMPLE MIXING OR STRAIGHT MIXING

Still another pressure of interest is the final pressure that results from mixing two quantities of gas in a nonflow system with mass ratios equal to the bypass ratio. We have referred to this as simple mixing or straight mixing. We can think of having two cylinders of gas: one with a mass equal to \dot{m}_p and total temperature and pressure of the primary; the other with a mass equal to \dot{m}_s and total temperature and pressure of the secondary. We then allow the two cylinders to communicate and mix adiabatically. Since the total volume remains unchanged we have in view of the energy equation and ideal gas relations

$$\dot{m}_s T_{os} + \dot{m}_p T_{op} = \dot{m}_m T_{om} = P_{om} (V_s + V_p) \quad (19)$$

where V_s and V_p are the total volumes of secondary and primary gas respectively. Eliminating the volumes yields

$$\dot{m}_s T_{os} + \dot{m}_p T_{op} = P_{om} \left(\frac{\dot{m}_p T_{op}}{P_{os}} + \frac{\dot{m}_s T_{os}}{P_{op}} \right) \quad (20)$$

Solving for P_{om}/P_{os} yields:

$$\frac{P_{om}}{P_{os}} = \frac{P_{op}}{P_{os}} \left[\frac{\frac{\dot{m}_p T_{op}}{\dot{m}_s T_{os}} + 1}{\frac{P_{op}}{P_{os}} + \frac{\dot{m}_p T_{op}}{\dot{m}_s T_{os}}} \right] \quad (21)$$

Equation (21) gives the pressure that can be achieved in a simple mixing of the two gases in a nonflow process. However, a cyclic, quasi-steady-flow device can be envisioned that would mix two quantities of gases according to Equation (21). Thus, it is reasonable to compare the performance of an ejector to the simple mixing case.

It can be formally shown that if one expands the primary fluid in a reversible adiabatic process and uses the work to compress the secondary fluid in a reversible adiabatic process and then mixes the two fluids by simple mixing, then a maximum value of P_{om} is achieved if the pressures are equalized before mixing. The value of this maximum pressure, P_{om} , is again given by Equation (15) and shows that conserving kinetic energy is the optimum that can be achieved by the use of isentropic machines in the nonflow case.

Having determined a number of limiting pressures it is of interest to determine the minimum total pressure of the mixed flow which gives a thrust augmentation of one for various conditions.

5.4 TOTAL PRESSURE NEEDED FOR THRUST AUGMENTATION

The overall efficiency of an aircraft engine is defined as the power out (thrust, τ , of the engine times the flight velocity, V_f) divided by the heat rate, \dot{Q} , supplied to the engine:

$$\eta_{OA} = \frac{\tau V_f}{\dot{Q}} = \frac{\Delta KE_j}{\dot{Q}} \cdot \frac{\tau V_f}{\Delta KE_j} = \eta_{th} \cdot \eta_{PR} \quad (22)$$

As shown in Equation (22) the overall efficiency, η_{OA} , is the product of the engine efficiency, η_{th} , and the propulsion efficiency, η_{PR} . ($\eta_{th} = \Delta KE_j / \dot{Q}$ and $\eta_{PR} = \tau V_f / \Delta KE_j$ where ΔKE_j is the increase in jet kinetic power, $1/2 \dot{m}_p (V_{jp}^2 - V_f^2)$). If the thrust of an engine is augmented while holding the flight speed constant and engine heat rate fixed (which is the case of the mixer) we see from Equation (22) that

$$\frac{\eta_{OA2}}{\eta_{OA1}} = \frac{\tau_2}{\tau_1} \equiv \phi \quad (23)$$

where subscripts 2 and 1 refer to augmented and unaugmented values, respectively.

Hence, the ratio of overall efficiencies is equal to the ratio of thrust (the thrust augmentation, ϕ). Equation (23) is valid even if η_{PR} is unchanged but η_{th} is changed. This can happen, for example, if the jet velocity and \dot{Q} are fixed but the mass flow is increased (decreased) because η_{th} is increased

(decreased). (Note that we are concerned with a given engine in combination with a mixer and, therefore, the heat rate, \dot{Q} , is fixed). From Equation (22) we see that η_{OA} can increase because, either η_{th} increases or η_{PR} increases or both increase. If the kinetic energy decreases, η_{th} will decrease but η_{OA} can still increase if η_{PR} is sufficiently increased (e.g., as happens with a turbofan).

For the case of a mixer we have for complete expansion to atmospheric pressure:

$$\phi = \frac{\tau_2}{\tau_1} = \frac{\dot{m}_m (V_{JM} - V_f)}{\dot{m}_p (V_{JP} - V_f)} \quad (24)$$

where V_{JM} is the jet velocity of the mixed flow, V_{JP} is the jet velocity of primary flow without the mixer and V_f is the flight velocity.

If we set the thrust augmentation to one we can solve Equation (24) for the jet velocity ratio:

$$\frac{V_{JM}}{V_{JP}} = \frac{\dot{m}_s}{\dot{m}_m} \frac{V_f}{V_{JP}} + \frac{\dot{m}_p}{\dot{m}_m} \quad (25)$$

Now for an ideal gas with constant specific heats we have for the jet velocity ratio:

$$\left(\frac{V_{JM}}{V_{JP}} \right)^2 = \frac{T_{om}}{T_{op}} \left[\frac{1 - \left(\frac{P_{amb}}{P_{om}} \right)^{\frac{\gamma-1}{\gamma}}}{1 - \left(\frac{P_{amb}}{P_{op}} \right)^{\frac{\gamma-1}{\gamma}}} \right] \quad (26)$$

If we combine Equations (25) and (26) we can solve for P_{om}/P_{os} :

$$\frac{P_{om}}{P_{os}} = \frac{P_{amb}}{P_{os}} \left\{ 1 - \frac{T_{op}}{T_{om}} \left(\frac{\dot{m}_s}{\dot{m}_m} \frac{V_f}{V_{JP}} + \frac{\dot{m}_p}{\dot{m}_m} \right)^2 \times \right. \\ \left. \left[1 - \left(\frac{P_{amb}}{P_{os}} \cdot \frac{P_{os}}{P_{op}} \right)^{\frac{\gamma-1}{\gamma}} \right]^{\frac{-\gamma}{\gamma-1}} \right\} \quad (27)$$

If we assume that P_{os} is the isentropic stagnation pressure resulting from the flight velocity then:

$$\left(\frac{V_f}{V_{JP}} \right)^2 = \frac{T_{os}}{T_{op}} \frac{1 - \left(\frac{P_{amb}}{P_{os}} \right)^{\frac{\gamma-1}{\gamma}}}{1 - \left(\frac{P_{amb}}{P_{os}} \cdot \frac{P_{os}}{P_{op}} \right)^{\frac{\gamma-1}{\gamma}}} \quad (28)$$

and

$$\frac{P_{amb}}{P_{os}} = \left(1 + \frac{\gamma-1}{2} M_\infty^2 \right)^{-\frac{\gamma}{\gamma-1}} \quad (29)$$

Clearly, in view of Equations (27), (28) and (29) we see that

$$\frac{P_{om}}{P_{os}} = f \left(M_\infty, \frac{T_{op}}{T_{os}}, \frac{P_{op}}{P_{os}}, \frac{\dot{m}_p}{\dot{m}_m} \right) \quad (30)$$

An explicit expression will be derived in the next section. Equations (27) through (29) were solved and P_{om}/P_{os} was plotted versus M_∞ on Figure 14 for P_{op}/P_{os} and $T_{op}/T_{os} = 3.7$. The curve parameters is \dot{m}_p/\dot{m}_m . If the mixed total pressure is greater than the value, read off the appropriate curve of Figure 14, then the thrust augmentation would be greater than one.

The data for Figure 14 can be used to draw lines on a T-s diagram where $\phi = 1$, as shown in Figure 15. We have also shown the locus of states for reversible mixing (Equation 12), constant kinetic energy (Equation 15), simple mixing (Equation 21) along with the values for $\phi = 1$ at the indicated Mach numbers. We have only shown supersonic flight Mach numbers, but the subsonic curves would lie between the $M = 1$ and $M = 2$ curves or just slightly to the left of the Mach one curve. The peaks of the curves of Figure 14 are just slightly subsonic, like $M = 0.85$.

Since T_{om}/T_{os} is fixed for a given mass flow, we have shown lines of constant \dot{m}_p/\dot{m}_m on Figure 15, which are, of course, horizontal lines on the T-s diagram. If the total pressure out of a given mixer lies between the reversible mixing curve and the constant kinetic energy curve, both η_{th} and η_{PR} would be increased in Equation (22). If the total pressure lies between the constant kinetic energy curve and the appropriate ϕ curve for the flight Mach number, then η_{th} decreases but η_{PR} increases sufficiently to give a thrust augmentation greater than one. If the total pressure lies to the right of the appropriate ϕ curve for the flight Mach number, then the thrust augmentation is less than one and the overall efficiency will have decreased.

In the next section we will generalize the thrust augmentation curves for any mixer in terms of the efficiency of the mixing process.

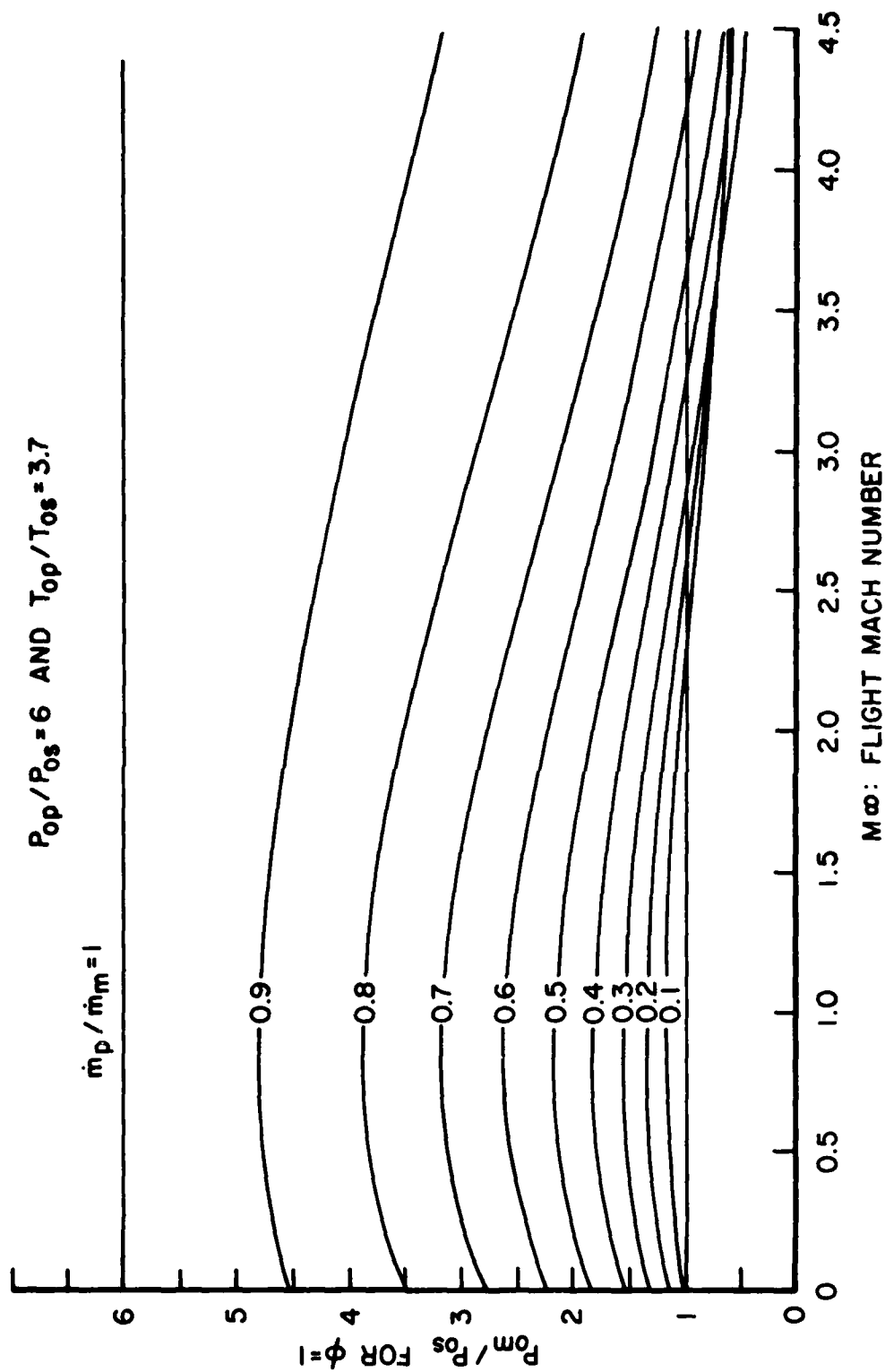


Figure 14. Total Pressure that Gives a Thrust Augmentation of 1.

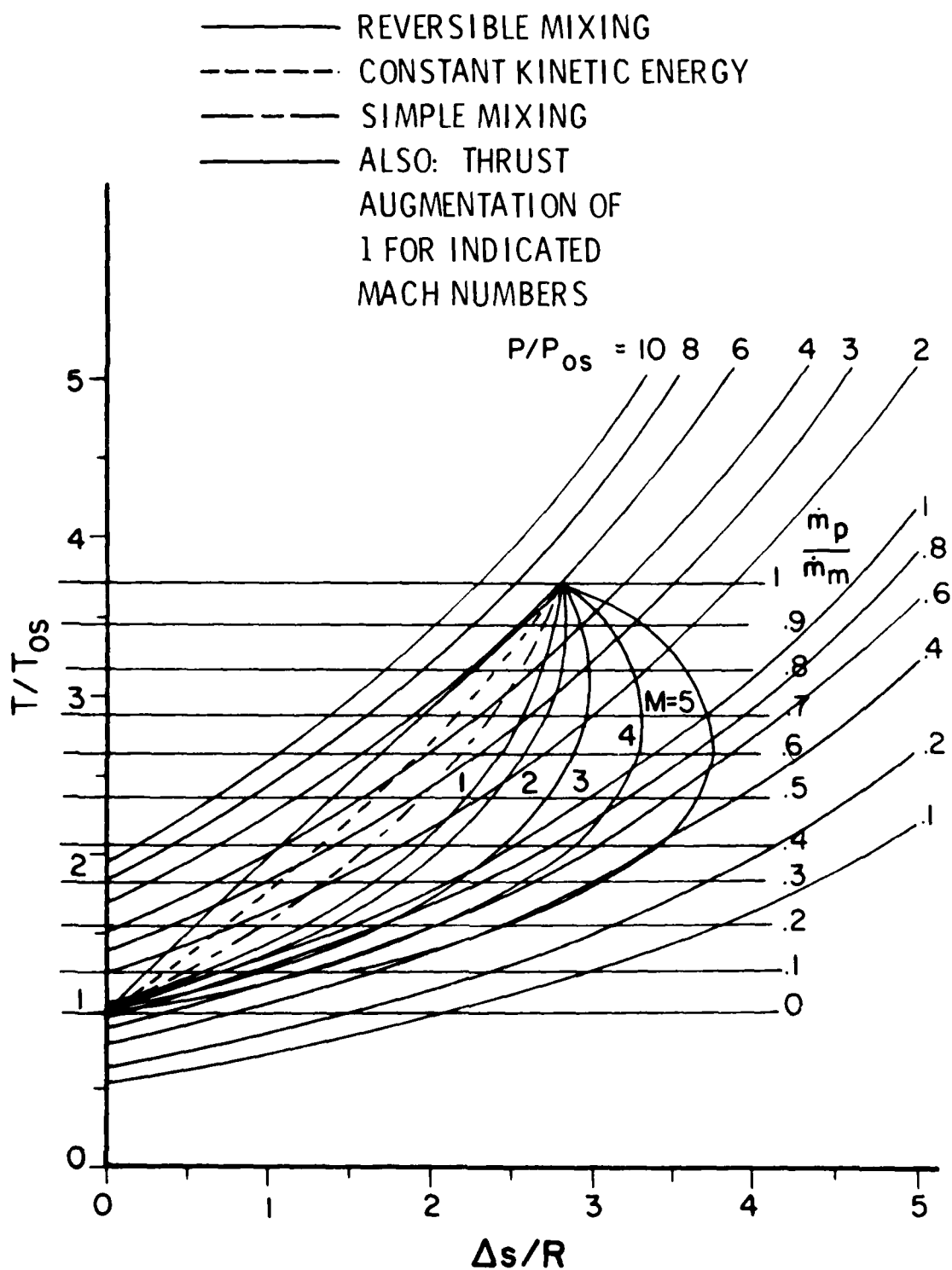


Figure 15. T-s Diagram for $P_{op}/P_{os} = 6$ and $T_{op}/T_{os} = 3.7$, Showing States for Reversible Mixing, Constant Kinetic Energy, Simple Mixing, and Thrust Augmentation of 1.

5.5 THRUST AUGMENTATION AS A FUNCTION OF MIXER EFFICIENCY

When the velocity of a fluid is achieved in an isentropic flow, we can relate the velocity to the temperature as

$$v = \sqrt{2C_p T_o \left(1 - \frac{T}{T_o}\right)} \quad (31)$$

In view of Equations (31) and (24), we have for the thrust augmentation

$$\phi = \frac{\dot{m}_m}{\dot{m}_p} \frac{\sqrt{\frac{T_{om}}{T_{os}}} \sqrt{1 - \frac{T_m}{T_{om}}} - \sqrt{1 - \frac{T_{amb}}{T_{os}}}}{\sqrt{\frac{T_{op}}{T_{os}}} \sqrt{1 - \frac{T_p}{T_{op}}} - \sqrt{1 - \frac{T_{amb}}{T_{os}}}} \quad (32)$$

Using the energy equation and the well-known isentropic relationships, we can show:

$$\phi = \frac{\dot{m}_m}{\dot{m}_p} \frac{\sqrt{\frac{\dot{m}_p}{\dot{m}_m} \frac{T_{op}}{T_{os}} + \frac{m_s}{m_m}} \sqrt{\left(1 + \frac{\gamma-1}{2} M_\infty^2\right) - \left(\frac{P_{om}}{P_{os}}\right)^{-\frac{\gamma-1}{\gamma}}} - \sqrt{\frac{\gamma-1}{2} M_\infty^2}}{\sqrt{\frac{T_{op}}{T_{os}}} \sqrt{\left(1 + \frac{\gamma-1}{2} M_\infty^2\right) - \left(\frac{P_{op}}{P_{os}}\right)^{-\frac{\gamma-1}{\gamma}}} - \sqrt{\frac{\gamma-1}{2} M_\infty^2}} \quad (33)$$

We can relate the total pressure to the efficiency based on availability by using Equation (A-34) of Appendix A and the energy equation:

$$\frac{P_{om}}{P_{os}} = \text{Exp} (D\eta - N) \quad (34)$$

where

$$D = \frac{\gamma}{\gamma-1} \frac{\dot{m}_p}{\dot{m}_m} \left[\frac{T_{op}}{T_{os}} - 1 - \ln \left(\frac{T_{op}}{T_{os}} \right) \right] + \frac{\dot{m}_p}{\dot{m}_m} \ln \left(\frac{P_{op}}{P_{os}} \right) \quad (35)$$

and

$$N = \frac{\gamma}{\gamma-1} \left[\frac{\dot{m}_p}{\dot{m}_m} \left(\frac{T_{op}}{T_{os}} - 1 \right) - \ln \left(\frac{\dot{m}_p}{\dot{m}_m} \frac{T_{op}}{T_{os}} - \frac{\dot{m}_s}{\dot{m}_m} \right) \right] \quad (36)$$

Of course the bypass ratio, \dot{m}_s/\dot{m}_p , is easily determined from either of the other mass flow ratios.

We have used Equations (33) through (36) to construct Figures 17 and 18, which show thrust augmentation versus Mach number. In all of the three figures, P_{op}/P_{os} is 6 and T_{op}/T_{os} is 3.7. The page parameter is the bypass ratio, \dot{m}_s/\dot{m}_p , which is 14.9, 5, and 2 on Figures 16, 17, and 18, respectively. Each of the figures has the efficiency as the curve parameter; 100 percent efficiency is, of course, reversible mixing. Since both of these pressures are independent of the flight Mach number, they correspond to only one value of efficiency on a given figure; e.g., the ideal turbo-fan corresponds to about 80 percent efficiency on Figure 16.

From the figures we see that the highest thrust augmentation occurs at subsonic flight Mach numbers for the higher

efficiencies. The lower efficiencies, however, have higher thrust augmentations at the higher Mach numbers. In Figures 16, 17, and 18 the pressure ratios and temperature ratios are held constant and no attempt was made to model these parameters to fit actual engine performance as a function of flight Mach number. We plan to do this as part of our future work.

There is still one limit value of pressure that can be determined with the aid of Fanno lines generated for the mixed flow.

5.6 MINIMUM TOTAL PRESSURE FOR A GIVEN BYPASS RATIO

If the exit flow is completely mixed, as we have assumed, then we can evaluate a minimum total pressure that is consistent with the mass flow ratio or bypass ratio. Fanno line flow is developed from considerations of only the continuity and energy equations for a constant area channel. The mass flow parameter, G (the mass velocity) is defined as

$$G \equiv \frac{\dot{m}_m}{A} \quad . \quad (37)$$

For a given geometry and given states of primary and secondary fluids, the value of G is fixed as soon as the total mass flow, \dot{m}_m , is known. Of course, the total temperature is determined by knowledge of the mass flow. Thus, we can immediately construct a T-s diagram for the given conditions. Such a T-s diagram is sketched on Figure 19 for values of T_{op}/T_{os} of 3.7 and P_{op}/P_{os} of 6. If we know the geometry (e.g., as in the case of the ejector of Figure 1) we could also determine a value of M_s (inlet secondary Mach number) required to give the mass flow ratio under consideration. Thus, we have indicated values of M_s on Figure 19 that might be valid for a particular geometry of the type shown on Figure 1. For any given flow rate, two values of M_s are valid: one subsonic, and the other supersonic.

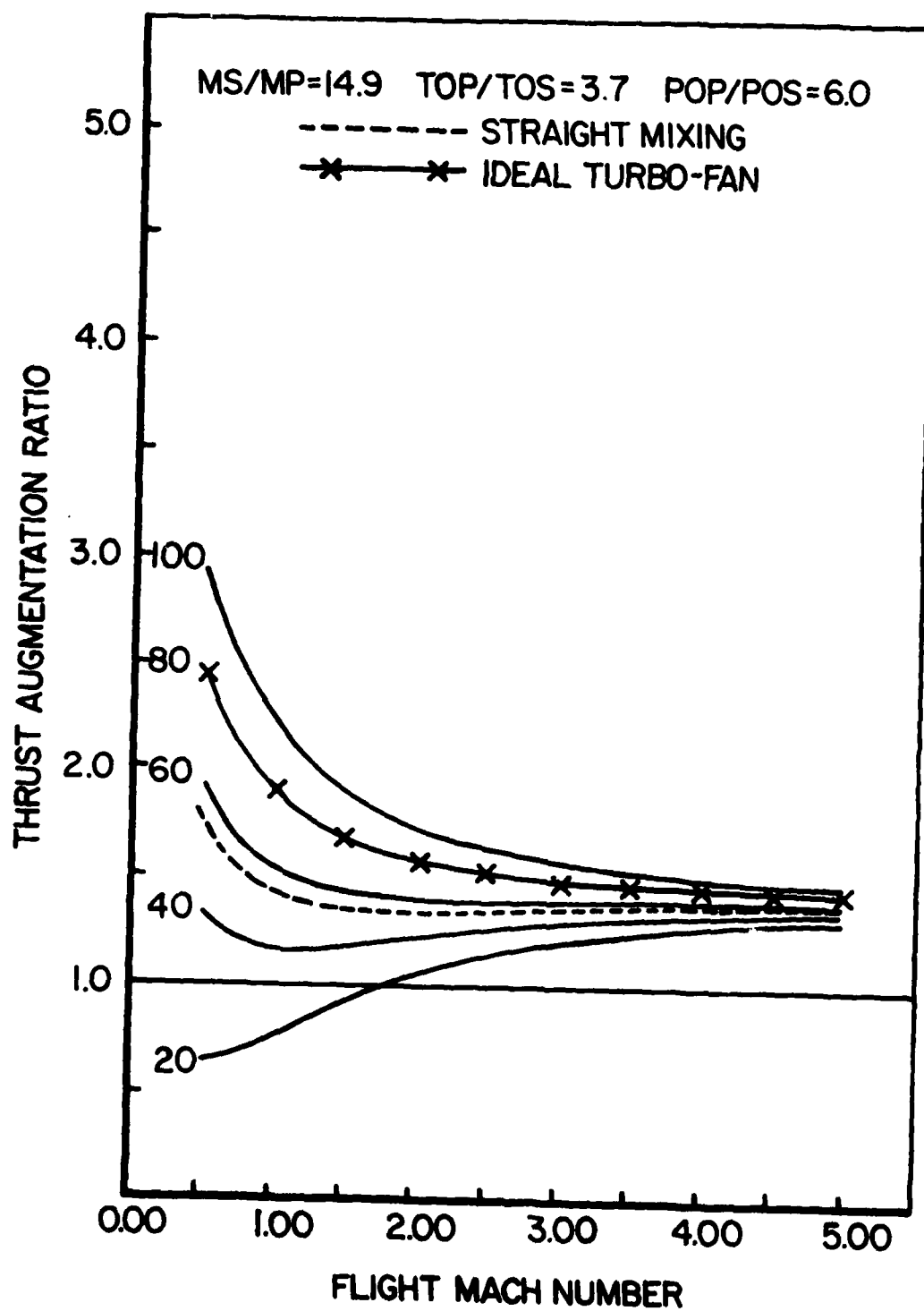


Figure 16. Thrust Augmentation as a Function of Flight Mach Number for a Bypass Ratio of 14.9. Curve parameter is efficiency.

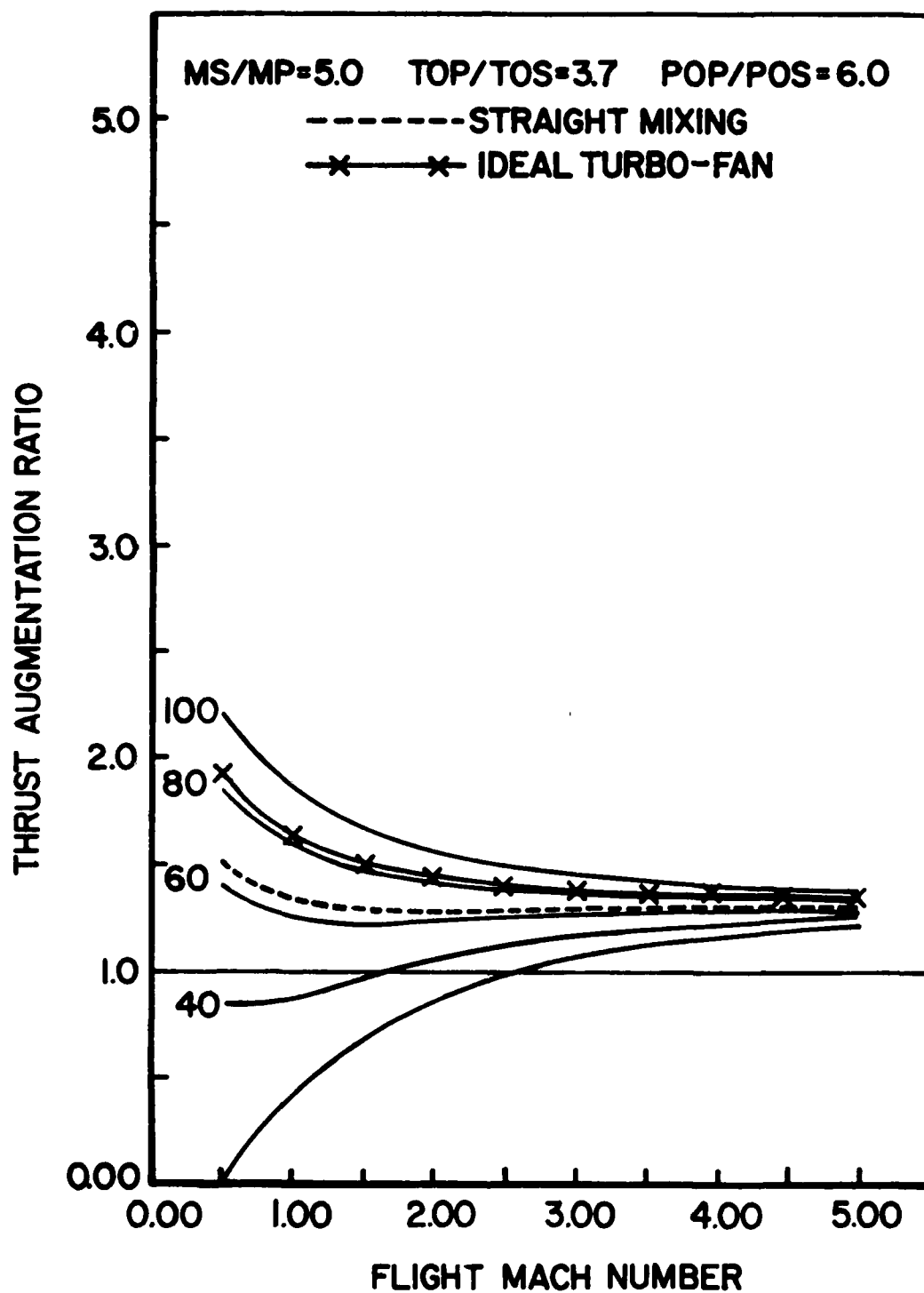


Figure 17. Thrust Augmentation as a Function of Flight Mach Number for a Bypass Ratio of 5.0; Curve Parameter is Efficiency.

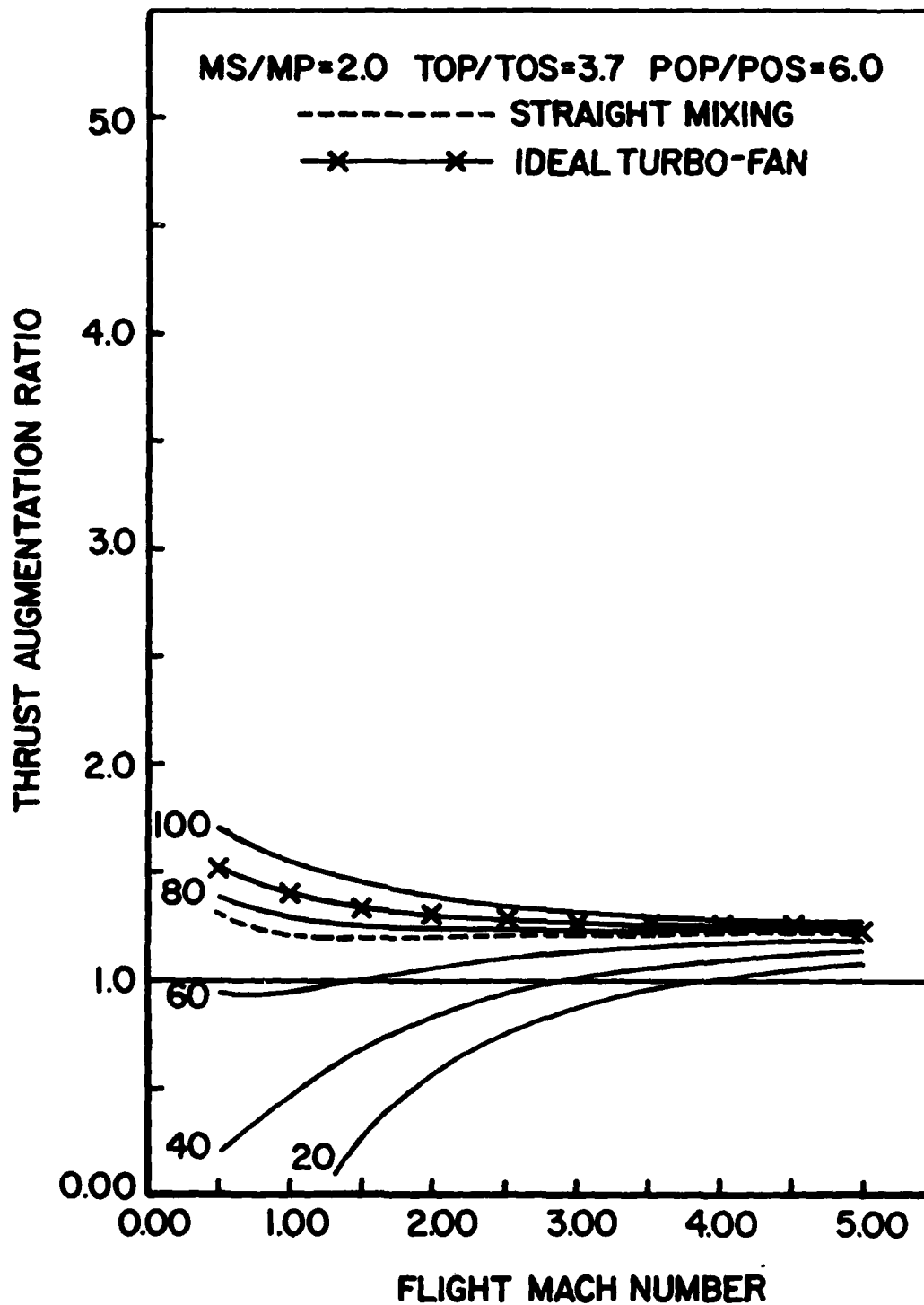


Figure 18. Thrust Augmentation as a Function of Flight Mach Number for a Bypass Ratio of 2.0; Curve Parameter is Efficiency.

As an example, on Figure 19 we have labeled a value of T_{om}/T_{os} that corresponds to a value of $M_s = 0.6$ (or $M_s = 1.52$). The intersection of this particular temperature line and the straight line joining the primary and secondary stagnation conditions gives the state for reversible mixing.

If we drop an isentropic (vertical) line from this stagnation state for reversible mixing we can find the two intersections with the appropriate Fanno line. We have shown these intersections as small circles on the T-s diagram of Figure 19. The intersections represent the static properties of the flow that correspond to the given flow rate and the stagnation conditions of the mixed flow. Of course, the flow on the upper branch is subsonic and that along the lower branch is supersonic.

We have also indicated a pair of points connected by a dashed line which represents a normal shock. These points represent the pair of solutions that can be obtained for the ejector. Isentropic lines connecting these points to the appropriate total temperature gives the stagnation states which correspond to the two solutions.

Additional dissipative mechanisms (such as friction) would move the resulting solutions to the right (increasing the entropy) on the T-s diagram. As is well known, there is a limit to the dissipation that can take place without decreasing the mass flow. At this limit point, the mixed flow Mach number is one. The intersection of the isentropic line drawn from the limit point to the appropriate total temperature gives the minimum value of the total pressure that is consistent with the exit area and the mixed flow mass-flow rate.

The value of this minimum total pressure can be found in a straightforward manner. The value of the mass velocity can be written in terms of Mach number and stagnation conditions:

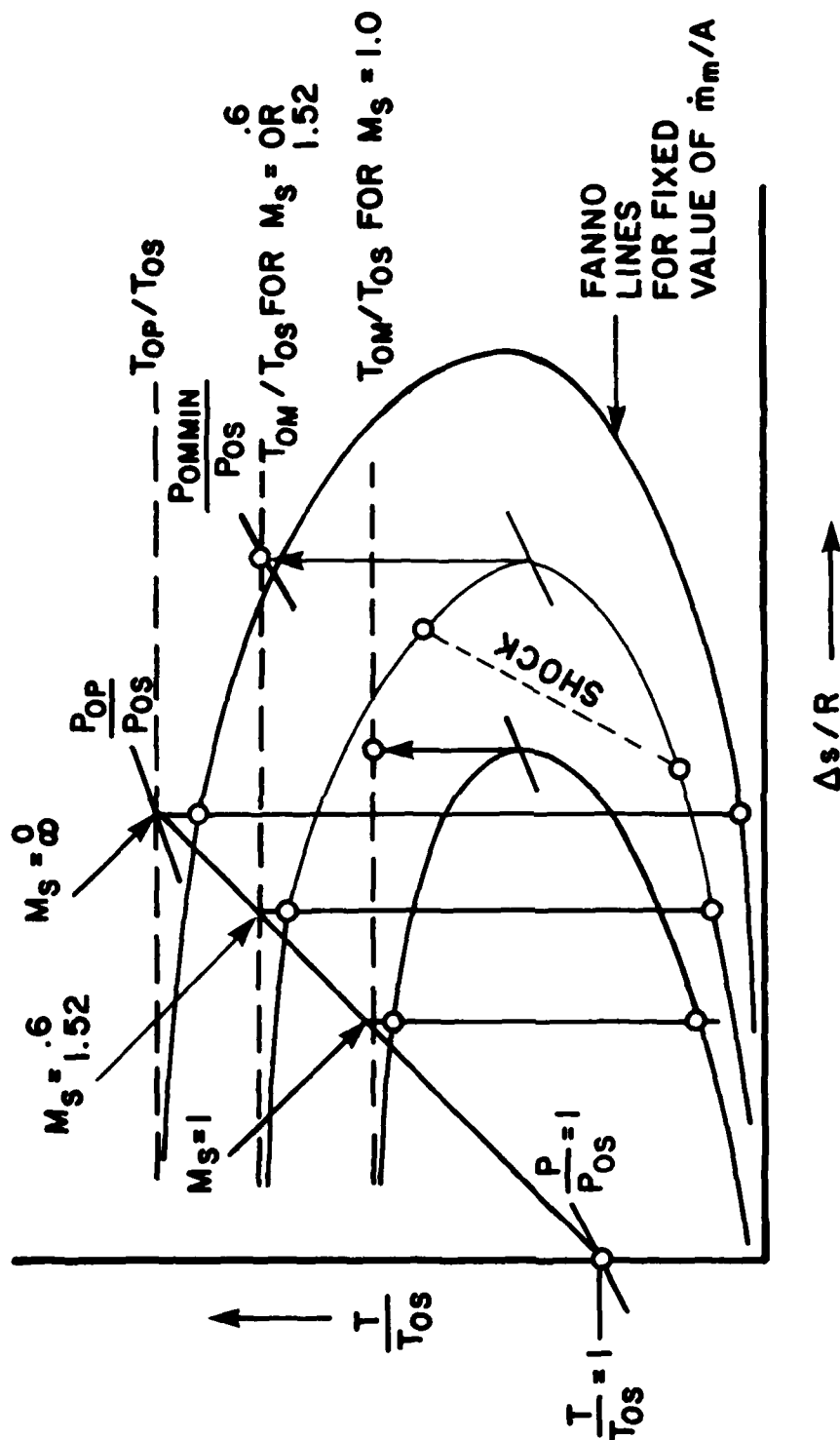


Figure 19. Fanno Lines for the Mixed Flow on a T-s Diagram. Reversible Mixing Would Occur on the Straight Line Joining the Primary and Secondary Total Condition.

$$G = \sqrt{\frac{\gamma}{R}} \frac{P_o}{\sqrt{T_o}} \frac{M}{\left(1 + \frac{\gamma-1}{2} M^2\right)^{\frac{\gamma+1}{2(\gamma-1)}}} \quad (38)$$

Thus, for the mixed flow at the point where the Mach number is one:

$$G_m = \frac{P_{om_{min}}}{\sqrt{T_{om}}} \sqrt{\frac{\gamma}{R}} \left(\frac{2}{\gamma+1}\right)^{\frac{\gamma+1}{2(\gamma-1)}} \quad (39)$$

or

$$G = f(\gamma, R) \cdot \frac{P_{om_{min}}}{\sqrt{T_{om}}} \quad (40)$$

Now

$$f(\gamma, R) \cdot \frac{P_{om_{min}}}{\sqrt{T_{om}}} = \frac{\dot{m}_m}{A} \cdot \frac{A_p^*}{\dot{m}_p} \cdot \frac{\dot{m}_p}{A_p^*} = \frac{\dot{m}_m}{\dot{m}_p} \cdot \frac{A_p^*}{A} \cdot G_p \quad (41)$$

We have assumed the P_{op} is high enough that the primary nozzle flows full. Therefore, an equation similar to Equation (40) is also valid for the primary flow when the Mach number is one at the nozzle throat. Using this condition we can easily obtain:

$$\frac{P_{om_{min}}}{P_{os}} = \frac{\dot{m}_m}{\dot{m}_p} \cdot \frac{A_p^*}{A} \cdot \frac{P_{op}}{P_{os}} \frac{\sqrt{T_{om}/T_{os}}}{\sqrt{T_{op}/T_{os}}} \quad (42)$$

In view of the energy equation

$$\frac{P_{om_{min}}}{P_{os}} = \frac{\dot{m}_m}{\dot{m}_p} \frac{A_p}{A} \frac{P_{op}}{P_{os}} \sqrt{\frac{\dot{m}_p}{\dot{m}_m} + \left(1 - \frac{\dot{m}_p}{\dot{m}_m}\right) \frac{T_{os}}{T_{op}}} \quad (43)$$

Thus, the minimum pressure can be determined immediately from the geometry and the stagnation conditions once the mass flow ratio is given. If the dissipative processes required a lower pressure than the value given by Equation (43) the flow would choke and the mass flow ratio would be reduced. For the case of a constant area ejector the inlet Mach number of the secondary flow would be reduced.

Figure 20 shows the results of calculations for a constant geometry ejector. The conditions are shown on Figure 20 for which the curve was constructed. We show the total pressure resulting from reversible mixing, Equation (12), constant kinetic energy, Equation (15), straight mixing, Equation (21) and the minimum possible total pressure Equations (43) for the indicated secondary Mach number.

We have also shown results from our computer program for constant area ejectors with friction. We have shown both solutions for two values of $f(L/D)$: 0 and 0.1.

The significance of the minimum pressure curve is apparent for the value of $f(L/D) = 0.1$: both branches terminate on this limit curve where the mixed flow is Mach one. The same is true for each of the other supersonic branches that terminate on the minimum pressure curve: the subsonic branch also terminates at the same point. Each value of M_s represents one Fanno line for the mixed flow. Thus, if a value of P_{om} greater than $P_{om_{min}}$ is achieved at some value of M_s we could increase the length of the mixing tube, thereby causing the value of $f(L/D)$ to increase, until the minimum pressure is reached, at which point the flow

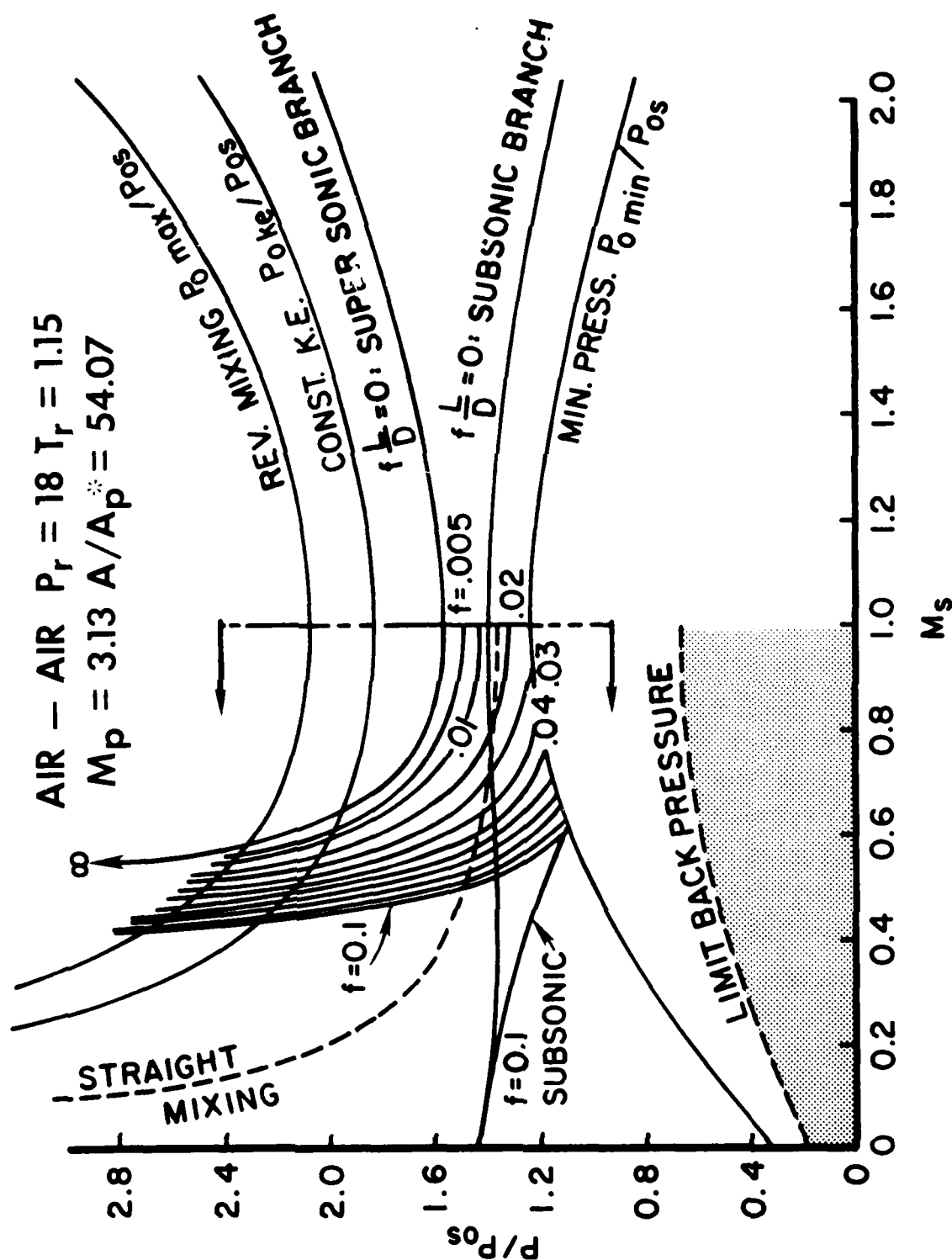


Figure 20. Composite Curve Showing Various Limit Lines and Ejector Curves for Various Values of Friction.

would be choked. On the other hand, if we could reduce the length and still have the flow completely mixed we could increase the total pressure. This increase would terminate on one of the two branches for which $f(L/D) = 0$.

If the mixed flow is subsonic the operating point is uniquely determined by the back pressure for the appropriate $f(L/D)$.

Referring again to Figure 19 we can determine a value of the back pressure for which the flow must be supersonic. Since the Fanno line represents the locus of all possible static states that are consistent with the area and M_g (or mass flow ratio) we can determine the minimum static pressure that is consistent with subsonic flow at the point where the Mach number approaches one. This limiting back pressure is also indicated on Figure 20. If the back pressure is below this curve in the shaded region the exit flow must be supersonic. Since we are concerned at this time only with a configuration like Figure 1 the inlet secondary Mach number must be equal to or less than one.

Clearly, in an experiment we could set the back pressure low enough to insure supersonic operation. However, as stated earlier, this boundary condition can not by itself enable us to determine the operating point since the mixed flow is supersonic and the exit pressure does not have to match the back pressure. Of course in a flying ejector we would want to adjust the flow through a suitably designed diffuser or nozzle in order to match the back pressure since this would optimize the thrust.

However, no matter how well we design the exit diffuser or nozzle we can not improve the performance of the ejector: we can in fact only lower the value of the exit total pressure. The operating point on the supersonic branch is not determined by either the back pressure or the exit diffuser (or nozzle design). It is in fact uniquely determined by the inlet conditions as discussed in the next section.

SECTION 6

DETERMINATION OF THE SUPERSONIC OPERATING POINT

Fabri and Siestrunk³ in 1958 presented the results of an extensive study of air-to-air ejectors with high pressure ratios in which the primary air flow is supersonic. Although they were primarily concerned with jet pumps they presented a theory that was in good agreement with their experimental results for the predicted rates of induced mass flows if the mixing tube is long enough and the geometric configuration of the set up is similar to the theoretical one. Thus, even though our application is vastly different we can use their approach to determine the operating point on the supersonic branch.

For the case of supersonic mixed flows and a supersonic primary flow Fabri and Siestrunk³ state that the inlet flow pattern is similar to that shown on Figure 21. This flow pattern represents the case where the inlet pressure in the primary flow exceeds the inlet pressure of the secondary flow. Therefore, the primary flow must undergo an additional expansion in the entrance region of the mixing tube. The case where the two inlet pressures match is a limiting case and therefore can be determined from this analysis. Since the expansion takes place very quickly in the entrance region the flows will remain unmixed and the slip line between the the primary and secondary flow is shown as a double line emanating from the primary nozzle. (The double line was originally drawn by Fabri and Siestrunk³ to account for the wake effect due to the wall thickness of the primary nozzle which they could not neglect since they were working with very small ejectors. We will neglect the effect in our analysis since it can be accounted for in a simple adjustment of the area ratio.)

If one considers the case where the primary inlet pressure is less than the secondary inlet pressure, there would be a shock in the primary fluid immediately at the entrance that increases the pressure in the primary fluid. This requires the slip line at

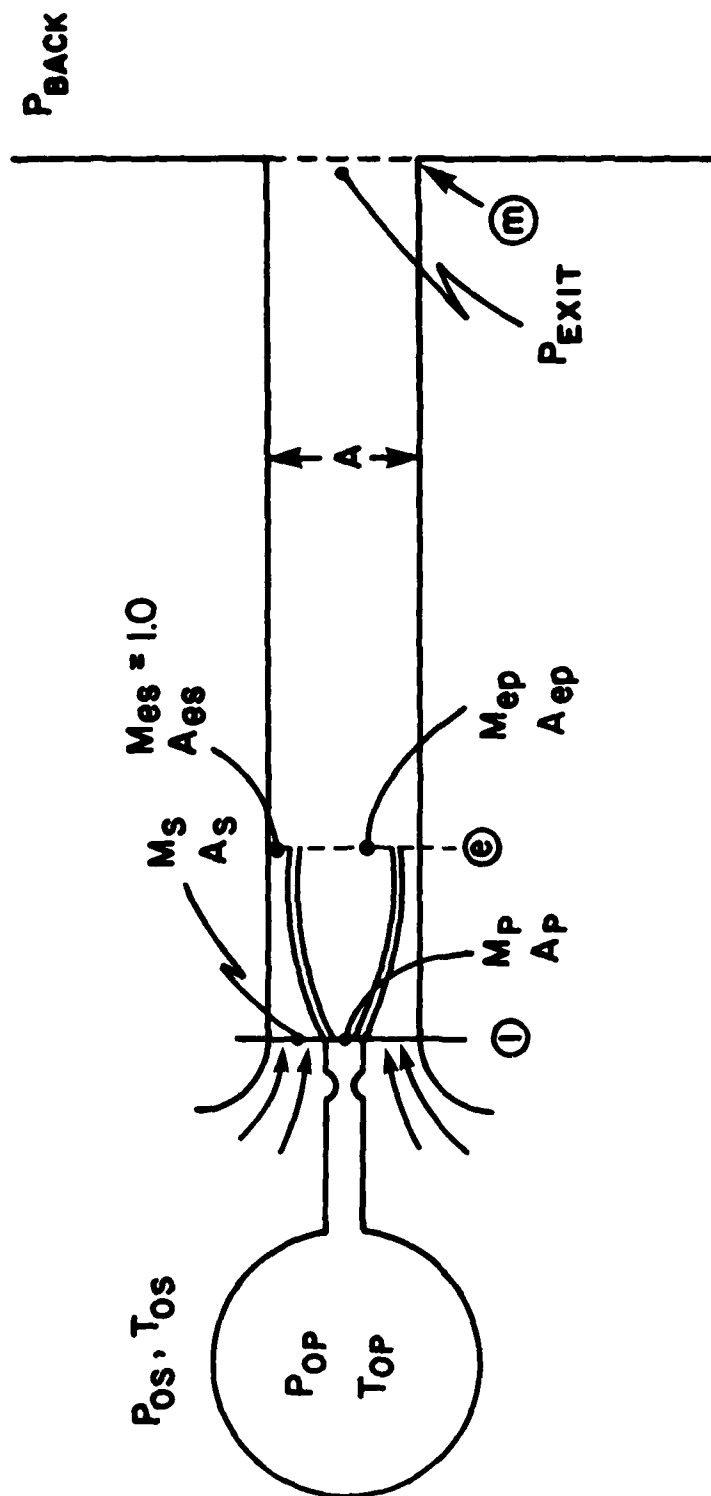


Figure 21. Inlet Flow Pattern for an Ejector Operating with a Supersonic Mixed Flow and Having a Supersonic Primary Flow and a Subsonic Secondary Flow.

the nozzle lip to turn inward. Thus, the secondary flow sees a minimum area at the inlet and the inlet secondary Mach number will be Mach one for the supersonic mixed flow case because of the flow pressure in the mixing tube required for the supersonic branch. (If this were not the case the pressure in the secondary flow would increase after the flow entered the mixing tube and this requires a still further shock compression in the primary flow which eventually would lead to a breakdown of the supersonic flow in the primary jet. This breakdown would lead to a subsonic mixed flow.) The case where the pressures are equal is again a limiting case. But the inlet Mach number is always one, including the limiting case.

These arguments do not hold if a throat is placed in the secondary stream ahead of the inlet since the secondary flow could then be supersonic when the pressures were matched at the inlet.

The continuity and momentum equations can be written for the control volume shown on Figure 21. The supersonic primary flow expands and the Mach number increases to station e. The subsonic secondary flow also undergoes an expansion and the Mach number increases until it reaches Mach one at the station e; in fact, this is the criteria by which we select the station e. The method of characteristics would be required to study the supersonic primary flow. However, the good agreement with experiment obtained by Fabri and Siestrunk shows that it is adequate to treat both flows by simple one-dimensional isentropic equations.

Since the secondary Mach number is one at station e we can write for the constant area channel.

$$\frac{A_{p_e} + A_s^*}{A_p^*} = \frac{A}{A_p^*} \quad (44)$$

or

$$\frac{A_{pe}}{A_p^*} = \frac{A}{A_p^*} - \frac{A_s}{A_p^*} \cdot \frac{A_s^*}{A_s} \quad (45)$$

Using the well known isentropic flow equations for the area ratios we have

$$\frac{1}{M_{ep}^*} \left(\frac{\gamma+1}{2} - \frac{\gamma-1}{2} M_{ep}^{*2} \right)^{-\frac{1}{\gamma-1}} = \frac{A}{A_p^*} - \frac{A_s}{A_p^*} M_s^* \left(\frac{\gamma+1}{2} - \frac{\gamma-1}{2} M_s^{*2} \right)^{\frac{1}{\gamma-1}} \quad (46)$$

The isentropic relationships for the pressures can also be used.

$$P_{ep} = P_{op} \left(1 - \frac{\gamma-1}{\gamma+1} M_{ep}^{*2} \right)^{\frac{\gamma}{\gamma-1}} \quad (47)$$

and since $M_{es}^* = 1$

$$P_{es} = P_{os} \left(\frac{2}{\gamma+1} \right)^{\frac{\gamma}{\gamma-1}} \quad (48)$$

using the momentum equation along with the isentropic relations and the fact that $M_{es}^* = 1$ enables one to derive the following equation.

$$\frac{1 + M_{ep}^{*2}}{M_{ep}^*} = \frac{1 + M_p^{*2}}{M_p^*} + \frac{A_s}{A_p^*} \frac{P_{os}}{P_{op}} \left(\frac{\gamma+1}{2} - \frac{\gamma-1}{2} M_s^{*2} \right)^{\frac{1}{\gamma-1}} \left(1 - M_s^* \right)^2 \quad (49)$$

A computer program was written to solve these equations for a given geometry which fixes M_p^* . The continuity equation, Equation (46), was solved for M_{ep} for given choice of M_s^* . These values were then used in Equation (49) to determine the value of P_{os}/P_{op} that was consistent with the choice of M_s^* . In this way the curve shown on Figure 22 was constructed for the geometric values (including M_p) shown on Figure 22.

In Figure 22 we show the total pressure required to achieve the value of M_s^* . Since the geometry is fixed the value, of the mass flow ratio is determined by M_s^* and we can use the mass flow ratio and the values of P_{op}/P_{os} to determine the various limit lines that we have previously discussed. These are also shown on Figure 22. Finally, we have also shown the total pressure achieved by the mixed flow on the supersonic branch.

When $M_s^* = 1$, it is clear from Equation (46) that $M_{ep}^* = M_p^*$ since the right side of Equation (46) is simply A_p/A_p^* (note $A_p = A - A_s$).

If we solve Equation (49) for P_{op}/P_{os} for the conditions where $M_s^* = 1$ and $M_{pe}^* = M_p^*$, we obtain the indeterminate form of zero over zero. However, using L'Hospital's rule, we can show that the value of P_{op}/P_{os} is related to M_p^* :

$$\frac{P_{op}}{P_{os}} = \left(\frac{\gamma+1}{2} - \frac{\gamma-1}{2} M_p^{*2} \right)^{-\frac{\gamma}{\gamma-1}} \quad (50)$$

Since $M_s^* = 1$ when equation (50) is valid, it can be shown, using the isentropic relations for pressure, that $P_{lp} = P_{ls}$ at this condition also. This is indicated on Figure 22. Fabri and Siestrunck refer to this condition as saturated flow.

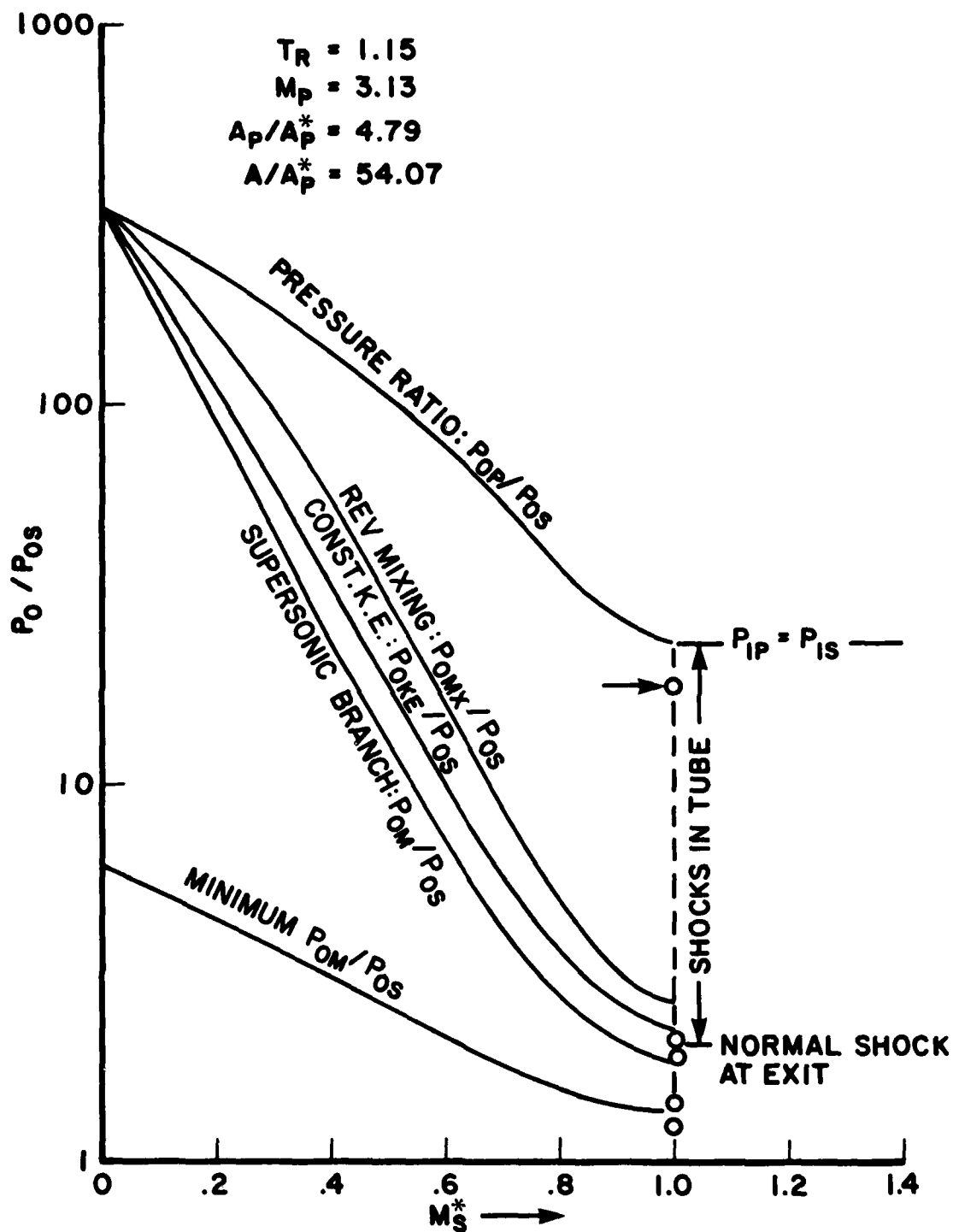


Figure 22. Pressure Ratio Required to Achieve a Given Value of M_s^* Along with Limit Lines and the Supersonic Branch Solution.

Dr. Morton Alperin has pointed out⁸ that there may also be a point where M_s^* is less than 1 and $P_{1p} = P_{1s}$. The value of M_s^* at which this occurs depends upon M_p^* and the geometry.

For still lower values of the pressure ratio, the inlet static pressure of the primary flow is lower than the static pressure in the secondary flow. Thus, the primary fluid experiences shocks within the mixing tube as indicated on Figure 22. Finally, we reach the point where a normal shock stands in the exit of the primary nozzle and for lower pressures we would have subsonic primary exit flow into the mixing tube.

It is of value to consider the following thought experiment. If we assumed that we have value of $P_{op}/P_{os} = 100$ for the ejector of Figure 22, we see that $M_s^* = 0.55$. With this value of P_{op}/P_{os} , suppose that we set the value of the back pressure such that the value of M_s^* is 0.1 and the mixed flow is subsonic. As we lower the back pressure, the value of M_s^* increases toward 0.55. (For an example of how back pressure affects M_s^* , see Figure 9.) When we reach $M_s^* = 0.55$, a further reduction in back pressure would require a higher value of M_s^* and consequently, a higher value of \dot{m}_s/\dot{m}_p . The experimental work of Fabri and Siestrunk³ show definitely that this will not happen. Rather, the flow will make a transition to the supersonic branch, and from then on it will be independent of the back pressure. Thus, we can determine the value of the transition back pressure from the subsonic branch by evaluating the back pressure at the same value of M_s^* at which the supersonic branch will operate.

We can use the kinds of information shown on Figure 22 to construct a graph like that shown on Figure 23. We have chosen various area ratios and plotted the efficiency versus the mass flow ratio achieved for values of other parameters shown on the figure. Each curve terminates at the point where the value of M_s^* first reaches Mach one. The points are indicated by the hack marks on Figure 23 along each area ratio curve. Now it is clear from Figure 23 that the maximum efficiency is achieved for a given mass flow ratio with the smallest diameter tube operating at a value of $M_s^* = 1$.

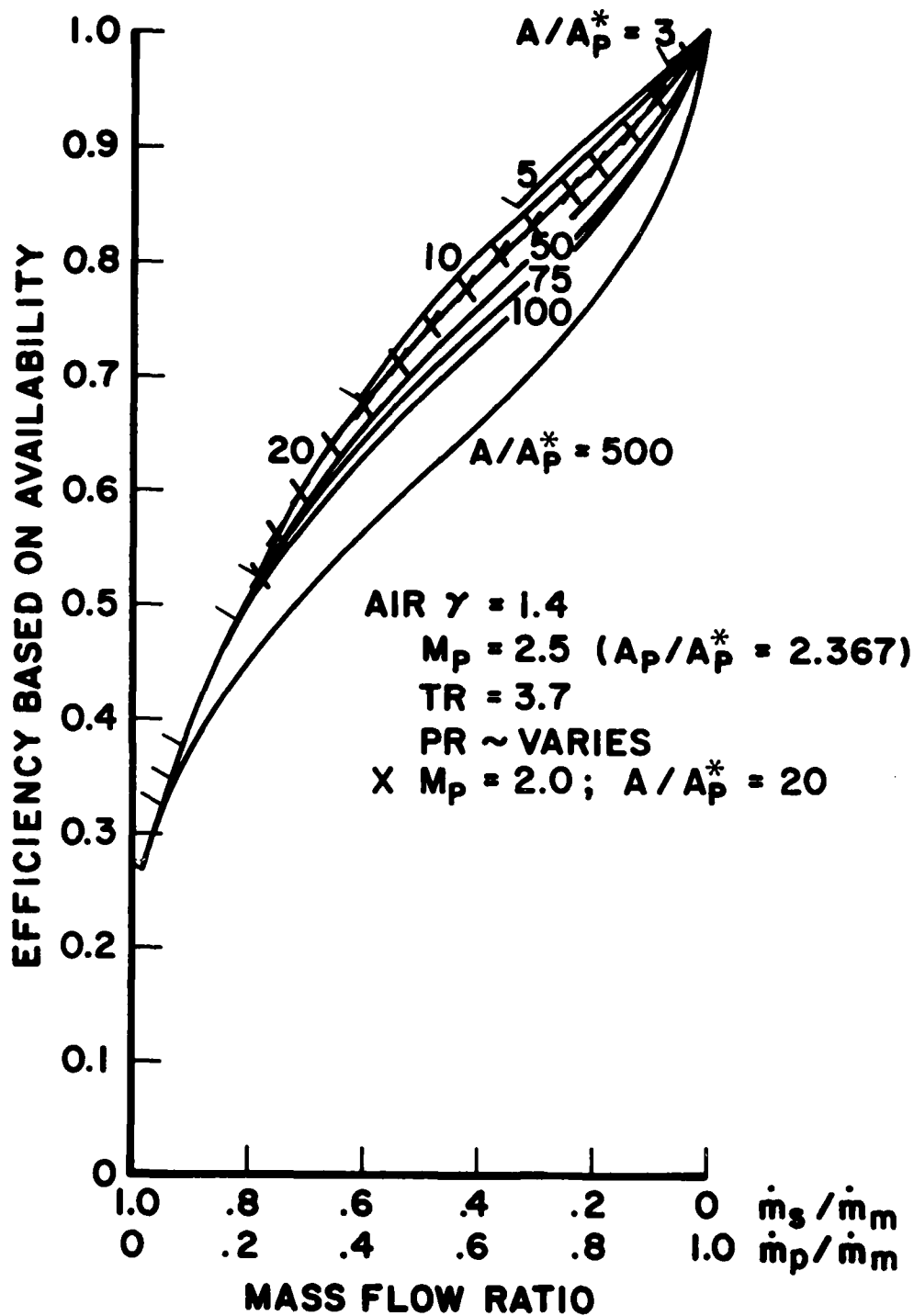


Figure 23. Efficiency Versus Mass Flow Ratio for Different Geometry Mixing Tubes.

SECTION 7
SUMMARY AND RECOMMENDATION

The results of our study have shown:

- 1) The supersonic branch can be achieved at subsonic, secondary inlet Mach numbers.
- 2) The extremely high values of efficiency obtained on both solution branches can be explained by the observation that the constant area geometry is a sufficient condition but not a necessary condition for deriving the set of equations used for analyzing an ejector.
- 3) Since the constant area condition is not a necessary condition, it explains why some of the solutions obtained with the equations could not be achieved in an ejector.
- 4) Since the constant area condition is a sufficient condition for deriving the set of equations, all of the physically possible operating points (which conform to the assumptions) for an ejector will be included in the set of solutions.
- 5) The Fabri and Siestrunk³ inlet condition uniquely determines the single operating point for a given ejector that can be obtained on the supersonic branch with $M_s \leq 1$.
- 6) The back pressure at which the supersonic solution is acquired can also be determined.
- 7) Operation at values of $M_s \geq 1$ can be forced by the presence of a throat in the secondary flow before the inlet.
- 8) The optimum efficiency for a given mass flow ratio occurs when $M_s = 1$ and the mixing tube has the smallest area consistent with the mass flow requirements.
- 9) Limit lines were established for generalized mixers. These limit lines include:
 - Reversible mixing;
 - Constant kinetic energy;

Simple mixing;
Minimum total pressure.

10) Methods were shown for constructing T-s diagrams which show the limit lines and the stagnation states required for thrust augmentation at given flight Mach numbers.

11) Generalized thrust augmentation curves were constructed using the efficiency, based on availability, as a parameter.

12) The analysis presented will enable the complete determination of performance of an ejector when used for thrust augmentation. Thus, we are now in a position to determine realistic estimates of the upper performance limits of ejectors for thrust augmentation over a wide range of flight conditions.

We therefore make the following recommendations for future work:

1) The current ejector investigation be extended toward establishing a theory and analysis of the upper bound of ejector performance obtainable with the "second solution." Obtain upper limits of ejector thrust augmentation characteristics over various flight, altitude regimes and bypass ratios, and compare them with turbofan engine performance characteristics.

2) Based on the analytical results achieved in 1), we would:

a) Conduct theoretical studies of new methods of achieving high performance ejector devices that are characterized by compactness, light weight, and high efficiency; and

b) Outline the methods to be used in an experimental verification of the theory that would define the fundamental limitations of constant area ejectors operating with supersonic mixed flow.

REFERENCES

1. J. L. Porter, R. A. Squyers, A Summary/Overview of Ejector Augmentor Theory and Performance, USAF Technical Report No. R-91100-9CR-47, April 1981, Volumes I and II.
2. E. D. Kennedy, "The Ejector Flow Process," Master of Science Thesis, University of Minnesota, Minneapolis, Minn., 1955.
3. J. Fabri and R. Siestrunk, "Supersonic Air Ejectors," Advances in Applied Mechanics, Vol. 5, Academic Press, Inc., New York, NY, 1958.
4. H. J. Hoge, On the Theory of Mixing of Fluid Streams, Quartermaster Research and Engineering Center, Pioneering Research Division, Technical Report PR-2, February 1959.
5. B. Kiselev, Calculation on One-Dimensional Gas Flows, USAF Technical Report NO. F-TS-1209-1A, January 1949, (translated from the Russian by Brown University).
6. M. Alperin and J. Wu, High Speed Ejectors, AFFDL-TR-79-3048, May 1979.
7. J. E. Minardi, et al., Rankine Cycle Augmented Light Gas Turbine, UDR-TR-80-53, May 1980.
8. M. Alperin, personal communication, 1982.

APPENDIX A
COMPRESSIBLE FLOW EJECTOR ANALYSES FROM REFERENCE 7

COMPRESSIBLE FLOW EJECTOR ANALYSES

In this section we present a compressible flow analysis of an ejector for both constant area and constant pressure. Both problems can be solved in closed form if the fluids are assumed to be ideal gases. However, the solutions are somewhat complex and, therefore, computer programs were developed to obtain solutions over a wide range of parameters for a number of combinations of fluids.

We will first present the constant area analysis, then the constant pressure analysis, and finally some results from the computer runs.

Constant Area Analysis

A schematic of a constant area ejector is shown on Figure A-1. Also shown is the control volume used in the analysis.

At station 1 the flows are completely unmixed and each flow is assumed to be uniform and parallel. Station 1 is located at the exit plane of the primary nozzle. The exit area of the nozzle is A_p and the area occupied by the secondary flow at station 1 is A_s . The exit area, A , at station 2 is the sum of the areas:

$$A = A_p + A_s \quad (A-1)$$

Station 2 is assumed to be located far enough downstream from station 1 so that complete mixing has taken place and the flow is uniform and parallel.

For the control volume shown we can write the continuity, momentum, and energy solutions:

$$\dot{m}_p + \dot{m}_s = \dot{m}_m \quad (A-2)$$

$$P_m A - P_{1p} A_p - P_{1s} A_s + 2\pi r l \tau = \dot{m}_p (V_p - V_m) + \dot{m}_s (V_s - V_m) \quad (A-3)$$

$$\dot{m}_p h_{op} + \dot{m}_s h_{os} = \dot{m}_m \left(h_m + \frac{V_m^2}{2} \right) \quad (A-4)$$

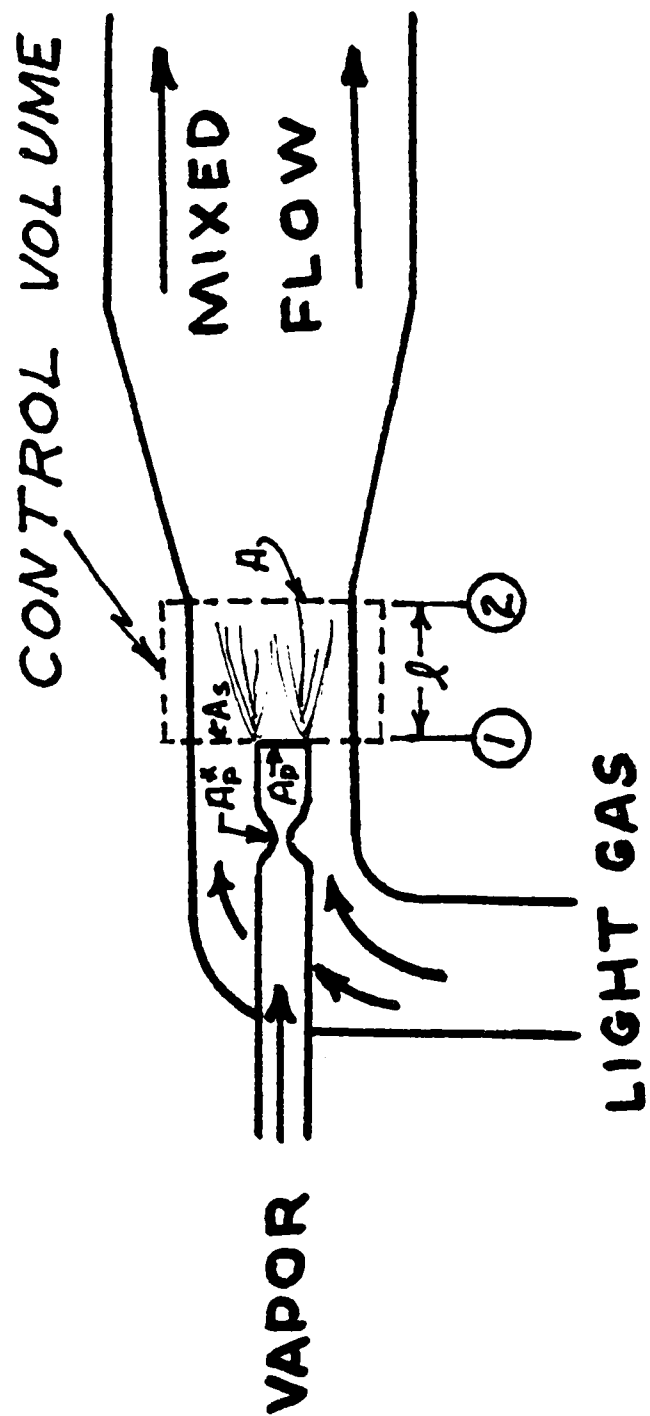


Figure A-1. Constant Area Ejector.

In Equations (A-2) to (A-4) \dot{m} is the mass flow rate and the subscript designates the primary flow at station 1, s designates the secondary flow at station 1, and m the mixed flow at station 2.

In the momentum equation, P is the pressure and V the velocity; r is the radius of the tube at station 2 and ℓ is the distance between station 1 and 2. The pressure P_{1p} does not have to be equal to P_{1s} since the primary nozzle will be a supersonic nozzle in the applications of interest.

In the energy equation h_{op} and h_{os} are the stagnation enthalpies of the primary and secondary flows, respectively, and h_m is the static enthalpy of the mixed flow.

The mass flow rates of both the primary and secondary flows can be adjusted at will by controlling the stagnation conditions. Thus, in view of (A-2), all mass flow rates are known.

Of course the uniform flow assumption allows us to write:

$$\rho_{1p} A_p V_p = \dot{m}_p \quad (A-5)$$

$$\rho_{1s} A_s V_s = \dot{m}_s \quad (A-6)$$

$$\rho_m A V_m = \dot{m}_m \quad (A-7)$$

Hence, from the known geometry of the nozzle and ejector we can obtain V_p and V_s if we assume an isentropic expansion from the known stagnation conditions for the flow in the primary nozzle and for the secondary fluid.

Consequently, the only unknowns in equations (A-3), (A-4), and (A-7) are P_m , h_m , ρ_m and V_m . However, we also know an equation of state:

$$P_m = f(h_m, \rho_m) \quad (A-8)$$

If conditions are such that condensation of the primary vapor occurs in the ejector, an iterative procedure would be required to obtain a solution since Equation (A-8) would not be simple. However, for many cases of interest, it will be

satisfactory to assume ideal gas behavior between station 1 and 2 for both the vapor and the secondary gas. (It is not required that the primary gas expand as an ideal gas in the nozzle).

In the remainder of this section we will assume that the gases are ideal gases with constant specific heats. Thus, we can write:

$$h = C_p T \quad (A-9)$$

and

$$P = \rho RT \quad (A-10)$$

where C_p is the specific heat at constant pressure and R is the gas constant for the particular gas. For the mixed flow at station 2 we have:

$$h_m = C_{p_m} T_m \quad (A-11)$$

$$P_m = \rho_m R_m T_m \quad (A-12)$$

Combining (A-12) and (A-7) yields

$$P_m = \frac{\dot{m}_m R_m}{AV_m} T_m \quad (A-13)$$

(note that Equations (A-13) and (A-11) could be combined to form an equation in the form of Equation (A-8) is desired).

We can obtain the following two equations from the momentum and energy equations:

$$\begin{aligned} \frac{\dot{m}_m R_m}{AV_m} T_m A - (P_{1p} A_p + P_{1s} A_s - 2\pi r l \tau) = \\ \dot{m}_p (V_p - V_m) + \dot{m}_s (V_s - V_m) \end{aligned} \quad (A-14)$$

$$\dot{m}_p h_{op} + \dot{m}_s h_{os} = \dot{m}_m (C_p T_m + \frac{V_m^2}{2}) \quad (A-15)$$

Now R_m can be determined from the following simple mixing formula for an ideal gas.

$$\dot{m}_m R_m = \dot{m}_p R_p + \dot{m}_s R_s \quad (A-16)$$

Thus, (A-14), (A-15), and (A-16) can be combined to obtain a closed form solution to V_m , T_m and R_m . From Equation (A-14)

$$T_m = \frac{1}{\dot{m}_m R_m} [(P_{1p} A_p + P_{1s} A_s - 2\pi r l \tau) V_m + \dot{m}_p (V_p - V_m) V_m + \dot{m}_s (V_s - V_m) V_m] \quad (A-17)$$

while from Equation (A-15) and (A-9) we have

$$T_m = \frac{C_{pp} \dot{m}_p}{C_{pm} \dot{m}_m} T_{op} + \frac{C_{ps} \dot{m}_s}{C_{pm} \dot{m}_m} T_{os} - \frac{V_m^2}{2C_{pm}} \quad (A-18)$$

Substituting for T_m in Equation (A-17) from Equation (A-18) and dividing by T_{1s} yields

$$\left[\frac{C_{pp} \dot{m}_p}{C_{pm} \dot{m}_m} \frac{T_{op}}{T_{os}} \cdot \frac{T_{os}}{T_{1s}} + \frac{C_{ps} \dot{m}_s}{C_{pm} \dot{m}_m} \right] \frac{T_{os}}{T_{1s}} - \frac{V_m^2}{2C_{pm} T_{os}} \frac{T_{os}}{T_{1s}} =$$

$$\left[\left(\frac{P_{1p}}{P_{os}} \right) \left(\frac{P_{os}}{P_{1s}} \right) \frac{A_p}{A} + \frac{A_s}{A} - \frac{2\tau l}{P_{1s} r} \right] \frac{AP_{1s}}{\dot{m}_m R_m T_{1s}} V_m$$

$$+ \frac{\dot{m}_p V_p}{\dot{m}_m R_m T_{1s}} V_m + \frac{\dot{m}_s V_s}{\dot{m}_m R_m T_{1s}} V_m - \frac{\dot{m}_p + \dot{m}_s}{\dot{m}_m R_m} \frac{V_m^2}{T_{1s}} \quad (A-19)$$

Equation (A-19) is a quadratic equation in V_m and can, therefore, be solved since all the quantities in the equation are known once the geometry and stagnation conditions are known.

Of course, a suitable estimate of the shear stress, τ , needs to be available. However, for our first estimates we have assumed that $\tau = 0$ (Equation A-19).

The formulas of Table A-1 are helpful in obtaining a solution to Equation (A-19). In Table A-1, W is the molecular weight of the fluid.

With the exception of the fluid gas constant, \bar{R} , in equation T6 of Table A-1, all of the quantities with a bar over them are ratios of the primary flow value to the secondary flow value. If we cast each of the terms (excluding V_m) in Equation (A-19) in terms of these ratios, we obtain the following set of terms which we designate with C's:

$$C1 = \frac{\bar{\Gamma}_m \bar{T}_o + W}{\bar{\Gamma}_m + \bar{W}} \left(1 + \frac{\gamma_s - 1}{2} M_s^2 \right) \quad (A-20)$$

$$C2 = \frac{\bar{W}(\bar{m} + 1)}{\bar{\Gamma}_m + \bar{W}} \frac{\gamma_s - 1}{2} M_s^2 \quad (A-21)$$

$$C3 = \left(\bar{P}_1 \bar{A} + 1 - \frac{2\tau\ell}{\bar{P}_1 s r} (1 + \bar{A}) \right) \frac{\bar{W}}{\bar{m} + \bar{W}} \quad (A-22)$$

$$C4 = \frac{\bar{m} \bar{W} \bar{V}}{\bar{m} + \bar{W}} \gamma_s M_s^2 \quad (A-23)$$

$$C5 = \frac{\bar{W}}{\bar{m} + \bar{W}} \gamma_s M_s^2 \quad (A-24)$$

$$C6 = \frac{\bar{W}(\bar{m} + 1)}{\bar{W} + \bar{m}} \gamma_s M_s^2 \quad (A-25)$$

Setting the ratio $V_m/V_{1s} \equiv \bar{V}_m$, we can write Equation (A-19) in terms of the C's as:

$$(C2 + C6) \bar{V}_m^2 + (C3 + C4 + C5) \bar{V}_m - C1 = 0 \quad (A-26)$$

TABLE A-1
USEFUL OTHER EQUATIONS FOR AN IDEAL GAS

ISENTROPIC FLOW

$$\frac{T_o}{T} = 1 + \frac{\gamma - 1}{2} M^2 \quad (A-T1)$$

$$\frac{P_o}{P} = \left(1 + \frac{\gamma - 1}{2} M^2\right)^{\frac{\gamma}{\gamma - 1}} \quad (A-T2)$$

$$\frac{\rho_o}{\rho} = \left(1 + \frac{\gamma - 1}{2} M^2\right)^{\frac{1}{\gamma - 1}} \quad (A-T3)$$

$$\frac{A}{A^*} = \frac{1}{M} \left[\frac{2}{\gamma + 1} \left(1 + \frac{\gamma - 1}{2} M^2\right) \right]^{\frac{\gamma + 1}{2(\gamma - 1)}} \quad (A-T4)$$

$$\frac{T_o}{T} \frac{V^2}{2h_o} = \frac{\gamma - 1}{2} M^2 \quad (A-T5)$$

$$\frac{\dot{m}}{A} = \frac{\gamma W}{R} \frac{P_o}{\sqrt{T_o}} \frac{M}{\left(1 + \frac{\gamma - 1}{2} M^2\right)^{\frac{\gamma + 1}{2(\gamma - 1)}}} \quad (A-T6)$$

MIXING FORMULA

$$C_{p_m} \dot{m}_m = C_{p_p} \dot{m}_p + C_{p_s} \dot{m}_s \quad (A-T7)$$

$$C_{v_m} \dot{m}_m = C_{v_p} \dot{m}_p + C_{v_s} \dot{m}_s \quad (A-T8)$$

$$R_m \dot{m}_m = R_p \dot{m}_p + R_s \dot{m}_s \quad (A-T9)$$

$$\gamma_m = \gamma_p \frac{1 + \frac{W_p}{W_s} \frac{m_s}{m_p} \frac{\gamma_p - 1}{\gamma_p} \cdot \frac{\gamma_s}{\gamma_s - 1}}{1 + \frac{W_p}{W_s} \frac{m_s}{m_p} \cdot \frac{\gamma_p - 1}{\gamma_s - 1}} \quad (A-T10)$$

TABLE A-1 (Concluded)
USEFUL OTHER EQUATIONS FOR AN IDEAL GAS

$$\Gamma \equiv [\gamma_p/(\gamma_p - 1)]/[\gamma_s/(\gamma_s - 1)] \quad (\text{A-T11})$$

$$C_{pp}/C_{ps} = \Gamma/\bar{W}$$

$$C_{pm}/C_{ps} = (\Gamma\bar{m} + \bar{W})/[\bar{W}(\bar{m} + 1)] \quad (\text{A-T12})$$

$$R_m/R_s = (\bar{m} + \bar{W})/[\bar{W}(\bar{m} + 1)] \quad (\text{A-T13})$$

$$C_{pp}\dot{m}_p/C_{pm}\dot{m}_m = \Gamma\bar{m}/(\Gamma\bar{m} + \bar{W}) \quad (\text{A-T14})$$

$$R_p\dot{m}_p/R_m\dot{m}_m = \bar{m}/(\bar{m} + \bar{W}) \quad (\text{A-T15})$$

If we evaluate Equation (A-6) for the secondary flow rate and the primary flow rate, we can show that

$$\frac{\bar{m}}{\bar{A}} = \sqrt{\bar{\gamma} \bar{W}} \left(\frac{P_O}{\sqrt{T_O}} \right) \left(\frac{2}{\gamma_p + 1} \right)^{\frac{\gamma_p + 1}{2(\gamma_p - 1)}} \left(\frac{A_p^*}{A_p} \right) \frac{\left(1 + \frac{\gamma_s - 1}{2} M_s^2 \right)^{\frac{\gamma_s + 1}{2(\gamma_s - 1)}}}{M_s} \quad (A-27)$$

In Equation (A-27) we have assumed the primary nozzle is choked. The value of M_s can be controlled in an experiment by adjusting the back pressure on the ejector at station 2 for a given value of P_{O_s} . Thus, we have used M_s as our independent variable in our computer calculations. A geometry, pair of fluids, and stagnation conditions are chosen and Equation (A-27) is solved for \bar{m} (or we hold \bar{m} fixed and calculate \bar{A}) for various values of M_s . Equations (A-20) through (A-26) can then be solved for each value of M_s . Once V_m is determined, either Equation (A-27) or (A-28) can be used to determine T_m . The density and pressure can be determined by Equations (A-7) and (A-13). Therefore, all of the properties at station 2 are completely determined.

Ejector "Efficiency"

Many definitions of ejector efficiency can be made and found to be useful. Some of them, however, are pseudo efficiencies since they can be greater than one under certain conditions of operation.

For our purposes we have calculated at this time four pseudo efficiencies. Each is briefly discussed below.

The first pseudo efficiency that we have considered is based on the thermodynamic availability, ψ , of the primary vapor and the availability of the mixed gas and vapor leaving the ejector. If we neglect potential energy terms we have, in general, for the availability of a fluid in steady flow:

$$\psi = h_O - h_R - T_R (s - s_R) \quad (A-28)$$

where h_R is the reference enthalpy and s_R is the reference entropy and h_O is the stagnation enthalpy of the fluid (therefore, it

includes kinetic energy) and s is the static entropy of the fluid. Ordinarily, the reference values would be evaluated at atmospheric pressure and temperature; however, for our purposes we will evaluate the reference values at the stagnation temperature and pressure of the secondary gas. This insures us that the secondary gas will have zero availability before mixing and that all the availability results only from the primary flow.

For an ideal gas with constant specific heats, we have:

$$h_O - h_R = C_P (T_O - T_R) \quad (A-29)$$

and since the entropy can be found from the isentropic stagnation conditions, we have:

$$s - s_R = C_P \ln \left(\frac{T_O}{T_R} \right) - R \ln \left(\frac{P_O}{P_R} \right) \quad (A-30)$$

Therefore, we can write for the general case

$$\psi = C_P T_R \left(\frac{T_O}{T_R} - 1 - \ln \left[\frac{T_O}{T_R} \left(\frac{P_R}{P_O} \right)^{\frac{\gamma-1}{\gamma}} \right] \right) \quad (A-31)$$

Evaluating Equation (A-31) for the primary flow and the secondary stagnation conditions for the reference state, we have

$$\psi_P = C_{PP} T_{Os} \left(\frac{T_{Op}}{T_{Os}} - 1 - \ln \left[\frac{T_{Op}}{T_{Os}} \left(\frac{P_{Os}}{P_{Op}} \right)^{\frac{\gamma_p-1}{\gamma_p}} \right] \right) \quad (A-32)$$

and for the mixed gas we have

$$\psi_m = C_{P_m^*} T_{Os} \left(\frac{T_{Om}}{T_{Os}} - 1 - \ln \left[\frac{T_{Om}}{T_{Os}} \left(\frac{P_{Os}}{P_{Om}} \right)^{\frac{\gamma_m-1}{\gamma_m}} \right] \right) \quad (A-33)$$

Thus, the efficiency based on availability, η_{av} , is

$$\eta_{av} = \frac{\dot{m}_m C_{pm}}{\dot{m}_p C_{pp}} \frac{\frac{T_{om}}{T_{os}} - 1 - \ln \left[\frac{T_{om}}{T_{os}} \left(\frac{P_{os}}{P_{om}} \right)^{\frac{\gamma_m - 1}{\gamma_m}} \right]}{\frac{T_{op}}{T_{os}} - 1 - \ln \left[\frac{T_{op}}{T_{os}} \left(\frac{P_{os}}{P_{op}} \right)^{\frac{\gamma_p - 1}{\gamma_p}} \right]} \quad (A-34)$$

Since all the quantities in Equation (A-34) are known from the previous calculations, we can determine η_{av} , and it is a true efficiency for the ejector if primary and secondary gases are the same, but a pseudo efficiency if not, since we neglected the availability due to dissimilar gases.

In the other pseudo efficiencies that we have looked at, we divide the enthalpy change of the mixed flow for an isentropic expansion from the stagnation conditions of the mixed flow to the secondary stagnation pressure, P_{os} , by three different changes in enthalpy of the primary.

In the first case, we use the change in the enthalpy of the primary for an isentropic expansion from the primary stagnation conditions to the secondary stagnation pressure.

$$\eta_{pos} = \frac{\dot{m}_m}{\dot{m}_p} \frac{(h_{om} - h_{m@Pos})}{(h_{op} - h_{p@Pos})} \quad (A-35)$$

In the second case we use the change in the enthalpy of the primary for an isentropic expansion from the primary stagnation conditions to the static pressure, P_{lp} at the inlet to the ejector.

$$\eta_{plp} = \frac{\dot{m}_m}{\dot{m}_p} \frac{(h_{om} - h_{m@Pos})}{(h_{op} - h_{p@Plp})} \quad (A-36)$$

Finally in the third case we use the change in the enthalpy of primary for an isentropic expansion from the primary stagnation conditions to the secondary stagnation temperature.

$$\eta_{Tos} = \frac{\dot{m}_m}{\dot{m}_p} \frac{(h_{om} - h_{m@Pos})}{(h_{op} - h_{eTos})} \quad (A-37)$$

Under certain conditions the "efficiencies" in Equations (A-35) to (A-37) can be greater than one and, therefore, they are not true efficiencies.

Constant Pressure Analysis

For the constant pressure case, the momentum equation takes a very simple form if we neglect shear stress:

$$\dot{m}_p (V_p - V_m) + \dot{m}_s (V_s - V_m) = 0. \quad (A-38)$$

Equation (A-38) can be immediately solved for V_m . Using the same notation as for the constant area case we obtain the result:

$$\bar{V}_m = \frac{\bar{m} \bar{V} + 1}{\bar{m} + 1} \quad (A-39)$$

The temperature can be found from the energy equation, Equation (A-18), which is also valid for the constant pressure case. The pressure is, of course, equal to the inlet value, therefore Equation (A-13) can be solved for the exit area. Thus, a complete solution can be found for constant pressure which is simpler than the constant area case. The efficiency definitions can be used for either the constant pressure or constant area case.

Computer Results of Ejector Studies

A large number of computer runs have been made for various combinations of fluids and geometries. Data for the runs presented in the main body are presented in this section.

The first set of data is presented for air driving air in the constant area case. The mass flow ratio was set to 0.1. All of the tables present the tabulated computer results used to plot Figures 2 and 3 in the main body. The first column contains the secondary Mach number, M_s , which is taken as the independent variable. The second column is P_{1s}/P_{0s} (because of lack of space, it is labeled $P_{1s}/$ and the third column is the temperature ratio T_{1s}/T_{0s}). Each of these values are obtained from M_s using isentropic relations. The exit area of the primary nozzle is chosen to match the pressure of the primary to the secondary. This sets the value of the primary Mach number, M_p (located in column 10) and enables one to find T_{1p}/T_{0p} and P_{1p}/P_{0p} (located in columns 11 and 12).

Column four gives the ratio of the primary velocity to the secondary velocity V_p/V_s and column five gives the ratio of the mixed velocity to the secondary velocity.

Column six gives the mixed flow Mach number. Column seven is the pressure ratio P_m/P_{0s} and column eight is the temperature ratio T_m/T_{0s} . The gamma value of the mixture is given in column nine.

Column thirteen gives the area ratio A_p/A_s required to match the exit pressure and column fourteen gives the value of A/R_p^* . The last four columns give the three efficiencies discussed in this Appendix and the entropy increase.

CONSTANT AREA CALCULATIONS

SUBSONIC BRANCH

PRIMARY VAPOR AIR SECONDARY GAS AIR

PR= 6.000 TR= 3.700 GP=1.400 GS=1.400 WR= 1.00 WP= 29.00 WS= 29.00

M P/M S= 0.100

MS	PIS/	TIS/	VP/VS	VM/VS	MM	PM/	TM/	GM	MP	TIP/TOP	PIP/POP	AP/AS	A/AP*	EFPOS	EFTOS	EFAVL	SR
0.0500	0.998	1.000	54.485	1.341	0.040	1.016	1.245	1.400	1.83	0.599	0.166	0.004	363.838	0.85	0.03	0.180	0.497
0.1000	0.993	0.998	27.293	1.316	0.118	1.024	1.242	1.400	1.83	0.598	0.166	0.008	183.073	0.09	0.05	0.206	0.481
0.1500	0.984	0.996	18.252	1.295	0.174	1.027	1.238	1.400	1.84	0.597	0.164	0.012	123.455	0.13	0.07	0.229	0.467
0.2000	0.972	0.992	13.748	1.277	0.229	1.025	1.233	1.400	1.85	0.595	0.162	0.016	93.931	0.16	0.09	0.250	0.454
0.2500	0.957	0.988	11.059	1.261	0.283	1.017	1.226	1.400	1.86	0.592	0.160	0.020	76.449	0.19	0.10	0.269	0.443
0.3000	0.939	0.982	9.277	1.247	0.334	1.004	1.218	1.400	1.87	0.589	0.157	0.024	64.996	0.21	0.12	0.285	0.433
0.3500	0.919	0.976	8.013	1.234	0.388	0.987	1.209	1.400	1.88	0.585	0.153	0.028	56.994	0.24	0.13	0.300	0.424
0.4000	0.896	0.969	7.073	1.224	0.440	0.966	1.199	1.400	1.90	0.581	0.149	0.031	51.156	0.26	0.14	0.312	0.417
0.4500	0.870	0.961	6.349	1.214	0.492	0.942	1.188	1.400	1.92	0.576	0.145	0.035	46.766	0.27	0.15	0.323	0.410
0.5000	0.843	0.952	5.775	1.206	0.543	0.914	1.176	1.400	1.94	0.571	0.141	0.038	43.398	0.29	0.16	0.333	0.404
0.5500	0.814	0.943	5.311	1.200	0.594	0.884	1.163	1.400	1.96	0.565	0.136	0.042	40.780	0.30	0.16	0.341	0.399
0.6000	0.784	0.933	4.928	1.194	0.645	0.852	1.150	1.400	1.99	0.559	0.131	0.045	38.731	0.31	0.17	0.348	0.395
0.6500	0.753	0.922	4.609	1.190	0.697	0.817	1.135	1.400	2.01	0.553	0.125	0.048	37.127	0.32	0.18	0.353	0.392
0.7000	0.721	0.911	4.339	1.188	0.750	0.781	1.120	1.400	2.04	0.546	0.120	0.051	35.881	0.33	0.18	0.357	0.389
0.7500	0.689	0.899	4.108	1.188	0.804	0.742	1.103	1.400	2.07	0.539	0.115	0.054	34.928	0.33	0.18	0.361	0.387
0.8000	0.656	0.887	3.909	1.194	0.864	0.699	1.084	1.400	2.10	0.531	0.109	0.057	34.222	0.33	0.18	0.363	0.386
0.8500	0.624	0.874	3.736	1.220	0.942	0.643	1.058	1.400	2.13	0.524	0.104	0.059	33.727	0.34	0.18	0.364	0.385
0.9000	IMAGINARY SOLUTION																
0.9500	IMAGINARY SOLUTION																
1.0000	IMAGINARY SOLUTION																
1.0500	IMAGINARY SOLUTION																
1.1000	IMAGINARY SOLUTION																
1.1500	0.440	0.791	3.050	0.920	0.911	0.662	1.068	1.400	2.36	0.474	0.073	0.073	34.844	0.32	0.18	0.356	0.390
1.2000	0.412	0.776	2.974	0.853	0.866	0.691	1.083	1.400	2.40	0.465	0.069	0.075	34.538	0.31	0.17	0.347	0.396
1.2500	0.386	0.762	2.906	0.798	0.832	0.710	1.094	1.400	2.44	0.457	0.064	0.076	35.143	0.29	0.16	0.334	0.403
1.3000	0.361	0.747	2.844	0.750	0.803	0.724	1.102	1.400	2.48	0.448	0.060	0.078	35.855	0.27	0.15	0.319	0.413
1.3500	0.337	0.733	2.787	0.709	0.777	0.734	1.111	1.400	2.53	0.439	0.056	0.080	36.673	0.24	0.13	0.299	0.425
1.4000	0.314	0.718	2.735	0.673	0.755	0.740	1.118	1.400	2.57	0.431	0.052	0.081	37.597	0.20	0.11	0.276	0.438
1.4500	0.293	0.704	2.688	0.640	0.734	0.742	1.124	1.400	2.62	0.422	0.049	0.082	38.627	0.16	0.09	0.250	0.454
1.5000	0.272	0.690	2.645	0.611	0.716	0.742	1.130	1.400	2.66	0.413	0.045	0.084	39.764	0.11	0.06	0.220	0.472
1.5500	0.253	0.675	2.605	0.584	0.699	0.738	1.135	1.400	2.71	0.405	0.042	0.085	41.009	0.06	0.03	0.187	0.492
1.6000	0.235	0.661	2.568	0.560	0.683	0.733	1.139	1.400	2.76	0.396	0.039	0.086	42.365	0.00	0.00	0.151	0.514
1.6500	0.218	0.647	2.534	0.538	0.669	0.724	1.143	1.400	2.81	0.388	0.036	0.088	43.835	-0.06	-0.03	0.113	0.537
1.7000	0.203	0.634	2.503	0.519	0.655	0.715	1.147	1.400	2.86	0.380	0.034	0.089	45.420	-0.13	-0.07	0.071	0.563
1.7500	0.188	0.620	2.474	0.500	0.643	0.703	1.150	1.400	2.91	0.372	0.031	0.090	47.125	-0.20	-0.11	0.027	0.589
1.8000	0.174	0.607	2.447	0.484	0.631	0.690	1.153	1.400	2.96	0.364	0.029	0.091	48.953	-0.28	-0.15	-0.020	0.618
1.8500	0.161	0.594	2.422	0.468	0.621	0.676	1.156	1.400	3.01	0.356	0.027	0.092	50.909	-0.36	-0.20	-0.068	0.647
1.9000	0.149	0.581	2.399	0.454	0.611	0.660	1.159	1.400	3.06	0.348	0.025	0.092	52.997	-0.44	-0.24	-0.119	0.678
1.9500	0.138	0.568	2.377	0.441	0.601	0.644	1.161	1.400	3.11	0.340	0.023	0.093	55.223	-0.53	-0.29	-0.172	0.710
2.0000	0.128	0.556	2.356	0.429	0.593	0.627	1.164	1.400	3.16	0.333	0.021	0.094	57.591	-0.62	-0.34	-0.227	0.743
2.0500	0.118	0.543	2.337	0.418	0.585	0.610	1.166	1.400	3.22	0.326	0.020	0.095	60.107	-0.72	-0.40	-0.284	0.778

CONSTANT AREA CALCULATIONS
 SUPERSONIC BRANCH
 PRIMARY VAPOR: AIR SECONDARY GAS: AIR
 PR= 4.000 TR= 3.700 GP=1.400 GS=1.400 WR= 1.00 WP= 29.00 WS= 29.00
 M.P/M.S= 0.100

MS	PIS/	TIS/	VP/VS	VN/VS	MM	PM/	TM/	GM	MP	TIP/TOP	PIP/POP	AP/AS	A/AP*	EFPOS	EFTOS	EFAVL	SR
0.0500	VIOLATION OF 2ND LAW: REQUIRES NEGATIVE TEMPERATURES																
0.1000	VIOLATION OF 2ND LAW: REQUIRES NEGATIVE TEMPERATURES																
0.1500	VIOLATION OF 2ND LAW: REQUIRES NEGATIVE TEMPERATURES																
0.2000	VIOLATION OF 2ND LAW: REQUIRES NEGATIVE TEMPERATURES																
0.2500	VIOLATION OF 2ND LAW: REQUIRES NEGATIVE TEMPERATURES																
0.3000	VIOLATION OF 2ND LAW: REQUIRES NEGATIVE TEMPERATURES																
0.3500	VIOLATION OF 2ND LAW FOR ADIABATIC SYSTEMS: REQUIRES WORK INPUT AND COOLING																
0.4000	VIOLATION OF 2ND LAW FOR ADIABATIC SYSTEMS: REQUIRES WORK INPUT AND COOLING																
0.4500	VIOLATION OF 2ND LAW FOR ADIABATIC SYSTEMS: REQUIRES WORK INPUT AND COOLING																
0.5000	VIOLATION OF 2ND LAW FOR ADIABATIC SYSTEMS: REQUIRES WORK INPUT AND COOLING																
0.5500	0.814	0.943	5.311	3.033	1.908	0.217	0.721	1.400	1.94	0.565	0.136	0.042	40.780	0.96	0.53	0.784	0.129
0.6000	0.784	0.933	4.928	2.580	1.682	0.272	0.795	1.400	1.99	0.559	0.131	0.045	38.731	0.68	0.37	0.590	0.248
0.6500	0.753	0.922	4.489	2.239	1.511	0.327	0.855	1.400	2.01	0.553	0.125	0.048	37.127	0.51	0.28	0.480	0.315
0.7000	0.721	0.911	4.339	1.958	1.377	0.382	0.903	1.400	2.04	0.546	0.120	0.051	35.881	0.42	0.23	0.418	0.352
0.7500	0.689	0.899	4.108	1.728	1.265	0.437	0.944	1.400	2.07	0.539	0.115	0.054	34.928	0.37	0.20	0.384	0.372
0.8000	0.656	0.887	3.909	1.532	1.166	0.492	0.979	1.400	2.10	0.531	0.109	0.057	34.222	0.35	0.19	0.370	0.381
0.8500	0.624	0.874	3.736	1.348	1.063	0.558	1.016	1.400	2.13	0.524	0.104	0.059	33.727	0.34	0.19	0.365	0.385
0.9000	IMAGINARY SOLUTION																
0.9500	IMAGINARY SOLUTION																
1.0000	IMAGINARY SOLUTION																
1.0500	IMAGINARY SOLUTION																
1.1000	IMAGINARY SOLUTION																
1.1500	0.440	0.791	3.050	1.070	1.102	0.530	1.002	1.400	2.36	0.474	0.073	0.073	34.044	0.33	0.18	0.358	0.389
1.2000	0.412	0.776	2.974	1.089	1.163	0.490	0.980	1.400	2.40	0.465	0.069	0.075	34.538	0.32	0.18	0.354	0.391
1.2500	0.386	0.762	2.906	1.093	1.217	0.455	0.961	1.400	2.44	0.457	0.064	0.076	35.143	0.31	0.17	0.349	0.394
1.3000	0.361	0.747	2.844	1.095	1.268	0.424	0.943	1.400	2.48	0.448	0.060	0.078	35.855	0.31	0.17	0.344	0.397
1.3500	0.337	0.733	2.787	1.096	1.317	0.395	0.925	1.400	2.53	0.439	0.056	0.080	36.473	0.30	0.16	0.339	0.401
1.4000	0.314	0.718	2.735	1.096	1.366	0.368	0.907	1.400	2.57	0.431	0.052	0.081	37.597	0.29	0.16	0.333	0.404
1.4500	0.293	0.704	2.688	1.096	1.413	0.343	0.890	1.400	2.62	0.422	0.049	0.082	38.627	0.28	0.15	0.326	0.408
1.5000	0.272	0.690	2.645	1.095	1.460	0.319	0.873	1.400	2.66	0.413	0.045	0.084	39.764	0.27	0.15	0.319	0.412
1.5500	0.253	0.675	2.605	1.095	1.507	0.297	0.856	1.400	2.71	0.405	0.042	0.085	41.009	0.25	0.14	0.312	0.417
1.6000	0.235	0.661	2.568	1.094	1.554	0.276	0.840	1.400	2.76	0.396	0.039	0.086	42.365	0.24	0.13	0.304	0.422
1.6500	0.218	0.647	2.534	1.094	1.600	0.257	0.824	1.400	2.81	0.388	0.036	0.088	43.835	0.23	0.13	0.295	0.427
1.7000	0.203	0.634	2.503	1.093	1.645	0.239	0.808	1.400	2.86	0.380	0.034	0.089	45.428	0.22	0.12	0.286	0.432
1.7500	0.188	0.620	2.474	1.092	1.691	0.222	0.792	1.400	2.91	0.372	0.031	0.090	47.125	0.20	0.11	0.277	0.438
1.8000	0.174	0.607	2.447	1.091	1.736	0.206	0.777	1.400	2.96	0.364	0.029	0.091	48.953	0.19	0.10	0.267	0.444
1.8500	0.161	0.594	2.422	1.091	1.781	0.191	0.762	1.400	3.01	0.356	0.027	0.092	50.909	0.17	0.09	0.257	0.450
1.9000	0.149	0.581	2.399	1.090	1.826	0.177	0.747	1.400	3.06	0.348	0.025	0.092	52.997	0.15	0.08	0.247	0.456
1.9500	0.138	0.568	2.377	1.089	1.870	0.165	0.733	1.400	3.11	0.340	0.023	0.093	55.223	0.14	0.07	0.236	0.463
2.0000	0.128	0.556	2.356	1.089	1.915	0.153	0.719	1.400	3.16	0.333	0.021	0.094	57.591	0.12	0.07	0.225	0.470
2.0500	0.118	0.543	2.337	1.088	1.959	0.142	0.705	1.400	3.22	0.326	0.020	0.095	60.107	0.10	0.06	0.213	0.477

CONSTANT PRESSURE CALCULATIONS
SINGLE SOLUTION
PRIMARY VAPOR AIR SECONDARY GAS AIR
PR= 4.000 TR= 3.700 GP=1.400 GS=1.400 WR= 0.00 WP= 29.00 VS= 29.00
N.P/M.S= 0.100

MS	PI5/	TIS/	VP/VS	VN/VS	MM	PM/	TM/	GN	MP	TIP/TOP	PIP/POP	AP/AS	A/AP*	EFPOS	EFTOS	EFAVL	SR
0.0500	0.998	1.000	54.485	5.862	0.264	0.998	1.228	1.400	1.83	0.599	0.166	0.004	363.038	0.12	0.07	0.227	0.468
0.1000	0.993	0.998	27.293	3.390	0.306	0.993	1.223	1.400	1.83	0.598	0.166	0.008	183.073	0.15	0.08	0.246	0.457
0.1500	0.984	0.996	18.252	2.568	0.349	0.984	1.216	1.400	1.84	0.597	0.164	0.012	123.455	0.18	0.10	0.263	0.447
0.2000	0.972	0.992	13.748	2.159	0.391	0.972	1.208	1.400	1.85	0.595	0.162	0.016	93.931	0.20	0.11	0.278	0.437
0.2500	0.957	0.988	11.059	1.914	0.434	0.957	1.200	1.400	1.86	0.592	0.160	0.020	76.449	0.22	0.12	0.292	0.429
0.3000	0.939	0.982	9.277	1.752	0.477	0.939	1.191	1.400	1.87	0.589	0.157	0.024	64.996	0.24	0.13	0.304	0.421
0.3500	0.919	0.976	8.013	1.638	0.521	0.919	1.181	1.400	1.88	0.585	0.153	0.028	56.994	0.26	0.14	0.316	0.415
0.4000	0.896	0.969	7.073	1.552	0.565	0.896	1.171	1.400	1.90	0.581	0.149	0.031	51.156	0.28	0.15	0.325	0.409
0.4500	0.870	0.961	6.349	1.484	0.609	0.870	1.159	1.400	1.92	0.576	0.145	0.035	46.766	0.29	0.16	0.334	0.403
0.5000	0.843	0.952	5.775	1.434	0.653	0.843	1.148	1.400	1.94	0.571	0.141	0.038	43.398	0.30	0.17	0.341	0.399
0.5500	0.814	0.943	5.311	1.392	0.698	0.814	1.135	1.400	1.96	0.565	0.136	0.042	40.780	0.31	0.17	0.348	0.395
0.6000	0.784	0.933	4.928	1.357	0.743	0.784	1.122	1.400	1.99	0.559	0.131	0.045	38.731	0.32	0.17	0.353	0.392
0.6500	0.753	0.922	4.609	1.328	0.788	0.753	1.108	1.400	2.01	0.553	0.125	0.048	37.127	0.33	0.18	0.357	0.390
0.7000	0.721	0.911	4.339	1.304	0.833	0.721	1.094	1.400	2.04	0.546	0.120	0.051	35.881	0.33	0.18	0.360	0.388
0.7500	0.689	0.899	4.108	1.283	0.878	0.689	1.079	1.400	2.07	0.539	0.115	0.054	34.928	0.33	0.18	0.362	0.386
0.8000	0.656	0.887	3.909	1.264	0.923	0.656	1.064	1.400	2.10	0.531	0.109	0.057	34.222	0.34	0.18	0.364	0.385
0.8500	0.624	0.874	3.736	1.249	0.969	0.624	1.049	1.400	2.13	0.524	0.104	0.059	33.727	0.34	0.18	0.364	0.385
0.9000	0.591	0.861	3.585	1.235	1.015	0.591	1.033	1.400	2.17	0.516	0.099	0.062	33.416	0.34	0.18	0.364	0.385
0.9500	0.559	0.847	3.452	1.223	1.060	0.559	1.017	1.400	2.20	0.508	0.093	0.064	33.268	0.33	0.18	0.363	0.386
1.0000	0.528	0.833	3.334	1.212	1.106	0.528	1.001	1.400	2.24	0.499	0.088	0.067	33.268	0.33	0.18	0.361	0.387
1.0500	0.498	0.819	3.228	1.203	1.152	0.498	0.984	1.400	2.28	0.491	0.083	0.069	33.403	0.33	0.18	0.359	0.388
1.1000	0.468	0.805	3.135	1.194	1.198	0.468	0.968	1.400	2.32	0.483	0.078	0.071	33.664	0.32	0.18	0.356	0.390
1.1500	0.440	0.791	3.050	1.186	1.244	0.440	0.951	1.400	2.36	0.474	0.073	0.073	34.044	0.32	0.17	0.352	0.392
1.2000	0.412	0.776	2.974	1.179	1.290	0.412	0.934	1.400	2.40	0.465	0.069	0.075	34.538	0.31	0.17	0.348	0.395
1.2500	0.386	0.762	2.906	1.173	1.336	0.386	0.918	1.400	2.44	0.457	0.064	0.076	35.143	0.30	0.17	0.343	0.398
1.3000	0.361	0.747	2.844	1.168	1.382	0.361	0.901	1.400	2.48	0.448	0.060	0.078	35.855	0.30	0.16	0.338	0.401
1.3500	0.337	0.733	2.787	1.162	1.428	0.337	0.884	1.400	2.53	0.439	0.056	0.080	36.673	0.29	0.16	0.332	0.405
1.4000	0.314	0.718	2.735	1.158	1.475	0.314	0.868	1.400	2.57	0.431	0.052	0.081	37.597	0.28	0.15	0.325	0.409
1.4500	0.293	0.704	2.688	1.153	1.521	0.293	0.852	1.400	2.62	0.422	0.049	0.082	38.627	0.27	0.15	0.318	0.413
1.5000	0.272	0.690	2.645	1.150	1.567	0.272	0.835	1.400	2.66	0.413	0.045	0.084	39.764	0.25	0.14	0.311	0.417
1.5500	0.253	0.675	2.605	1.146	1.613	0.253	0.819	1.400	2.71	0.405	0.042	0.085	41.009	0.24	0.13	0.303	0.422
1.6000	0.235	0.661	2.568	1.143	1.659	0.235	0.803	1.400	2.76	0.396	0.039	0.086	42.365	0.23	0.13	0.294	0.427
1.6500	0.218	0.647	2.534	1.139	1.705	0.218	0.788	1.400	2.81	0.388	0.036	0.088	43.835	0.21	0.12	0.285	0.433
1.7000	0.203	0.634	2.503	1.137	1.750	0.203	0.772	1.400	2.86	0.380	0.034	0.089	45.420	0.20	0.11	0.275	0.439
1.7500	0.188	0.620	2.474	1.134	1.796	0.188	0.757	1.400	2.91	0.372	0.031	0.090	47.125	0.18	0.10	0.266	0.444
1.8000	0.174	0.607	2.447	1.132	1.842	0.174	0.742	1.400	2.96	0.364	0.029	0.091	48.953	0.17	0.09	0.256	0.451
1.8500	0.161	0.594	2.422	1.129	1.888	0.161	0.727	1.400	3.01	0.356	0.027	0.092	50.909	0.15	0.08	0.245	0.457
1.9000	0.149	0.581	2.399	1.127	1.933	0.149	0.713	1.400	3.06	0.348	0.025	0.092	52.997	0.13	0.07	0.234	0.464
1.9500	0.138	0.568	2.377	1.125	1.978	0.138	0.699	1.400	3.11	0.340	0.023	0.093	55.223	0.12	0.06	0.223	0.471
2.0000	0.128	0.556	2.356	1.123	2.024	0.128	0.685	1.400	3.16	0.333	0.021	0.094	57.591	0.10	0.05	0.211	0.478
2.0500	0.118	0.543	2.337	1.122	2.069	0.118	0.671	1.400	3.22	0.326	0.020	0.095	60.107	0.08	0.04	0.199	0.485

CONSTANT AREA CALCULATIONS

SUBSONIC BRANCH

PRIMARY VAPOR: AIR SECONDARY GAS: AIR

PR= 4.000 TH= 3.700 CP=1.400 CS=1.400 WR= 1.00 WP= 29.00 WS= 29.00

M.P/M.S= 0.500

MS	PIS/	TIS/	VP/VS	VN/VS	MN	PN/	TH/	GN	MP	TIP/TOP	PIP/POP	AP/AS	A/AP*	EFPOS	EFTOS	EFAVL	SR
0.0500	0.998	1.000	54.405	2.574	0.093	1.002	1.097	1.400	1.03	0.599	0.166	0.020	73.785	0.09	0.05	0.445	1.233
0.1000	0.993	0.998	27.293	2.374	0.173	1.141	1.089	1.400	1.03	0.598	0.166	0.041	37.795	0.16	0.09	0.476	1.165
0.1500	0.984	0.996	18.252	2.220	0.242	1.183	1.078	1.400	1.04	0.597	0.164	0.061	25.877	0.22	0.12	0.501	1.108
0.2000	0.972	0.992	13.740	2.096	0.304	1.211	1.065	1.400	1.05	0.595	0.162	0.081	19.979	0.27	0.15	0.522	1.061
0.2500	0.957	0.988	11.059	1.994	0.364	1.227	1.051	1.400	1.06	0.592	0.160	0.100	16.492	0.31	0.17	0.540	1.021
0.3000	0.939	0.982	9.277	1.908	0.419	1.233	1.036	1.400	1.07	0.589	0.157	0.120	14.213	0.35	0.19	0.555	0.987
0.3500	0.919	0.976	8.013	1.833	0.470	1.231	1.020	1.400	1.08	0.585	0.153	0.138	12.627	0.38	0.21	0.569	0.958
0.4000	0.896	0.969	7.073	1.768	0.518	1.223	1.003	1.400	1.09	0.581	0.149	0.157	11.475	0.40	0.22	0.580	0.933
0.4500	0.870	0.961	6.349	1.709	0.564	1.209	1.786	1.400	1.92	0.576	0.145	0.175	10.616	0.42	0.23	0.589	0.912
0.5000	0.843	0.952	5.775	1.655	0.607	1.191	1.769	1.400	1.94	0.571	0.141	0.192	9.963	0.44	0.24	0.598	0.894
0.5500	0.814	0.943	5.311	1.605	0.648	1.170	1.753	1.400	1.96	0.565	0.136	0.209	9.464	0.45	0.25	0.604	0.879
0.6000	0.784	0.933	4.928	1.557	0.685	1.148	1.737	1.400	1.99	0.559	0.131	0.225	9.088	0.47	0.26	0.610	0.866
0.6500	0.753	0.922	4.609	1.510	0.718	1.126	1.722	1.400	2.01	0.553	0.125	0.241	8.789	0.48	0.26	0.615	0.855
0.7000	0.721	0.911	4.339	1.462	0.747	1.105	1.709	1.400	2.04	0.546	0.120	0.256	8.572	0.48	0.27	0.619	0.847
0.7500	0.689	0.899	4.108	1.412	0.771	1.088	1.698	1.400	2.07	0.539	0.115	0.270	8.417	0.49	0.27	0.622	0.840
0.8000	0.656	0.887	3.909	1.359	0.788	1.075	1.690	1.400	2.10	0.531	0.109	0.284	8.314	0.49	0.27	0.624	0.835
0.8500	0.624	0.874	3.736	1.303	0.797	1.068	1.686	1.400	2.13	0.524	0.104	0.297	8.257	0.50	0.27	0.625	0.833
0.9000	0.591	0.861	3.585	1.244	0.800	1.066	1.684	1.400	2.17	0.516	0.099	0.309	8.240	0.50	0.27	0.625	0.832
0.9500	0.559	0.847	3.452	1.184	0.797	1.068	1.686	1.400	2.20	0.508	0.093	0.321	8.260	0.50	0.27	0.625	0.833
1.0000	0.528	0.833	3.334	1.124	0.789	1.073	1.690	1.400	2.24	0.499	0.088	0.333	8.314	0.49	0.27	0.623	0.836
1.0500	0.498	0.819	3.228	1.066	0.778	1.079	1.695	1.400	2.28	0.491	0.083	0.343	8.398	0.49	0.27	0.621	0.841
1.1000	0.468	0.805	3.135	1.011	0.765	1.084	1.701	1.400	2.32	0.483	0.078	0.354	8.512	0.48	0.26	0.618	0.849
1.1500	0.440	0.791	3.050	0.960	0.752	1.088	1.707	1.400	2.36	0.474	0.073	0.363	8.655	0.47	0.26	0.613	0.859
1.2000	0.412	0.776	2.974	0.913	0.737	1.089	1.714	1.400	2.40	0.465	0.069	0.373	8.825	0.46	0.25	0.608	0.870
1.2500	0.386	0.762	2.906	0.870	0.723	1.088	1.720	1.400	2.44	0.457	0.064	0.382	9.022	0.45	0.25	0.602	0.884
1.3000	0.361	0.747	2.844	0.830	0.710	1.084	1.726	1.400	2.48	0.448	0.060	0.390	9.246	0.43	0.24	0.594	0.901
1.3500	0.337	0.733	2.787	0.793	0.697	1.077	1.732	1.400	2.53	0.439	0.056	0.398	9.497	0.41	0.23	0.586	0.919
1.4000	0.314	0.718	2.735	0.760	0.684	1.068	1.737	1.400	2.57	0.431	0.052	0.405	9.775	0.39	0.22	0.577	0.939
1.4500	0.293	0.704	2.688	0.729	0.672	1.055	1.743	1.400	2.62	0.422	0.049	0.412	10.080	0.37	0.20	0.567	0.961
1.5000	0.272	0.690	2.645	0.701	0.660	1.041	1.748	1.400	2.66	0.413	0.045	0.419	10.414	0.35	0.19	0.557	0.985
1.5500	0.253	0.675	2.605	0.675	0.650	1.024	1.752	1.400	2.71	0.405	0.042	0.426	10.776	0.32	0.18	0.545	1.010
1.6000	0.235	0.661	2.568	0.651	0.639	1.005	1.756	1.400	2.76	0.396	0.039	0.432	11.167	0.30	0.16	0.533	1.037
1.6500	0.218	0.647	2.534	0.629	0.630	0.985	1.760	1.400	2.81	0.388	0.036	0.438	11.589	0.27	0.15	0.520	1.066
1.7000	0.203	0.634	2.503	0.609	0.621	0.963	1.764	1.400	2.86	0.380	0.034	0.443	12.041	0.24	0.13	0.507	1.096
1.7500	0.188	0.620	2.474	0.590	0.612	0.939	1.768	1.400	2.91	0.372	0.031	0.448	12.524	0.20	0.11	0.492	1.127
1.8000	0.174	0.607	2.447	0.573	0.604	0.915	1.771	1.400	2.96	0.364	0.029	0.453	13.045	0.17	0.09	0.478	1.160
1.8500	0.161	0.594	2.422	0.557	0.596	0.890	1.774	1.400	3.01	0.356	0.027	0.458	13.598	0.13	0.07	0.463	1.194
1.9000	0.149	0.581	2.399	0.542	0.589	0.864	1.777	1.400	3.06	0.348	0.025	0.462	14.188	0.10	0.05	0.447	1.229
1.9500	0.138	0.568	2.377	0.528	0.582	0.838	1.780	1.400	3.11	0.340	0.023	0.466	14.815	0.06	0.03	0.431	1.265
2.0000	0.128	0.556	2.356	0.515	0.575	0.812	1.782	1.400	3.16	0.333	0.021	0.471	15.481	0.02	0.01	0.414	1.301
2.0500	0.118	0.543	2.337	0.503	0.569	0.786	1.784	1.400	3.22	0.326	0.020	0.474	16.188	-0.02	-0.01	0.397	1.339

CONSTANT AREA CALCULATIONS

SUPERSONIC BRANCH

PRIMARY VAPOR: AIR SECONDARY GAS: AIR

PR= 4.000 TR= 3.700 CP=1.400 CS=1.400 VR= 1.00 VP= 29.00 VS= 29.00

M.P/M.S= 0.500

MS	PIS/	TIS/	VP/VS	VH/VS	MM	PH/	TM/	GM	MP	TIP/TOP	PIP/POP	AP/AS	A/AP*	EFPOS	EFTOS	EFAVL	SR
0.0500	VIOLATION OF 2ND LAW: REQUIRES NEGATIVE TEMPERATURES																
0.1000	VIOLATION OF 2ND LAW: REQUIRES NEGATIVE TEMPERATURES																
0.1500	VIOLATION OF 2ND LAW: REQUIRES NEGATIVE TEMPERATURES																
0.2000	VIOLATION OF 2ND LAW: REQUIRES NEGATIVE TEMPERATURES																
0.2500	VIOLATION OF 2ND LAW: REQUIRES NEGATIVE TEMPERATURES																
0.3000	VIOLATION OF 2ND LAW FOR ADIABATIC SYSTEMS: REQUIRES WORK INPUT AND COOLING																
0.3500	VIOLATION OF 2ND LAW FOR ADIABATIC SYSTEMS: REQUIRES WORK INPUT AND COOLING																
0.4000	0.896	0.969	7.873	5.777	2.446	0.179	0.845	1.400	1.90	0.581	0.149	0.157	11.475	0.99	0.54	0.873	0.281
0.4500	0.870	0.961	6.349	4.760	2.081	0.247	1.018	1.400	1.92	0.576	0.145	0.175	10.616	0.77	0.43	0.761	0.531
0.5000	0.843	0.952	5.775	4.017	1.843	0.314	1.132	1.400	1.94	0.571	0.141	0.192	9.963	0.66	0.36	0.702	0.663
0.5500	0.814	0.943	5.311	3.458	1.673	0.377	1.218	1.400	1.96	0.565	0.136	0.209	9.464	0.59	0.32	0.669	0.735
0.6000	0.784	0.933	4.928	3.027	1.548	0.437	1.284	1.400	1.99	0.559	0.131	0.225	9.080	0.55	0.30	0.651	0.776
0.6500	0.753	0.922	4.609	2.691	1.454	0.490	1.336	1.400	2.01	0.553	0.125	0.241	8.789	0.53	0.29	0.641	0.797
0.7000	0.721	0.911	4.339	2.427	1.383	0.536	1.374	1.400	2.04	0.546	0.120	0.256	8.572	0.52	0.29	0.636	0.808
0.7500	0.689	0.899	4.108	2.217	1.331	0.572	1.403	1.400	2.07	0.539	0.115	0.270	8.417	0.52	0.28	0.634	0.813
0.8000	0.656	0.887	3.909	2.053	1.297	0.599	1.422	1.400	2.10	0.531	0.109	0.284	8.314	0.51	0.28	0.633	0.815
0.8500	0.624	0.874	3.736	1.925	1.278	0.614	1.432	1.400	2.13	0.524	0.104	0.297	8.257	0.51	0.28	0.633	0.816
0.9000	0.591	0.861	3.585	1.826	1.272	0.619	1.435	1.400	2.17	0.516	0.099	0.309	8.240	0.51	0.28	0.633	0.816
0.9500	0.559	0.847	3.452	1.750	1.278	0.614	1.432	1.400	2.20	0.508	0.093	0.321	8.260	0.51	0.28	0.633	0.816
1.0000	0.528	0.833	3.334	1.691	1.294	0.601	1.424	1.400	2.24	0.499	0.088	0.333	8.314	0.51	0.28	0.632	0.816
1.0500	0.498	0.819	3.228	1.644	1.315	0.582	1.412	1.400	2.28	0.491	0.083	0.343	8.398	0.51	0.28	0.632	0.818
1.1000	0.468	0.805	3.135	1.607	1.342	0.560	1.397	1.400	2.32	0.483	0.078	0.354	8.512	0.51	0.28	0.631	0.820
1.1500	0.440	0.791	3.050	1.577	1.372	0.536	1.380	1.400	2.36	0.474	0.073	0.363	8.655	0.51	0.28	0.630	0.823
1.2000	0.412	0.776	2.974	1.551	1.405	0.510	1.362	1.400	2.40	0.465	0.069	0.373	8.825	0.50	0.28	0.628	0.826
1.2500	0.386	0.762	2.906	1.529	1.440	0.483	1.343	1.400	2.44	0.457	0.064	0.382	9.022	0.50	0.27	0.626	0.831
1.3000	0.361	0.747	2.844	1.511	1.476	0.457	1.323	1.400	2.48	0.448	0.060	0.390	9.246	0.49	0.27	0.624	0.836
1.3500	0.337	0.733	2.787	1.494	1.513	0.430	1.303	1.400	2.53	0.439	0.056	0.398	9.497	0.49	0.27	0.621	0.841
1.4000	0.314	0.718	2.735	1.480	1.551	0.405	1.283	1.400	2.57	0.431	0.052	0.405	9.775	0.48	0.27	0.618	0.848
1.4500	0.293	0.704	2.688	1.467	1.589	0.380	1.263	1.400	2.62	0.422	0.049	0.412	10.080	0.48	0.26	0.615	0.855
1.5000	0.272	0.690	2.645	1.456	1.627	0.356	1.242	1.400	2.66	0.413	0.045	0.419	10.414	0.47	0.26	0.612	0.862
1.5500	0.253	0.675	2.605	1.445	1.666	0.334	1.222	1.400	2.71	0.405	0.042	0.426	10.776	0.46	0.25	0.608	0.870
1.6000	0.235	0.661	2.568	1.436	1.704	0.312	1.202	1.400	2.76	0.396	0.039	0.432	11.167	0.45	0.25	0.604	0.879
1.6500	0.218	0.647	2.534	1.427	1.743	0.291	1.182	1.400	2.81	0.388	0.036	0.438	11.589	0.44	0.24	0.600	0.888
1.7000	0.203	0.634	2.503	1.420	1.782	0.272	1.162	1.400	2.86	0.380	0.034	0.443	12.041	0.43	0.24	0.596	0.898
1.7500	0.188	0.620	2.474	1.412	1.821	0.254	1.142	1.400	2.91	0.372	0.031	0.448	12.526	0.42	0.23	0.591	0.908
1.8000	0.174	0.607	2.447	1.406	1.860	0.237	1.123	1.400	2.96	0.364	0.029	0.453	13.045	0.41	0.23	0.586	0.919
1.8500	0.161	0.594	2.422	1.399	1.898	0.220	1.104	1.400	3.01	0.356	0.027	0.458	13.598	0.40	0.22	0.581	0.930
1.9000	0.149	0.581	2.399	1.394	1.937	0.205	1.086	1.400	3.06	0.348	0.025	0.462	14.188	0.39	0.21	0.576	0.941
1.9500	0.138	0.568	2.377	1.388	1.975	0.191	1.067	1.400	3.11	0.340	0.023	0.466	14.815	0.38	0.21	0.571	0.953
2.0000	0.128	0.556	2.356	1.383	2.013	0.178	1.049	1.400	3.16	0.333	0.021	0.471	15.481	0.37	0.20	0.565	0.966
2.0500	0.118	0.543	2.337	1.379	2.051	0.166	1.032	1.400	3.22	0.326	0.020	0.474	16.188	0.35	0.19	0.559	0.978

CONSTANT PRESSURE CALCULATIONS
SINGLE SOLUTION
PRIMARY VAPOR: AIR SECONDARY GAS: AIR

PR= 6.000 TR= 3.700 GP=1.400 GS=1.400 WR= 1.00 WP= 29.00 VS= 29.00
N.P/M.S= 0.500

MS	PIS/	TIS/	VP/VS	VN/VS	MM	PM/	TM/	GM	MP	TIP/TOP	PIP/POP	AP/AS	A/AP*	EFPOS	EFTOS	EFAVL	SR
0.0500	0.998	1.000	54.485	10.828	0.717	0.998	1.723	1.400	1.83	0.599	0.166	0.020	73.785	0.36	0.20	0.560	0.977
0.1000	0.993	0.998	27.293	9.764	0.746	0.993	1.710	1.400	1.83	0.598	0.166	0.041	37.795	0.38	0.21	0.570	0.955
0.1500	0.984	0.996	18.252	6.751	0.776	0.984	1.696	1.400	1.84	0.597	0.164	0.061	25.877	0.40	0.22	0.579	0.935
0.2000	0.972	0.992	13.748	5.249	0.806	0.972	1.681	1.400	1.85	0.595	0.162	0.081	19.979	0.42	0.23	0.587	0.917
0.2500	0.957	0.988	11.059	4.353	0.838	0.957	1.666	1.400	1.86	0.592	0.160	0.100	16.492	0.43	0.24	0.594	0.901
0.3000	0.939	0.982	9.277	3.759	0.870	0.939	1.650	1.400	1.87	0.589	0.157	0.120	14.213	0.45	0.24	0.601	0.886
0.3500	0.919	0.976	8.013	3.338	0.903	0.919	1.634	1.400	1.88	0.585	0.153	0.138	12.627	0.46	0.25	0.607	0.873
0.4000	0.896	0.969	7.073	3.024	0.937	0.896	1.616	1.400	1.90	0.581	0.149	0.157	11.475	0.47	0.26	0.612	0.862
0.4500	0.870	0.961	6.349	2.783	0.971	0.870	1.599	1.400	1.92	0.576	0.145	0.175	10.616	0.48	0.26	0.617	0.852
0.5000	0.843	0.952	5.775	2.592	1.004	0.843	1.580	1.400	1.94	0.571	0.141	0.192	9.963	0.49	0.27	0.620	0.843
0.5500	0.814	0.943	5.311	2.437	1.042	0.814	1.561	1.400	1.96	0.565	0.136	0.209	9.464	0.49	0.27	0.624	0.836
0.6000	0.784	0.933	4.928	2.309	1.078	0.784	1.542	1.400	1.99	0.559	0.131	0.225	9.080	0.50	0.27	0.627	0.829
0.6500	0.753	0.922	4.609	2.203	1.115	0.753	1.522	1.400	2.01	0.553	0.125	0.241	8.789	0.51	0.28	0.629	0.825
0.7000	0.721	0.911	4.339	2.113	1.152	0.721	1.502	1.400	2.04	0.546	0.120	0.256	8.572	0.51	0.28	0.630	0.821
0.7500	0.689	0.899	4.100	2.036	1.190	0.689	1.481	1.400	2.07	0.539	0.115	0.270	8.417	0.51	0.28	0.632	0.818
0.8000	0.656	0.887	3.909	1.970	1.228	0.656	1.460	1.400	2.10	0.531	0.109	0.284	8.314	0.51	0.28	0.632	0.816
0.8500	0.624	0.874	3.734	1.912	1.267	0.624	1.438	1.400	2.13	0.524	0.104	0.297	8.257	0.51	0.28	0.633	0.816
0.9000	0.591	0.861	3.585	1.862	1.306	0.591	1.417	1.400	2.17	0.516	0.099	0.309	8.240	0.51	0.28	0.633	0.816
0.9500	0.559	0.847	3.452	1.817	1.345	0.559	1.395	1.400	2.20	0.508	0.093	0.321	8.260	0.51	0.28	0.632	0.817
1.0000	0.528	0.833	3.334	1.770	1.385	0.528	1.373	1.400	2.24	0.499	0.088	0.333	8.314	0.51	0.28	0.631	0.819
1.0500	0.498	0.819	3.220	1.743	1.425	0.498	1.351	1.400	2.28	0.491	0.083	0.343	8.398	0.51	0.28	0.630	0.822
1.1000	0.468	0.805	3.135	1.712	1.465	0.468	1.329	1.400	2.32	0.483	0.078	0.354	8.512	0.50	0.28	0.628	0.825
1.1500	0.440	0.791	3.050	1.683	1.504	0.440	1.307	1.400	2.36	0.474	0.073	0.363	8.655	0.50	0.27	0.626	0.830
1.2000	0.412	0.776	2.974	1.658	1.547	0.412	1.285	1.400	2.40	0.465	0.069	0.373	8.825	0.50	0.27	0.624	0.835
1.2500	0.384	0.762	2.906	1.635	1.587	0.384	1.263	1.400	2.44	0.457	0.064	0.382	9.022	0.49	0.27	0.621	0.841
1.3000	0.361	0.747	2.844	1.615	1.628	0.361	1.242	1.400	2.48	0.448	0.060	0.390	9.246	0.48	0.27	0.619	0.847
1.3500	0.337	0.733	2.787	1.596	1.670	0.337	1.220	1.400	2.53	0.439	0.056	0.398	9.497	0.48	0.26	0.615	0.854
1.4000	0.314	0.718	2.735	1.578	1.711	0.314	1.198	1.400	2.57	0.431	0.052	0.405	9.775	0.47	0.26	0.612	0.862
1.4500	0.293	0.704	2.688	1.563	1.752	0.293	1.177	1.400	2.62	0.422	0.049	0.412	10.080	0.46	0.25	0.608	0.870
1.5000	0.272	0.690	2.645	1.548	1.794	0.272	1.156	1.400	2.66	0.413	0.045	0.419	10.414	0.45	0.25	0.604	0.879
1.5500	0.253	0.675	2.605	1.535	1.835	0.253	1.135	1.400	2.71	0.405	0.042	0.426	10.776	0.44	0.24	0.600	0.888
1.6000	0.235	0.661	2.568	1.523	1.877	0.235	1.115	1.400	2.76	0.396	0.039	0.432	11.167	0.43	0.24	0.595	0.898
1.6500	0.218	0.647	2.534	1.511	1.918	0.218	1.095	1.400	2.81	0.388	0.036	0.438	11.589	0.42	0.23	0.591	0.909
1.7000	0.203	0.634	2.503	1.501	1.959	0.203	1.075	1.400	2.86	0.380	0.034	0.443	12.041	0.41	0.23	0.586	0.920
1.7500	0.188	0.620	2.474	1.491	2.001	0.188	1.055	1.400	2.91	0.372	0.031	0.448	12.524	0.40	0.22	0.581	0.931
1.8000	0.174	0.607	2.447	1.482	2.042	0.174	1.036	1.400	2.96	0.364	0.029	0.453	13.045	0.39	0.21	0.575	0.943
1.8500	0.161	0.594	2.422	1.474	2.083	0.161	1.017	1.400	3.01	0.356	0.027	0.458	13.598	0.38	0.21	0.570	0.956
1.9000	0.149	0.581	2.399	1.466	2.124	0.149	0.999	1.400	3.06	0.348	0.025	0.462	14.180	0.36	0.20	0.564	0.968
1.9500	0.138	0.568	2.377	1.459	2.165	0.138	0.981	1.400	3.11	0.340	0.023	0.466	14.815	0.35	0.19	0.558	0.982
2.0000	0.128	0.556	2.356	1.452	2.206	0.128	0.963	1.400	3.16	0.333	0.021	0.471	15.481	0.34	0.19	0.552	0.995
2.0500	0.118	0.543	2.337	1.446	2.247	0.118	0.945	1.400	3.22	0.326	0.020	0.474	16.188	0.32	0.18	0.543	1.009

APPENDIX B

DETAILED DESCRIPTION OF MACHINERY REQUIRED TO ACHIEVE ANY
DESIRED TOTAL PRESSURE FOR CONSTANT ENERGY STEADY FLOWS

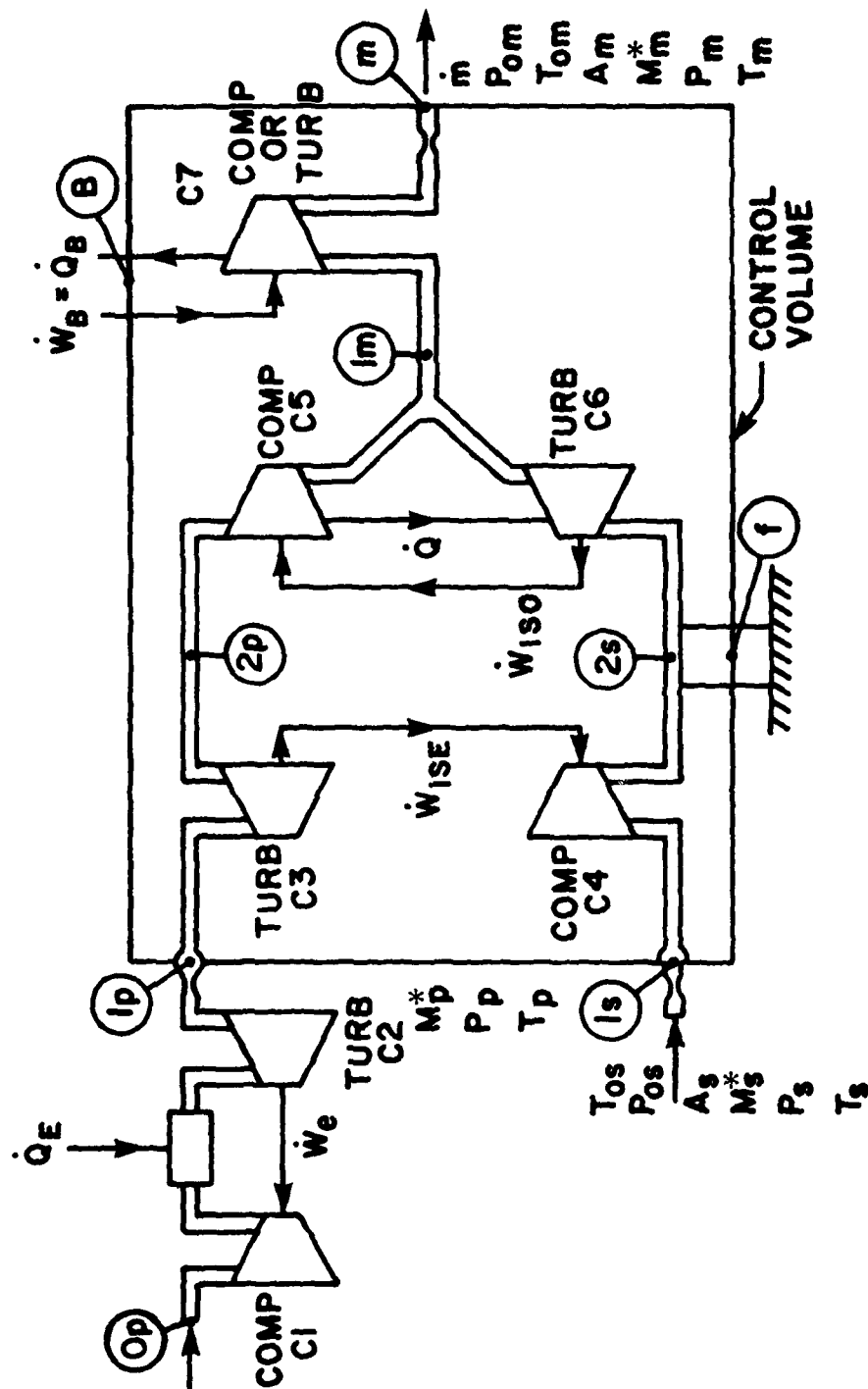


Figure B-1. Machinery for Producing Any Desired Total Pressure for Constant Enthalpy Steady Flows.

Components of Figure B-1

1. Reversible adiabatic components:

- C1: primary compressor
- C2: primary turbine that drives C1
- C3: primary turbine that drives C4
- C4: secondary compressor

2. Reversible isothermal components

- C5: primary isothermal compressor
- C6: secondary isothermal turbine that drives C5 and exchanges heat with C5
- C7: Mixed flow isothermal compressor (or turbine) that adjusts final stagnation pressure to any desired value

Stations

- 0p: We have shown a turbojet engine receiving mass flow \dot{m}_p at T_{0s} and P_{0s} and supplying conditions of P_{0p} and T_{0p} at station 1p.
- 1p: Conditions P_{0p} and T_{0p} and \dot{m}_p . The nozzle produces any desired Mach number M_p (or M_p^*) at station 1p with static pressure P_{1p} and static temperature T_{1p} . The flow can be diffused and fed to the reversible adiabatic turbine. Although we show that the stagnation conditions are supplied by a jet engine, they could also be provided by a boiler and the gas could be a primary vapor which may be a different gas than the secondary.
- 1s: A secondary gas flow is supplied at flow rate \dot{m}_s and stagnation conditions T_{0s} and P_{0s} . The nozzle supplies the flow at any desired Mach number, M_s (or M_s^*), at a static pressure of P_{1s} . The flow can be diffused to any desired value before entering the reversible adiabatic compressor C4.
- 2p: After passing through the reversible and adiabatic turbine the primary flow comes to the total temperature T_{0m} and a total pressure P_{02p} . Since the reversible adiabatic process is isentropic, the entropy is unchanged. Thus, $s_{2p} = s_{1p} = s_{0p}$ (i.e., the stagnation value of the entropy at station 1p).
- 2s: The secondary flow is compressed in a reversible adiabatic process in compressor C4 to a stagnation temperature of T_{0m} at stagnation pressure P_{02s} . Since this is an isentropic process, we have: $s_{2s} = s_{1s} = s_{0s}$ (i.e., the stagnation value of the entropy at station 1s).

Now the isentropic work, \dot{W}_{ISE} , transferred from turbine C3 to compressor C4 is:

$$\dot{W}_{ISE} = \dot{m}_p C_p (T_{0p} - T_{0m}) = \dot{m}_s C_p (T_{0m} - T_{0s})$$

Hence,

$$(\dot{m}_p + \dot{m}_s)T_{om} = \dot{m}_p T_{op} + \dot{m}_s T_{os} \quad . \quad (B-1)$$

Clearly, this is just the constant energy mixing condition.

lm: The conditions at lm result from mixing the secondary and primary gases that went through the reversible isothermal compressor C5 and the reversible isothermal turbine C6. We can relate the isothermal work to the heat transfer and to the entropy changes (since we have assumed reversible processes).

$$\dot{W}_{ISO} = \dot{Q} = \dot{m}_s T_{om} (s_m - s_{os}) = \dot{m}_p T_{om} (s_{op} - s_{om})$$

therefore

$$(\dot{m}_s + \dot{m}_p)s_{om} = \dot{m}_p s_{op} + \dot{m}_s s_{os} \quad . \quad (B-2)$$

Clearly, this is just the constant total entropy condition which is required for reversible mixing of the two incoming streams.

m: Finally, we take the mixed flow at conditions lm and compress the mixed flow with a reversible isothermal compressor C7. In this way, we can compress the mixed flow to any desired stagnation pressure while still keeping the total temperature the same: i.e., T_{om} . The work required for the compressor C7 is equal to the heat transfer. These quantities are shown crossing the control volume at the boundary station B. We may expand the mixed flow through a nozzle to any Mach number and exit area that we wish.

If we write the momentum equation for the control volume shown in Figure B-1, we must in general include the force in the strut at the boundary station f. Since we are free to produce any stagnation pressure we want at station m, we can produce any force we desire at station f. (Note: the couplings at lp and ls have seals that do not contribute any force on the control volume.)

Clearly, we can write the following equations for the control volume of Figure B-1 when we have steady flow conditions.

Continuity:

$$\dot{m} = \dot{m}_s + \dot{m}_p \quad (B-3)$$

or

$$\rho_m A_m V_m = \rho_s A_s V_s + \rho_p A_p V_p \quad (B-3a)$$

Energy:

$$\dot{m} T_{om} = \dot{m}_s T_{os} + \dot{m}_p T_{op} \quad (B-4)$$

and momentum

$$P_m A_m - P_{lp} A_p = P_{ls} A_s + f = \dot{m}_p (V_p - V_m) + \dot{m}_s (V_s - V_m) \quad (B-5)$$

Now if we arbitrarily require that

$$A_m = A_p + A_s \quad (B-6)$$

and that the force in the strut is zero

$$f = 0 \quad (B-7)$$

We have a set of equations that are formally identical to those that we write for a constant area ejector.

The complete solution to these equations for a given set of inlet conditons can be used to produce efficiency maps as shown on Figures 4 and 5 of the main body of the report for subsonic and supersonic solution branches.

All of these solutions could be achieved with the machinery shown in Figure B-1 of this Appendix, but all of them could not be achieved with a constant area ejector.

It is also quite clear that the ideal machinery of Figure B-1 could be replaced with real, inefficient machines and ordinary heat exchangers such that Equations (B-3) thorough (B-5) would still be valid. Thus, all of the solutions shown on Figures 4 and 5 of the main body of the report could be achieved with real machines. However, it is highly unlikely that such a device would have any practical significance.